# Exploring the role of the actin-MRTFA-SRF signalling pathway downstream of P-cadherin in basal-like breast cancer cells

Lídia Maria Pereira Faria

**M**

2021

---

INSTITUTO DE CIÊNCIAS BIOMÉDICAS ABEL SALAZAR

M.ICBAS 2021

Lídia Maria Pereira Faria

# Exploring the role of the actin-MRTFA-SRF signalling pathway downstream of P-cadherin in basal-like breast cancer cells

Dissertação de candidatura ao grau de **Mestre em Oncologia – Especialização em Oncologia Laboratorial –** submetida ao Instituto de Ciências Biomédicas Abel Salazar da Universidade do Porto

O trabalho aqui apresentado está incluído num manuscrito que irá ser submetido para publicação.

<u>Orientador</u>: **Doutora Florence Janody**

Investigador Principal

Cytoskeletal Regulation & Cancer
i3S-Instituto de Investigação e Inovação em Saúde – Universidade do Porto

<u>Coorientador:</u> **Doutora Sara Inês de Ascensão Tavares Canato**

Investigador em Pós-Doutoramento

Cancer and Stem Cell Biology
Champalimaud Foundation

Cytoskeletal Regulation & Cancer
i3S-Instituto de Investigação e Inovação em Saúde – Universidade do Porto

*"Above all, don't fear difficult moments.
The best comes from them"*

**Rita Levi-Montalcini**

## ACKNOWLEDGEMENTS

## ABSTRACT

Triple-Negative Breast Cancer (TNBC) remains by far the most lethal subtype of breast cancer, owing to their intrinsic and/or adaptive resistance to current chemotherapeutic drugs and to their inter- and intra-tumour heterogeneity. The cell-cell adhesion molecule P-cadherin (P-cad) is highly enriched in Basal-Like TNBC in the earlier stages of the malignant process in most cases, and significantly associated with worse prognosis. P-cad overexpression promotes *in vitro* cell migration, invasion and self-renewal potential, as well as tumourigenic and metastatic capacity in *in vivo* breast cancer models. Thus, P-cad signalling could hold the potential to delineate an aggressive molecular subtype of TNBC and to pinpoint to personalized therapeutic targets. Yet, the molecular pathways involved downstream of P-cad remain unclear.

Using a humanized *Drosophila* model expressing conditional P-cad, the Janody's group identified the actin/MRTF-A (Myocardin-related transcription factor A) /SRF (serum response factor) signalling pathway, as a P-cad effector. This pathway links actin filament (F-actin) dynamics and mechanical strains to gene transcription. The main goal of this project was to explore the role of the actin/MRTF-A/SRF signalling pathway downstream of P-cad in inducing tumourigenicity. To this end, we used the human mammary epithelial cell line MC10A-ER-Src, with conditional activation of the Src kinase proto-oncogene, which recapitulates the molecular events taking place during the development of basal-like TNBC upon Tamoxifen (TAM) treatment. During the first 12 hours of TAM treatment, pre-malignant MCF10A-ER-Src cells transiently upregulate P-cad and an SRF-dependent Luciferase reporter transgene, accumulate F-actin and acquire sustained proliferative abilities, prior to gain malignant transformed features. We show that pre-malignant MCF10A-ER-Src cells also transiently accumulate MRTF-A during the first 12 hours of TAM treatment. Moreover, inhibiting F-actin accumulation in pre-malignant MCF10A-ER-Src cells using Latrunculin A prevents the transient upregulation of the SRF-dependent Luciferase reporter transgene and could, in turn, stabilize P-cad and hinder cellular transformation. Inhibiting MRTF-A activity in pre-malignant MCF10A-ER-Src cells using CCG-203971 also impedes the upregulation of the SRF-dependent Luciferase reporter transgene and prevents cells from acquiring invading abilities in collagen and forming mammospheres. Taken all together, these observations and others provide evidences that in pre-malignant basal-like TNBC, the activation of MRTF-A/SRF signalling by P-cad through F-actin regulation is required for malignant progression. We believe that these findings open the possibility that targeting of this axis could be used as a therapeutic strategy to prevent the progression of a subset of pre-malignant basal-like TNBCs.

# RESUMO

O Cancro da Mama Triplo-Negativo (TNBC, do inglês Triple-Negative Breast Cancer) é o subtipo molecular de cancro da mama com maior taxa de mortalidade devido à sua resistência intrínseca e/ou adaptativa aos agentes quimioterapêuticos atualmente utilizados na prática clínica bem como à sua heterogeneidade inter- e intra-tumoral. A molécula de adesão celular P-caderina (P-cad) é sobre-expressa em TNBC do tipo Basal, na maioria dos casos numa fase inicial do desenvolvimento tumoral, o que está significativamente associado a pior prognóstico. A sobre-expressão de P-cad promove migração *in vitro*, invasão e capacidade de auto-renovação, bem como capacidade tumoral e metastática em modelos *in vivo* de cancro da mama. Deste modo, a sinalização da P-cad pode representar o potencial de delinear um subtipo molecular agressivo de TNBC e direcionar para alvos terapêuticos personalizados. No entanto, as vias de sinalização envolvidas a jusante da P-cad ainda não foram descritas.

Usando um modelo de *Drosophila* com expressão da P-cad humana, o grupo de Janody identificou a via de sinalização actina/MRTF-A (do inglês Myocardin-related transcription factor A) /SRF (do inglês Serum Response Factor) como efetor da P-cad, a qual liga a dinâmica do filamento de actina (F-actina) e as forças mecânicas à transcrição dos genes. O principal objetivo deste projeto foi explorar o papel da via de sinalização actina/MRTF-A/SRF a jusante da P-cad no desenvolvimento tumoral. Para isso, utilizamos a linha celular epitelial mamária MCF10A-ER-Src, com ativação condicional do proto-oncogene Src cinase, que recapitula os eventos moleculares que ocorrem durante o desenvolvimento de TNBC tipo basal após tratamento com Tamoxifeno (TAM). Durante as primeiras 12 horas de tratamento com TAM, as células MCF10A-ER-Src pré-malignas acumulam temporariamente P-cad e um transgene repórter de Luciferase dependente de SRF, bem como F-actina, e adquirem capacidade de proliferarem ininterruptamente, antes da aquisição de propriedades malignas, e nós mostramos que também acumulam temporariamente MRTF-A durante as primeiras 12 horas do tratamento com TAM. Além disso, a inibição da acumulação de F-actina em células pré-malignas usando Latrunculin A evita a sobre-expressão temporária do transgene repórter de Luciferase dependente de SRF e pode, por sua vez, estabilizar a P-cad e impedir a transformação celular. A inibição da atividade do MRTF-A em células pré-malignas usando CCG-203971 também evita a sobre-expressão temporária do transgene repórter de Luciferase dependente de SRF e impede que as células MCF10A-ER-Src adquiram capacidades de invasão em colagénio e de formação de mamosferas. Em suma, estas observações e outras fornecem evidências de que no TNBC pré-maligno do tipo basal, a ativação da via de sinalização actina/MRTF-A/SRF pela P-cad através da regulação da F-actina é necessária para a progressão

maligna. Acreditamos que esta descoberta abre a possibilidade de esta via ser usada como alvo terapêutico para prevenir a progressão de um subconjunto de TNBCs do tipo basal pré-malignos.

**TABEL OF CONTENTS**

## FIGURE INDEX

**TABLE INDEX**

## LIST OF ABREVIATIONS

| | |
|---|---|
| ABPs | Actin-Binding Proteins |
| AJ | Adherent Junctions |
| APS | Amonium Persulphate |
| BLBC | Basal-like Breast Cancer |
| BSA | Bovine Serum Albumin |
| $Ca^{2+}$ | Calcium |
| CAM | Cell Adhesion Molecules |
| CDKs | Cyclin-dependent Kinases |
| CGM | Complete Growth Medium |
| CK | Cytokeratins |
| CSC | Cancer Stem-like Cells |
| CSHS | Charcoal Stripped Horse Serum |
| D | *Drosophila melanogaster* |
| DMEM | Dulbecco's Modified Eagle Medium |
| DMSO | Dimethyl Sulfoxide |
| DTT | Dithiothreitol |
| E-cad | E-cadherin |
| ECM | Extracellular Matrix |
| EDTA | Ethylenediaminetetraacetic acid |
| EGF | Epidermal Growth Factor |
| EGFR | Epidermal Growth Factor Receptor |
| EGTA | Ethylene Glycol-bis(β-aminoethyl ether)-N,N,N′,N′-Tetraacetic Acid |
| EMT | Epithelial-to-Mesenchymal Transition |
| ER | Oestrogen Receptor |
| ER$^-$ | Oestrogen Receptor Negative |
| ER$^+$ | Oestrogen Receptor Positive |
| ERK | Extracellular-signal Regulated Kinase |
| EtOH | Ethanol |
| EVL | Ena/VASP-Like |
| F-actin | Filamentous actin |
| G-actin | Globular actin |
| H&E | Haematoxylin & Eosin |
| HEPES | 4-(2-hydroxyethyl)-1-piperazineethanesulfonic acid |
| HER2 | Human Epidermal Growth Factor Receptor 2 |
| HER2$^-$ | Human Epidermal Growth Factor Receptor 2 negative |
| HER2$^+$ | Human Epidermal Growth Factor Receptor 2 positive |
| IHC | Immunohistochemistry |
| IR | RNA Interference |
| LARII | Luciferase Assay Reagent II |
| LatA | Latrunculin A |
| LB | Luria Broth Miller |
| MAL | Megakaryocytic Acute Leukaemia |
| MAP | Mitogen-activated protein |
| MFE | Mammosphere formation efficiency |
| MRTF | Myocardin-Related Transcription Factor |
| NLS | Nuclear Localization Signal |
| *nub*-Gal4 | *nubbin*-Gal4 |
| P120ctn | p-120-catenin |
| PBS | Dulbecco's Phosphate Buffered Saline |
| P-cad | P-cadherin |
| PgR | Progesterone receptor |
| PgR$^-$ | Progesterone receptor negative |
| PgR$^+$ | Progesterone receptor positive |

| | |
|---|---|
| PI | Propidium Iodide |
| PIPES | Piperazine-N,N′-bis(2-ethanesulfonic acid) |
| PLB | Passive Lysis Buffer |
| PolyHEMA | Poly(2-hydrocyethyl methacrylate) |
| qRT-PCR | Real-time quantitative PCR |
| RB1 | Retinoblastoma 1 |
| RT | Room Temperature |
| SDS | Sodium Dodecyl Sulfate |
| SFK | Src family kinase |
| SRE | Serum Response Element |
| SRF | Serum Response Factor |
| TAD | Transactivation domain |
| TAM | Tamoxifen |
| TCF | Ternary Complex Factor |
| TEAD | TEA Domain |
| TEMED | N,N,N',N'-Tetramethyl-ethylenediamine |
| TME | Tumour Microenvironment |
| TNBC | Triple-Negative Breast Cancer |
| Tris | Tris(hydroxymethyl)aminomethane |
| WHO | World Health Organization |

# CHAPTER I

# INTRODUCTION

# 1. General concepts on cancer development

## 1.1. Worldwide impact of Cancer disease

According to the World Health Organization (WHO), Cancer is a genetic disease that comprises "a large group of disorders affecting any organ or tissue of the human body" (WHO, 2021).

In 2020, around 19 million new cases of cancer have been diagnosed worldwide (Figure 1-A). Cancer is the second leading cause of death, preceded by heart diseases, in both sexes and all ages (NCHS, 2021), with an estimate of 9.9 million deaths worldwide in 2020 (Figure 1.B), representing 1 in 6 people deaths (Sung et al., 2021).

The top 3 most common cancer types diagnosed worldwide are breast cancer, which accounts for 2.3 million new cases (11.7%), lung cancer with 2.2 million new cases (11,4%) and colorectal cancer with 1.9 million new cases every year (10%) (Figure 1.A). Regarding the impact of cancer on mortality rates, Lung cancer is responsible for 18% of all cancer deaths, followed by Colorectal cancer (9.4%), Liver cancer (8.3%), Stomach cancer (7.7%) and Breast cancer (6.9%) (Figure 1.B).
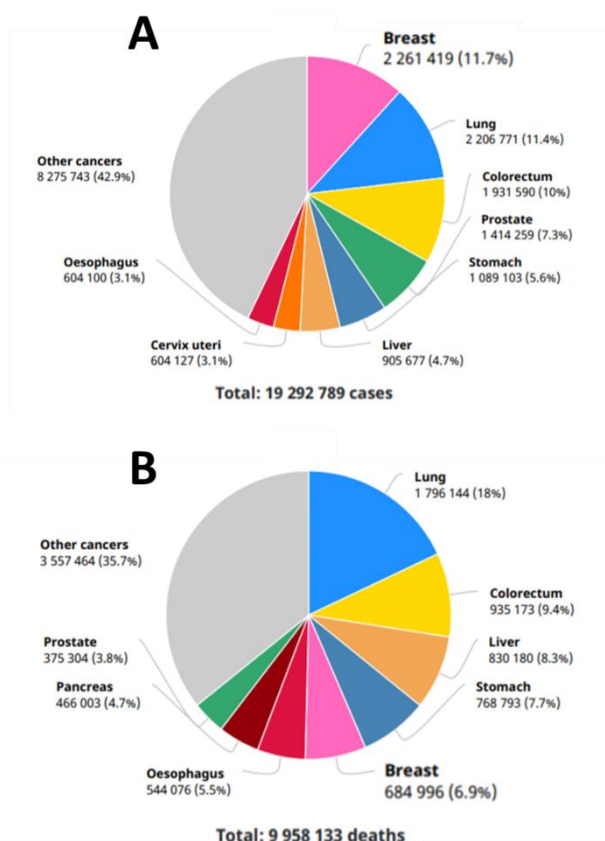


**Figure 1- Statistics of cancer worldwide**: Incidence (A) and mortality (B) distribution of the most common types of cancer in 2020 for both sexes and all ages. Adapted from Sung et al., 2021.

According to 2020 epidemiological data from the WHO, breast cancer is, worldwide, the second cancer with the highest incidence in both sexes, although more prevalent in the female gender. When narrowing this analysis to the female gender this is the most incident neoplasia, the most prevalent in five years and the one with the highest mortality, which makes it probably the most studied cancer in the world (Liga-Portuguesa-Contra-o-Cancro, 2021; WHO, 2021; Yip et al., 2008).

## 1.2.    From normal to malignant progression

The progression from a benign to a malignant phenotype is a complex process that starts with the transformation of a normal cell or group of cells. These cells are believed to acquire sustained proliferative abilities and an uncontrolled growth, being able to divide independently of external signalling, and to become resistant to apoptotic stimuli, allowing them to expand (Figure 2 – chart 2) and to ultimately give rise to a benign mass of tissue in any part of the human body, in case of a solid tumour, or to an outnumber of circulating blood cells in case of a haematological tumour (Saria, 2018; Witsch et al., 2010).

Although these alterations lead to modifications of the tissue structure, they are not always manifestations of a malignant phenotype. Figure 3 shows two of such examples. Hyperplasia is a tissue alteration characterized by a faster division rate than normal, which leads to overgrowth. Dysplasia is characterized by a modification in the tissue's organization. Although these alterations in the tissue's structure can evolve to malignancy, a malignant phenotype is characterized by a particular tissue morphology (Figure 3), showing that not all modifications in the organization of the tissue indicate a malignant phenotype (NIH, 2021).

However, these benign tumours can become malignant with the accumulation of more alterations that allow cells to become more aggressive. These cells abnormally differentiate and start expressing tumour markers. In addition, they lose contact inhibition, cohesiveness and adhesiveness which allows them to invade adjacent tissues (Figure 2 – chart 4) as well as to disseminate to the circulatory systems (Figure 2 – chart 5) and to colonize distant organs, a process called metastization (Figure 2 – chart 9) (Saria, 2018; Witsch et al., 2010).
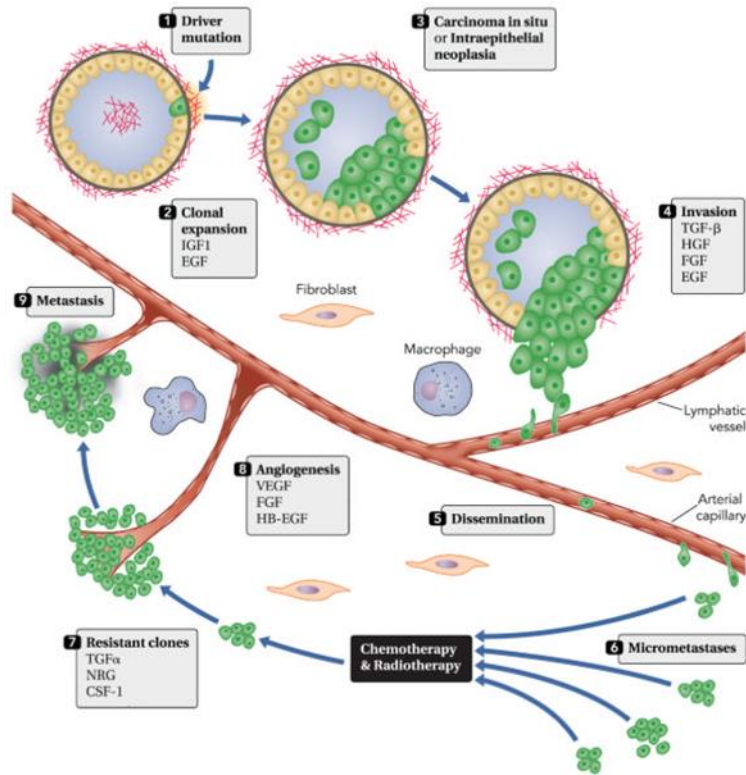
**Figure 2- Schematic representation of cancer development**. An alteration called driver mutation (1) originates initiated cells, which have the ability to undergo cell cycle control and survive. Then, these one's accumulate further oncogenic mutations and, driven by growth factors, undergo a clonal expansion (2) originating carcinomas *in situ* or intraepithelial neoplasias (3), which are circumscribed to that location. They can later acquire invasive properties (4), such as motility, which allow these cells to migrate through lymphatic and blood vessels and disseminate (5) to surrounding tissues, being able to metastasize in distant organs (9). From Witsch et al., 2010.
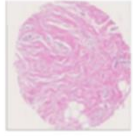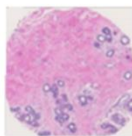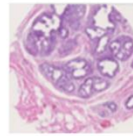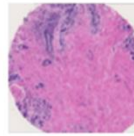


**Figure 3- Haematoxylin & Eosin (H&E) staining of normal, hyperplastic, dysplastic and malignant breast tissue**. H&E staining allows a complete visualization of a tissue's structure and identification of alterations that may or not induce malignancy. Scale bars = 250µm. Adapted from Ambekar et al., 2012.

### 1.3. Driver mutations are believed to induce cancer development

Cancer development is believed to occur primarily through the occurrence of driver mutations. These DNA modifications can be gain-of-function mutations in proto-oncogenes or loss-of-function mutations in tumour suppressor genes (Lee & Muller, 2010). Mutations in proto-oncogenes are translated in oncogenes, whose activity cannot be turned off as it happens in normal genes. Conversely, mutations in tumour suppressor genes abrogate the activity of these molecules to perform cell cycle control, as well as to induce apoptosis (López-Lázaro, 2018; NIH, 2021; Witsch et al., 2010).

The occurrence of mutations in these genes and progressive accumulation would lead to a significant increase in cell proliferation (López-Lázaro, 2018). Malignant progression is possible because these cells have the ability to escape cell cycle control and survive because they acquire characteristics so called hallmarks of cancer, nominated by Hanahan and Weinberg (Hanahan & Weinberg, 2011). Six of these hallmarks, were first described in 2000 and are the "integral components of most forms of cancer". Over the years, due to important progresses in cancer research, more hallmarks were added being in the total of 10 hallmarks represented in Figure 4. Also, once these hallmarks were identified, researchers have focused on developing new therapies in order to block each of these cancer cells advantages (Hanahan & Weinberg, 2011).
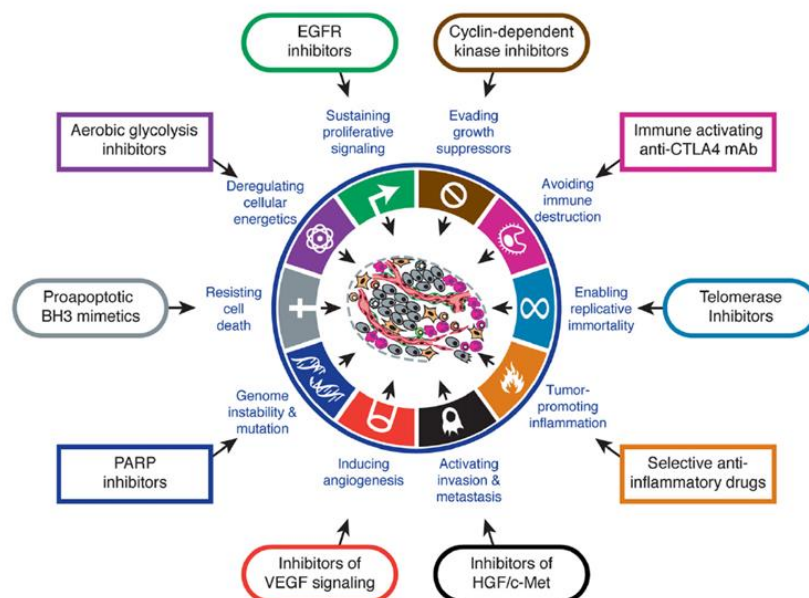


**Figure 4- Hallmarks of cancer and current available therapies**: these hallmarks of cancer constitute characteristics acquired by cancer cells that help them to move through the multistep development of cancer. From Hanahan & Weinberg, 2011.

These genetic alterations can be transmitted to the descendance, which increases their risk of developing cancer, hitting cancer as an hereditary disease. In addition, they can also

arise sporadically during lifetime due to external factors that induce DNA damage resulting in errors in cells division that can originate abnormal malignant cells. Since these environmental agents are responsible for inducing carcinogenesis, they are called carcinogens. They include exogenous risk factors, which can be chemical (tobacco smoke, organic and inorganic chemicals, unbalanced meals and pollution), physical (radiation) or biological (virus and bacteria) as well as endogenous risk factors, such as infections, gastric reflux, among others, which induce oxidative DNA damage (Montesano & Hall, 2001; NIH, 2021; Parsa, 2012).

Carcinogenic development can also be initiated by alterations in epigenetic mechanisms which regulate gene expression. Alterations in genes involved in the hypo and hypermethylation processes lead to DNA modifications in many important genes such as retinoblastoma 1 (RB1), p16, VHL and MLH1, promoting carcinogenesis (Feinberg et al., 2006). The occurrence of epigenetic alterations in progenitor cells can induce clonal expansion, giving rise to a benign tumour. These cells accumulate even more genetic and epigenetic alterations which trigger the acquisition of malignant properties (Figure 5).
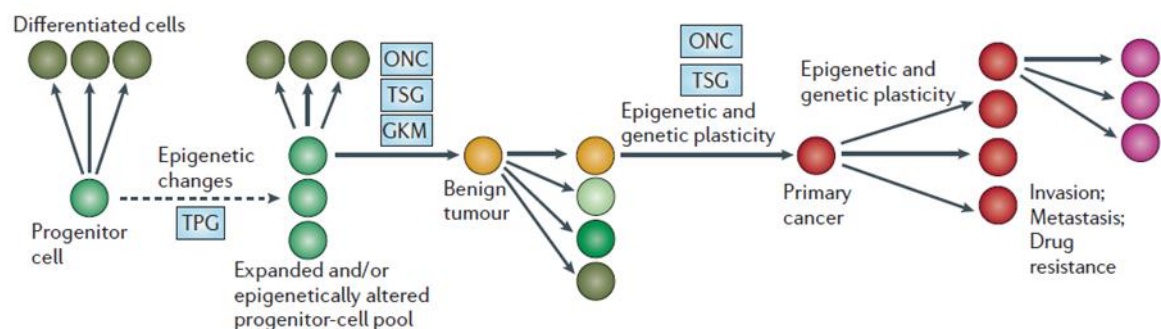


**Figure 5- Epigenetic development of cancer**. An epigenetic mutation in a progenitor cell is transmitted to the progeny which further accumulate additional epigenetic alterations that promote carcinogenesis. From Feinberg et al., 2006.

## 2. Breast Cancer

### 2.1. Structure of the normal breast tissue

The human mammary gland (Figure 6) undergoes a morphogenic transformation under puberty and originates a complex mature ductal tree that is enclosed by adipocytes, fibroblasts and endothelial cells that provide support and coordinate its development. The mammary duct presents a polarized layer of luminal epithelial cells surrounding the lumen that are responsible for milk production and an external layer of myoepithelial cells that provide contact with the basement membrane and are important for milk expulsion from the duct (Fu et al., 2019; Hansen & Bissell, 2000). Upon cancer development, the architecture of the human mammary gland is modified.
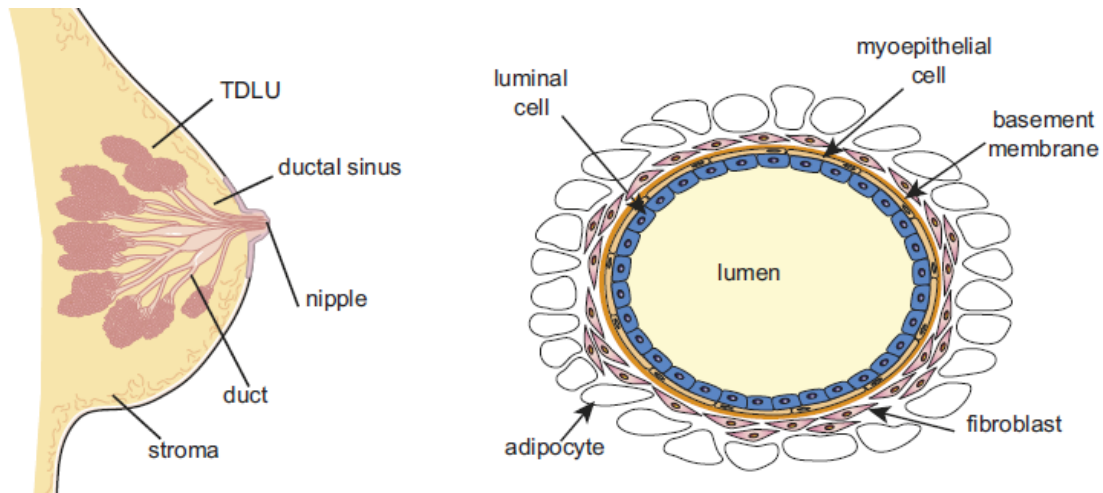
**Figure 6- Schematic representation of the human mammary gland tissue architecture**. Adapted from Fu et al., 2019.

## 2.2. Epidemiology and Risk Factors

The incidence of breast cancer has been increasing over the years due to several factors including an increase in average life expectancy and urbanization (Chen et al., 2017; Yip et al., 2008). Data from Globocan show that, in 2020, Portugal contributed to the statistics with more than 60 thousand new cases of breast cancer being the second most diagnosed type of cancer in our country with an incidence rate of 70.8% for both sexes and a mortality rate of 12.7%, which points breast cancer in the top 5 cancer types with higher mortality (WHO, 2021).

Looking at 2020 statistics for breast cancer in Portugal, the rise in breast cancer incidence correlates with an increase in average life expectancy. In addition, the majority of deaths were reported in women between 40 and 69 years old showing that aging is an important risk factor for breast cancer development (Sun et al., 2017; WHO, 2021). As breast cancer can be curable for many women when detected early, correctly diagnosed and submitted to appropriate treatments (Chen et al., 2017), screening programs were implemented. In Portugal, the Portuguese Association for Breast Cancer (Liga Portuguesa Contra o Cancro) took over this responsibility by encouraging mammography for women between 50 and 69 years old, every two years, assessed by two radiologists. In case of suspicion, women are referred to a hospital unit to perform ultrasounds that allows better visualization and diagnosis (Liga-Portuguesa-Contra-o-Cancro, 2021).

Family history is another important risk factor for breast cancer as women, whose mother or sister had a breast cancer, are more prone to develop this disease. Inheritable mutations in the BRCA 1 and 2 genes are well known genetic alterations that increase the susceptibility to develop breast cancer (Sun et al., 2017). In addition, "early menarche, late

menopause, late age at first pregnancy and low parity" are reproductive factors that contribute to increase the risk of developing breast cancer, as well as particular lifestyles including excessive alcohol intake or high levels of fat included in the diet. Although oral contraceptives are not described to potentiate the development of breast cancer, they constitute an external source of estrogen that, together with internal production from ovaries, may lead to higher levels of this hormone in the body, which is associated with a higher risk of developing breast cancer (Sun et al., 2017).

## 2.3. Breast cancer classification

Breast cancer is a very heterogeneous disease. This heterogeneity is observed between different individuals, referred to inter-tumour heterogeneity. Since heterogeneity is reflected in breast cancer diagnosis, prognosis and therapy response, it is important to have an uniformized organization of these subtypes (Malhotra et al., 2010; Turashvili & Brogi, 2017).

### 2.3.1. Histological classification

The histological classification of breast cancer is a simple and low-cost methodology, subdivided into two complementary analyses. The first evaluation classifies these cancers based on their histological type (*in situ* or invasive tumours) and grade (low- and high-grade tumours). *In situ* are non- or pre-invasive tumours that do not show infiltration, stromal invasion or diffusion below the basement membrane. When tumours acquire these capabilities, they are classified as invasive carcinomas. Low grade tumours are more alike normal breast tissue regarding their levels of tissue differentiation, which is indicative of a better prognosis. In opposite, high grade tumours display low levels of tissue differentiation. They have a worse prognosis and may require a more aggressive treatment (Ades et al., 2014; NIH, 2021). The histological classification of breast cancer can also be performed through a one-digit hierarchical code, an approach that stages tumours based on specific morphological or cytological patterns that are associated with clinical outcomes (NIH, 2021; Rakha et al., 2010; Weigelt et al., 2010).

### 2.3.2. Molecular classification

"Microarray-based gene expression analysis and unbiased hierarchical clustering" permitted to propose a molecular classification of breast cancer, which help to differentiate tumours in terms of treatment and prognosis. Although these molecular analyses allowed a better classification of each patient's tumour, these are high-price methodologies. For that reason, in clinical practice, only a panel of 50 genes (PAM50) are nowadays analysed, which allows to discriminate between five intrinsic molecular subtypes, defined as Luminal

A, Luminal B, HER2-positive, Claudin-Low and Triple-Negative (Table 1), based on the expression of the Estrogen Receptor (ER), Progesterone Receptor (PgR) and Human Epidermal Growth Factor 2 (HER2) (Malhotra et al., 2010).

| | Molecular markers | Histological grade | Prognosis |
|---|---|---|---|
| Luminal A | ER$^+$, PgR$^+$, HER2$^-$ | Low grade | Good |
| Luminal B | ER$^+$, PgR$^+$, HER2$^+$ | High grade | Poor |
| HER2 positive | ER$^-$, PgR$^-$, HER2$^+$ | High grade | Poor |
| Claudin-Low | ER$^-$, PgR$^-$, HER2$^-$ | High grade | Poor |
| Triple-negative | ER$^-$, PgR$^-$, HER2$^-$ | High grade | Poor |

**Table 1- Molecular classification of breast cancer**. This classification integrates the heterogeneity observed in breast cancer in five subtypes with different treatment approaches according to their differential expression of three molecular markers. From Malhotra et al., 2010.

Luminal breast cancer is the most common breast cancer subtype (Pandit et al., 2020) and can be classified into A and B. Both subtypes express ER and PgR but only luminal B tumours are positive for HER2 expression (Ades et al., 2014). Regarding their histological grade, luminal A tumours are described as low grade with a good prognosis while luminal B tumours display high grade characteristics associated with poor prognosis. Since both of these subtypes express ER, an hormonal or endocrine therapies can be used to block the ovarian production of estrogen or the activity of the ER in tumour cells (Drăgănescu & Carmocan, 2017).

HER2-positive are highly aggressive breast cancers representing 11 to 30% of all breast cancers and are characterized by one of the following: an overexpression of HER2 or an amplification of the HER2 gene. Given this, patients with this subtype of breast cancer benefit from therapies that block the activity of this overexpressed protein, which can include monoclonal antibodies, tyrosine kinase inhibitors or antibody-drug conjugates against HER2 (Schettini et al., 2020; Vernieri et al., 2019).

Claudin-Low breast cancer was later integrated in the molecular classification of breast tumours, constituting 1.5 to 14% of all breast cancers and is characterized by a low expression of genes involved in cell-cell adhesion but a higher expression of genes involved in Epithelial-to-Mesenchymal Transition (EMT) and stemness such as vimentin. These tumours lack expression of ER, PgR and HER2, which is reflected in their poor prognosis (Fougner et al., 2020; Malhotra et al., 2010; Prat et al., 2010).

Triple Negative Breast Cancer (TNBC) constitutes about 15 to 20% of all breast cancers. This subtype is more frequent in young and pre-menopausal African and African-American women and is strongly associated with increased parity, early stage of menarche and first full-term pregnancy before the age of 26. TNBCs are described by the absence of

expression of ER, PgR and HER2 overexpression, high aggressiveness and poor prognosis. In addition, they are characterized by the expression of basal-localized markers such as structural proteins (basal cytokeratins - CK, vimentin, fascin, nestin, moesin and Epidermal Growth Factor Receptor - EGFR), cell adhesion molecules (osteonectin, osteopontin, laminins, α6β4 integrin, P-cadherin, CD44, CD280, c-Met and CD146) and of transcription factors (c-Myc, Sox2, FOXC1/2, E2F-5, YB-1, p-JNK, p63 and p53), which are candidate biomarkers for this aggressive subtype of breast cancer (Alluri & Newman, 2014; Choo & Nielsen, 2010; Toft & Cryns, 2011; Yadav et al., 2015).

## 2.4. Triple-Negative Breast Cancer: the kiss of death

Contrarily to other breast cancer subtypes, TNBC does not have a targeted therapy which severely limits the treatment options that can be offered to these patients. Combinatorial chemotherapy is the standard neoadjuvant treatment to decrease tumour size following surgery. However, less than half of patients achieve pathological complete response. This is likely due to the heterogenous nature of TNBCs, not only between TNBC tumours (inter-tumour heterogeneity) but also within TNBC tumours (intra-tumour heterogeneity).

### 2.4.1. Inter-tumour heterogeneity

Although the TNBC subgroup is considered a single entity based on immunohistochemistry (IHC) and histopathological studies, molecular profiling has revealed an unexpected level of heterogeneity between TNBCs with up to 10 distinct subtypes. Among those, the basal-like subtype accounts 50 to 75% of cases. They are characterized by the expression of genes identifying normal basal and myoepithelial cells. In addition, a large majority of TNBCs carry mutations in the BRCA1 gene or have a defective DNA repair. Those can belong to the basal-like subgroup or to other subgroups. Thus, TNBC appears to comprise different disease entities, that urgently need to be stratified in order to identify relevant molecular targets for distinct TNBCs and develop novel therapies targeting specifically each of these diseases (Garrido-Castro et al., 2019; Lee & Muller, 2010; Marra et al., 2020; Toft & Cryns, 2011; Yin et al., 2020).

### 2.4.2. Intra-tumour heterogeneity

In addition, a patient's primary tumour and individual metastases can display enormous diversity of tumour cell populations. These cells can display differences in their genetic profiles, epigenome/transcriptome and proteome signatures, migration and invasion capabilities, proliferation, stemness and intrinsic cell plasticity. This intrinsic cell heterogeneity could be caused by clonal selection of individual cancer cells with distinct

genetic and/or epigenetic alterations (da Silva-Diz et al., 2018). In addition, a sub-population of multipotent cancer cells, defined as Cancer Stem-like cells (CSCs) or tumour-initiating cells, could give rise to all cell types that constitute a tumour, originating a "phenotypic copy of the original tumour". Although the exact location of these cells is not known, they appear to represent a very low percentage of cells constituting the tumour. This small subpopulation of cells was first described in the 1990's in human acute leukaemia and then identified by many other researchers in solid tumours, including breast cancer (Nassar & Blanpain, 2016; Toh et al., 2017). These cells are characterized for their self-renewal capability: they can divide asymmetrically, originating a daughter cell that maintain a self-renew ability, as well as a daughter cell that differentiate into a neoplastic cell (Atashzar et al., 2020; Pattabiraman & Weinberg, 2014; Toh et al., 2017; Toledo-Guzmán et al., 2018). Conversely, in some tumours and in cancer cell lines, non-CSCs can convert into CSCs under certain conditions (Visvader & Lindeman, 2012), indicating that CSCs and non-CSCs do not exist in static states but instead are highly plastic, being able to interconvert into one another state.

While non-CSCs are efficiently eliminated by currently available chemotherapeutic treatment, CSCs appear to have a low sensitivity to these treatment options. These small CSC cell populations that are capable to survive treatment have been proposed to reconstitute the tumour of origin, driving tumour recurrence (Figure 7) (Nassar & Blanpain, 2016).
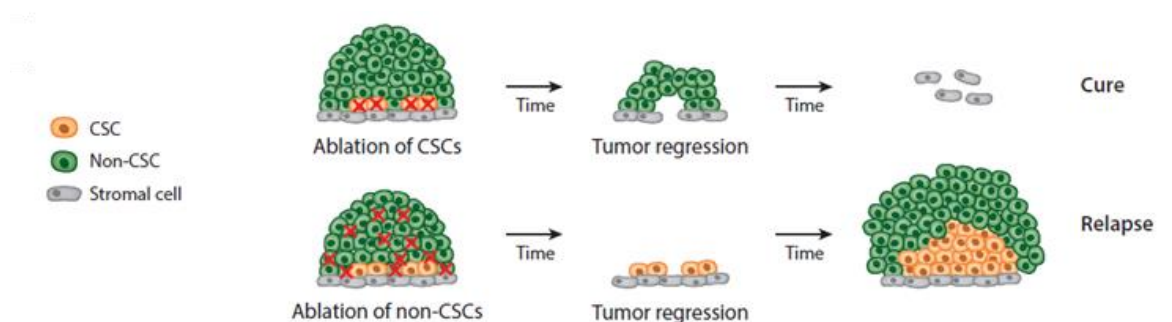


**Figure 7- Therapeutic effect on non and CSCs.** Only non-CSCs are eliminated in response to standard therapeutic options. Following treatment, remaining CSCs have the ability to drive tumour growth ultimately inducing relapse. From Nassar & Blanpain, 2016.

It is currently accepted that failure to eradicate this sub-population of cells severely limits the ultimate effectiveness of many current cancer therapies (Rossi et al., 2020). Thus, CSCs are considered critical targets for an important new generation of strategies to overcome cancer. However, little is known on the molecular pathways driving CSC phenotypes. They express characteristic proteins which constitute markers for their identification. Higher expression of the receptor for hyaluronic acid (CD44) and loss of expression of the heat-stable antigen (CD24) are the most reported breast CSC markers in the literature. They are transmembrane proteins that bind to the ExtraCellular Matrix (ECM) and regulate cell

adhesion. Aldehyde dehydrogenase 1 (ALDH1) has also been proposed as a breast CSC marker together with Prominin-1 (CD133), $\beta$1-integrin (CD29), $\alpha$6-integrin (CD49f) and $\beta$3-integrin (CD61). Yet, there is no consensus for CSC markers, even within the same molecular subtype. Moreover, the same tumour can harbour distinct populations of CSCs (Schmitt et al., 2012).

## 3. Cell Adhesion Molecules

Many of the stemness markers commonly used to identify populations of CSCs are actually Cell Adhesion Molecules (CAMs) (Farahani et al., 2014). CAMs are transmembrane proteins that are intimately linked to the actin cytoskeleton and play a crucial role in mediating cell-to-cell and cell-to-ECM anchoring and in functioning as transmitters of extracellular cues inside the cell (Samanta & Almo, 2015).

CAMs are classified in four main subtypes (integrins, selectins, immunoglobulin-like CAMs and cadherins) according to their structural differences as well as their binding partners (Figure 8) (Harjunpää et al., 2019; Lewczuk et al., 2019; Samanta & Almo, 2015). Integrins are heterodimeric calcium-dependent transmembrane proteins that bind to components of the ECM through their glycoprotein receptors. The human genome contains 18 $\alpha$ and 8 $\beta$ integrins (Takada et al., 2007), which heterodimerize forming many combinations that regulate different types of signalling (Figure 8.A). Selectins are a family of lectins that recognize carbohydrates (glycoproteins and glycolipids) from the cell surface, therefore mediating cell-cell adhesion. They can be subdivided in P, E and L-selectins according to the cell types in which they were found (platelets, endothelial cells or leukocytes), their binding being responsible for the "initial stage of the rolling cell adhesion cascade" (Figure 8.B). Immunoglobulin (Ig)-like CAMs are characterized by the presence of a compact Ig-fold, playing a major role in numerous biological processes (Figure 8.C) (Francavilla et al., 2009; Harjunpää et al., 2019; Lewczuk et al., 2019; Samanta & Almo, 2015).

### 3.1. Cadherins classification

Cadherins, the most studied group of CAMs, are calcium ($Ca^{2+}$)-dependent single pass cell transmembrane proteins, which are responsible for intercellular cell-cell adhesion as well as maintenance of normal tissue's architecture, development of critical embryogenesis steps and the "maintenance of cell polarity, tissue integrity and homeostasis" in mature tissues. The mammalian genome translates more than 20 subtypes of cadherins, each of them being responsible for different functions. This group is subdivided in two main classes: classical and non-classical cadherins. Classical cadherins are epithelial (E-), placental (P-) and neural (N-) cadherin, according to their specificity to each type of tissue. These

homophilic molecules interact with catenins through their cytoplasmic domain (Figure 8.D) and are also related to "specific junctional structures" denominated adherent junctions (AJ). These AJs are assembled through formation of a zipper-like conformation between cadherins, which is essential for the link between the actin cytoskeleton of adjacent cells (Francavilla et al., 2009; Harjunpää et al., 2019; Kaszak et al., 2020; Lewczuk et al., 2019; Samanta & Almo, 2015).

Despite the fact that classical cadherins are the most studied ones, mainly due to their link to carcinogenic development, cadherins also comprises non-classical cadherins, including desmossomal, atypical and protocadherins, which have several binding partners, perform different functions and present no homology to classical cadherins (Francavilla et al., 2009; Saito et al., 2012).
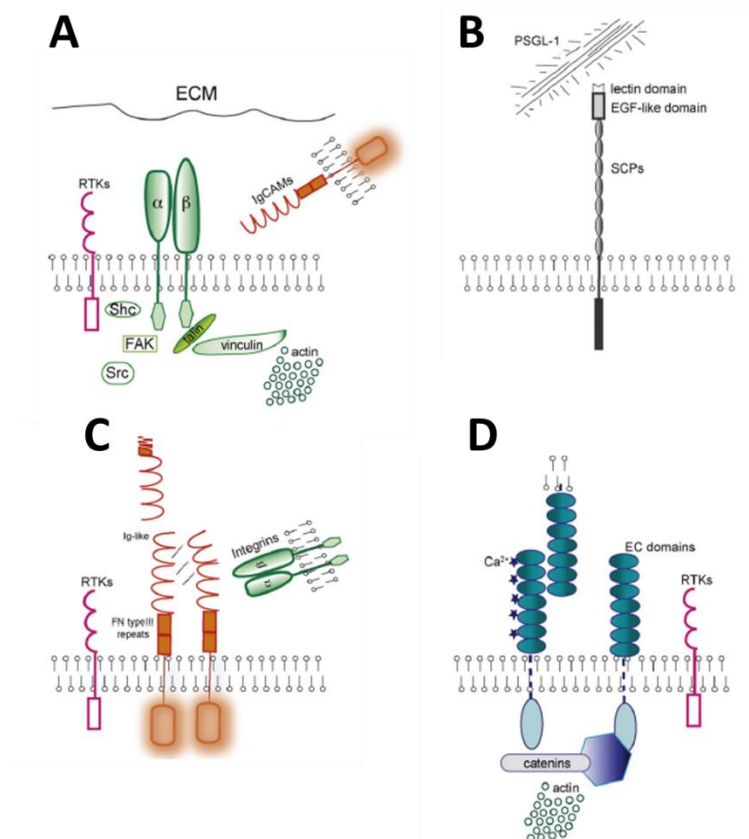


**Figure 8- Schematic representation of the domains that constitute (A) integrins, (B) selectins, (C) immunoglobulin-like CAMs and (D) cadherins**. Adapted from Francavilla et al., 2009.

### 3.2.    E-cadherin

E-cadherin (E-cad) was the first described cadherin in normal and pathological conditions that started with Takeichi in 1977. Later, when other cadherins were described, it received the designation E-cad from its epithelial localization (Takeichi, 1977; van Roy & Berx, 2008). This protein is encoded by the CDH1 gene, which encompasses a

transmembrane domain, a cytoplasmatic domain and an ectodomain (van Roy & Berx, 2008).

As a cadherin, E-cad mediates $Ca^{2+}$-dependent cell adhesion and the assembly of cell junctions mainly AJs (Mendonsa et al., 2018).

### 3.2.1. E-cadherin function in normal cells

E-cad function in normal cells starts from embryonic development as Fleming et al. have described its role in the adhesion of blastomeres and the compaction of early embryos (Fleming et al., 1992; Wong et al., 2018).

In normal epithelial cells, E-cad plays an important role in the assembly of AJs between two neighbouring cells. This cadherin binds to the armadillo domain of β-catenin, which interacts with the N-terminal domains of αE-catenin, originating the CCC complex. In turn, the vinculin homology domain 3 (VH3) of αE-catenin at the C-terminal end allows the interaction with the actin cytoskeleton, thus "mediating the organization and tethering of actin filaments at the zones of E-cad mediated cell-cell contact" (Mendonsa et al., 2018; Rimm et al., 1995; van Roy & Berx, 2008; Wong et al., 2018). E-cad has an important adhesive function, being responsible for holding the cell together, allowing its anchorage and interaction with other cells and promoting contact inhibition of proliferation (Knudsen & Wheelock, 2005). In the mammary tissue, E-cad is expressed in the luminal epithelial layer facing the lumen, where it is required for differentiation, cell survival, epithelial architecture and milk production (Knudsen & Wheelock, 2005).

### 3.2.2. E-cadherin function in breast cancer

Because E-cad plays a major role in the adhesion between epithelial cells, its loss has been described to be associated with the induction of EMT, characterized by the loss of cell-cell adhesions and polarity and the acquisition of a mesenchymal phenotype promoting cancer cell migration and invasion into distant tissues. In addition, loss of E-cad or disruption of the E-cad-β-catenin complex, for example through phosphorylation, leads to the translocation of β-catenin to the cytoplasm where it activates several signalling pathways, promoting cancer development. Accordingly, E-cad loss has been associated with patient poor survival, not only in breast cancer (Horne et al., 2018) but also in other types of cancer as gastric (Xing et al., 2013) and colon cancers (Jie et al., 2013) (Baranwal & Alahari, 2009; Horne et al., 2018; Wong et al., 2018).

In this context, E-cad act as a tumour suppressor. Consequently, breast cancer cells that do not express E-cad develop malignancy (Baranwal & Alahari, 2009; Horne et al., 2018). Studies performed by Mbalaviele et al. have shown that re-expressing E-cad in

breast cancer cells prevented the formation of bone metastasis by circulating breast cancer cells, which reassures its role as a tumour suppressor (Mbalaviele et al., 1996; Mendonsa et al., 2018).

Loss of E-cad can be a consequence of genetic and/or epigenetic alterations, including mutations in the coding sequence of the CDH1 gene and loss of heterozygosity (Wong et al., 2018). Some therapeutic approaches have been developed to target this prognostic marker and ultimately prevent tumourigenic development, such as α-solanine, which induces E-cad expression playing a major role in blocking EMT and metastatic process (Bruner & Derksen, 2018; David & Rajasekaran, 2012; Kaszak et al., 2020).

Although E-cad's role as a tumour suppressor has been well established, recent studies provide evidences that E-cad may also have a promoting role in tumour progression. Thus, E-cad has been shown to support intravasation and tumour cell survival in inflammatory breast carcinoma. Accordingly, most breast ductal carcinomas consistently express E-cad both in the primary tumour and in metastatic cells (Rodriguez et al., 2012).

### 3.3. P-cadherin

The classical cell adhesion molecule P-cadherin (P-cad) "was the third classical cadherin to be identified", being described for the first time by Nose and Takeichi in 1986, in developing mouse embryos, where they observed that this $Ca^{2+}$-dependent protein "plays a role in the implantation and morphogenesis of embryos by providing cells with heterogenous adhesive specificity" (Nose & Takeichi, 1986; Paredes et al., 2007).

Although P-cad shares above 67% homology with E-cad, it is poorly characterized. The CDH3 gene, which encodes for P-cad is shaped by 16 exons (Figure 9). The mature P-cad protein, composed of an extracellular, a transmembrane and an intercellular domain, allows interaction between cells through the formation of zipper-like structures (Albergaria et al., 2011).
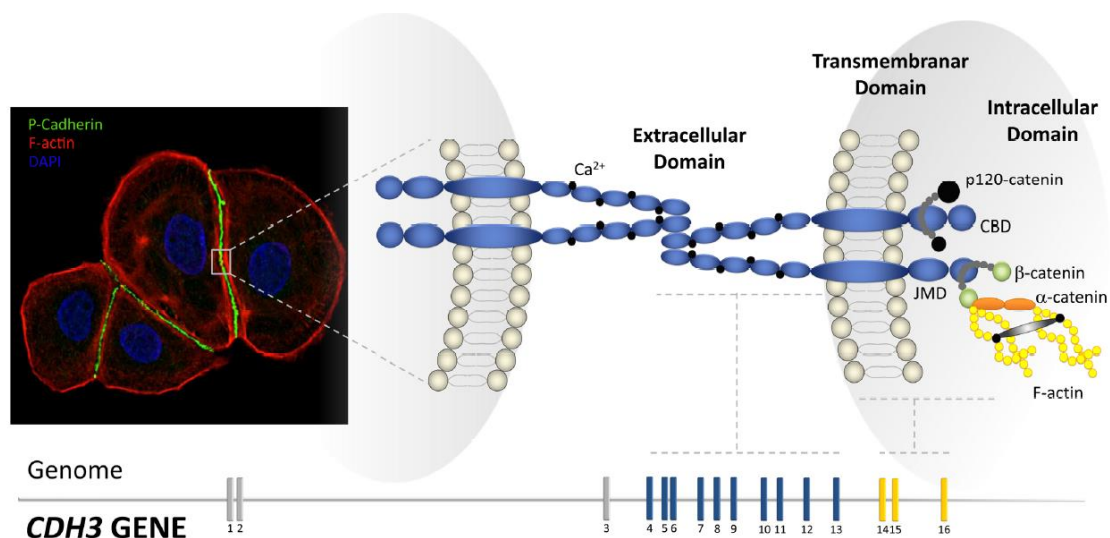
**Figure 9- Schematic representation of P-cad domains**. P-cad, codified by CDH3 gene, is required to establish cell-cell contact through the interaction of several intra and extracellular domains. From Albergaria et al., 2011.

P-cad is mainly localized in the basal myoepithelial layer of the human mammary gland, where this protein promotes cell-cell adhesion. In normal cells, P-cad is partially co-localized with E-cad (Paredes et al., 2007; Paredes et al., 2012; Vieira & Paredes, 2015).

### 3.3.1. P-cadherin function in normal cells

Like other cadherins, P-cad functional effect requires the formation of a cadherin-catenin complex, which is critical for the connection with the actin cytoskeleton and the maintenance of the structural integrity of epithelial tissues (Albergaria et al., 2011).

As just mentioned, P-cad plays an important role in tissues development, mainly in the development of the mammary gland (Albergaria et al., 2011; Paredes et al., 2007). To determine its function, scientists have performed over the years inactivation studies using mice models which led to the discover that P-cad plays an important role in normal mammopoiesis: the normal development of the mammary gland, where it is required to prevent precocious mammary gland differentiation and to reduce the risk of developing pre-neoplastic lesions. Furthermore, this protein also maintains an "undifferentiated state of the normal mammary gland" by preventing the growth of mature luminal epithelial cells, which suggests that this protein can identify cells with stemness properties and plays a role in promoting a stemness phenotype. Other authors have come up to the conclusion that the expression of this $Ca^{2+}$-dependent molecule is critical for the "maintenance of normal breast epithelial architecture" since it prevents mammary epithelial cells migration (Vieira & Paredes, 2015). All these functions have been associated to full length P-cad associated to the cellular membrane. In addition, P-cad ectodomain can also be cleaved to give rise to a

soluble form found in human breast milk (Vieira & Paredes, 2015), although the role of this processed P-cad form in normal breast tissues is not yet fully understood.

### 3.3.2. P-cadherin function in cancer

Depending on the context, P-cad acts either as a tumour suppressor or as an oncogene. In some tumours, like non-small cell lung cancer or melanoma, P-cad has been described as a tumour suppressor, as re-expressing P-cad in cellular models of melanoma or of lung carcinoma promotes the re-assembly of cell-cell contacts and prevents invasion *in vivo*. In contrast, in other tumours, like, among others, gastric, endometrial, colorectal and breast cancers, P-cad has been described to act as an oncogene, since its over-expression in these tumours correlates with invasion and higher aggressiveness and, therefore, patient's poorer survival (Paredes et al., 2007; Vieira & Paredes, 2015).

Immunohistochemistry studies have shown that P-cad is aberrantly expressed in around 30% of human breast carcinomas (Paredes et al., 2007), being aberrantly overexpressed in the earliest stages of cancer development (Hardy et al., 2002; Vieira & Paredes, 2015). Consistent with this finding, Joana Paredes lab has shown that P-cad overexpression is associated with higher histological grade tumours, being highly enriched in basal-like TNBC, independently from tumour size, lymph node metastasis and angiogenesis (Paredes et al., 2005; Paredes et al., 2007; Paredes et al., 2002; Paredes et al., 2004). The aberrant expression of this protein is significantly associated to a worse disease-free and overall patient survival (Paredes et al., 2007; Peralta Soler et al., 1999). Thus, P-cad constitutes a molecular marker for these highly aggressive subtypes of breast cancers.

P-cadherin overexpression has been shown to promote *in vivo* cell migration, invasion and self-renewal potential, as well as tumourigenic and metastatic capacity in *in vivo* breast cancer models (Ribeiro et al., 2010; Ribeiro et al., 2013; Vieira et al., 2014). Vieira et al. have shown that in breast cancer cells, P-cad overexpression is directly correlated with the expression of stem cell markers, including CD44, CD49f and aldehyde dehydrogenase, and that expressing P-cad in the luminal breast cancer cell line MCF7 increases *in vitro* mammospheres-forming efficiency and capacity to grow colonies in three-dimensional cultures. Conversely, knocking down P-cad in the basal-like breast cancer cell line BT-20 has the opposite effect (Vieira & Paredes, 2015; Vieira et al., 2014; Vieira et al., 2012). In addition, P-cad promotes cell motility, cell migration, as well as invasion capacity through Matrigel in breast cancer (Ribeiro et al., 2010).

Because P-cad appears a critical player of the aggressiveness of Basal-Like Breast Cancer (BLBC), it has received a lot of attention over the years, with the main goal of trying

to understand which signalling pathways activated by P-cad can possibly explain the acquisition of malignant phenotypes and the development of breast cancer stemness phenotypes. Ribeiro et al have reported that, to induce breast cancer cell invasion and tumourigenicity, P-cad requires the co-expression of E-cad. In these cells, P-cad disrupts the complex between E-cad and catenins, inhibiting E-cad's tumours suppressor function. These observations also open the possibility that P-cad converts the tumour suppressor function of E-cad into a tumour promoting one (Ribeiro et al., 2013). Consistent with these observations, tumours that present a simultaneous overexpression of P- and E-cad harbour a poorer prognosis (Peralta Soler et al., 1999).

In addition, the Paredes' lab has shown that P-cad modulates the expression of α6β4 integrins, which promote the acquisition of stemness properties downstream of P-cad (Vieira et al., 2014). In addition, P-cad overexpression increases *in vivo* tumourigenic ability, as well as *in vitro* cell invasion, by activating Src family kinase (SFK) signalling (Ribeiro et al., 2018). Src might also be critical for P-cad to affect cell morphology and the actin-myosin network, as inhibition of SFK signalling, using Dasatinib, revealed that P-cad induces a decrease in cell-cell adhesion and cell stiffness (Ribeiro et al., 2016). According to a role of P-cad in controlling the actin cytoskeleton, in breast carcinomas that co-express P- and E-cad, p120-catenin (p120ctn) is lost at the cell membrane and accumulates in the cytoplasm, which once in the cytoplasm has been shown to activate Rho-GTPases, altering actin cytoskeleton polymerization and promoting cell motility (Cheung et al., 2010; Ribeiro et al., 2013; Taniuchi et al., 2005).

However, we still do not have a complete picture of the molecular pathways that trigger tumourigenic capacity downstream of P-cad.

## 4. The actin cytoskeleton

The actin cytoskeleton is a multifunctional system that plays a major role in cell physiology, mediating various important cellular processes, such as controlling cell morphology, polarity, allowing cells movement and changes in cell shape (Blanchoin et al., 2014).

### 4.1. Actin cytoskeleton dynamics

Actin is one of the most abundant and highly conserved proteins in eukaryotes, which exists in a cell in two main forms: monomeric globular actin (G-actin), and polymeric filamentous actin (F-actin). Polymerization occurs predominantly by extension of the fast-growing barbed ends of the filaments, while filaments are disassembled by loss of

monomers from the slow-growing pointed ends. *In vitro*, actin polymerization can occur *de novo* through a thermodynamical process, starting from G-actin, which undergoes a nucleation step originating actin dimers and trimers (Figure 10). These trimers can rapidly elongate and originate actin filaments, an assembly process that occurs through ATP hydrolysis at a higher rate at the barbed end of the filament (Blanchoin et al., 2014).
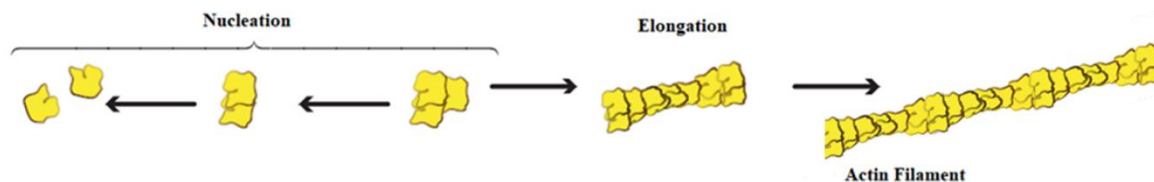


**Figure 10- Schematic representation of actin filament polymerization**. F-actin assembly is a process by which actin monomer (G-actin) are polymerized in actin filaments (F-actin) through hydrolysis of ATP. Adapted from Blanchoin et al., 2014.

F-actin occurs in many different forms: as cortical actin found in all cells, as bundled or branched assembles building up filopodia and lamellipodia, as thin filaments found in muscle sarcomeres, and many more. Each of these particular networks is likely to have specialized function within the cell. In cells, the assembly and disassembly of actin filaments, and also their organization into functional higher-order networks, is regulated by a plethora of actin-binding proteins (ABPs). Some ABPs link filaments to one another or to other organelles within the cell. Others, such as myosin motor, use actin filaments as tracks upon which to move vesicles and organelles. In addition, many regulate the proper cycle of polymerization and depolymerization of actin filaments. Actin nucleating factors control the rate, extent and spatial pattern of actin polymerization. The first described actin nucleator was the Arp2/3 complex, a complex of 7 proteins (Arp2, Arp3 and ArpC1-5) that interacts with actin filaments and allows the assembly of a branched actin network through the polymerization of daughter filaments from the side of an already existing filament, generating forces required for cell movement and cell shape changes. Unlike the Arp2/3 complex, all other known actin nucleators produce unbranched filaments. Formins allow the assembly of several structures as actin stress fibres through the high affinity binding of their FH2-domain to the barber ends of actin filaments. WH2 domain-containing actin nucleators, which includes Spire, allow elongation of free barbed ends through interaction of its tandem actin-monomer binding domains with the actin monomers (Blanchoin et al., 2014; Chesarone & Goode, 2009).

## 4.2. Role of the actin cytoskeleton in cancer

Actin and ABPs are involved in all stages of carcinogenesis. The actin cytoskeleton plays an important role in the EMT process and in the acquisition of motility capabilities by

cancer cells. These processes are triggered by chemotactic stimuli that promote the protrusion of several cells through the assembly of protrusive actin structures, including filopodia, lamellipodia and invadopodia, which are prerequisite for morphological alterations, migration and invasion to adjacent tissues of cancer cells (Yamaguchi & Condeelis, 2007).

The actin cytoskeleton is also a central contributor of the CSC and non-CSCs states. Studies in different cancers had demonstrated that reducing actin-myosin contractility, strongly promotes stem cell characteristics. Liu et al. have shown, using an inhibitor of Rho kinase, that dysregulation of the actin cytoskeleton is responsible for cells' stemness reprogramming (Liu et al., 2012; Ohata et al., 2012; Watanabe et al., 2007). Moreover, actin deregulation is a main transcriptional signature of human myeloma cell lines resistant to chemotherapeutic inhibitors against Histone deacetylase. Combinatory treatment with agents targeting the actin cytoskeleton can overcome this resistance (Mithraprabhu et al., 2014). Among ABPs involved, the bundling protein Fascin is a likely candidate, as it is involved in breast cancer chemotherapeutic resistance (Ghebeh et al., 2014).

One way by which the actin cytoskeleton can trigger the emergence of these cancer phenotype is by controlling the activity of signalling pathways, including Ras-MAPK, PI3K, NF-kB and the Hippo signalling pathways (Kustermans et al., 2008). The canonical Hippo pathway consists of the MST (sterile 20-like kinase) kinases, which activate the LATS1/2 (large tumour suppressor, Warts-) kinases through phosphorylation. In turn, LATS phosphorylates the transcriptional co-activators YAP and TAZ, thereby, limiting their nuclear import. In contrast, when the Hippo pathway is deactivated, YAP and TAZ translocate into the nucleus where they drive gene expression in complex with transcription factors, such as TEA-domain containing sequence specific transcription factors (TEAD), promoting the development of malignancy, including cell proliferation and survival, the acquisition of stemness properties and EMT as well as cancer cells' resistance to treatment (Plouffe et al., 2016; Shreberk-Shaked & Oren, 2019; Zheng & Pan, 2019).

Several studies have demonstrated that alteration of actin dynamics has a strong impact on the activity of YAP/TAZ. For example, inducing F-actin accumulation promotes nuclear enrichment of YAP/TAZ. Conversely, treating cells with F-actin-disrupting agents causes retention of YAP/TAZ in the cytoplasm in many cellular contexts (Seo & Kim, 2018). Actin dysregulation has also been described as an activator of Wnt signalling pathway in human mammary cells, promoting cells proliferation and EMT (Xuan Zhang, 2017).

## 5. The MRTF-SRF signalling pathway

## 5.1. Regulation of MRTF by actin

Actin is also a major regulator of the localization and activity of Myocardin-Related Transcription Factors (MRTFs) (Figure 11). This family of co-transcription factors include three members: myocardin is expressed in cardiac smooth muscle cells, MRTF-A (also known as MKL1 or Megakaryocytic Acute Leukaemia – MAL) is the most ubiquitously expressed in mammals and MRTF-B. MRTFs contain, in their N-terminal region, RPEL (arginine-proline-glutamine-leucine consensus sequence containing) motifs, that include two or three actin-binding motifs, which are critical for the interaction with G-actin monomers, overlapping with a nuclear localization signal (Gasparics & Sebe, 2018; Gau & Roy, 2018; Posern & Treisman, 2006). The B region contains a Nuclear Localization Signal (NLS) and is therefore important for its accumulation in the nucleus. In contrast, the Q region is required to promote the nuclear export of MRTFs into the cytoplasm and the binding to the transcription factor Serum Response Factor (SRF). All the members of this family also contain an SAP domain: a putative DNA binding domain found in other nuclear proteins, which allows MRTFs to transcribe gene expression independently of SRF, as well as a Leucine zipper domain and a transactivation domain (TAD) (Gasparics & Sebe, 2018; Pipes et al., 2006; Wang et al., 2001).

While myocardin is exclusively localized in the nucleus due to divergent RPEL motifs that have a lower affinity for actin, the cytoplasm-nuclear shuttling of MRTF-A and B is tightly controlled by actin. In resting conditions, G-actin binds to the MRTF RPEL motifs, which occludes the NLS, preventing its recognition by the importin-α/β heterodimer and thus blocking nuclear import of MRTF-A. In the presence of mitogenic signals or mechanical stimuli, activation of Rho-GTPase promotes actin polymerization, which reduces the pool of G-actin in the cells. This allows MRTF dissociation from G-actin, the access of the NLS by the importin-α/β heterodimer, which will translocate MRTF-A to the nucleus (Figure 12) (Gasparics & Sebe, 2018; Gau & Roy, 2018; Sidorenko & Vartiainen, 2019).

Besides MRTF-A regulation by cytoplasmic actin pools, nuclear actin also plays a key role in the regulation of this co-transcription factor. Although MRTF-A translocation to the nucleus is required for MRTF-A-dependent SRF transcriptional activity, it was shown that it is not sufficient. Indeed, nuclear actin plays a major role in this process since MRTF-A needs to be free in the nucleus to promote SRF transcriptional activity as actin-monomer binding inhibits this process under a mechanism that is not yet well understood (Sidorenko & Vartiainen, 2019).
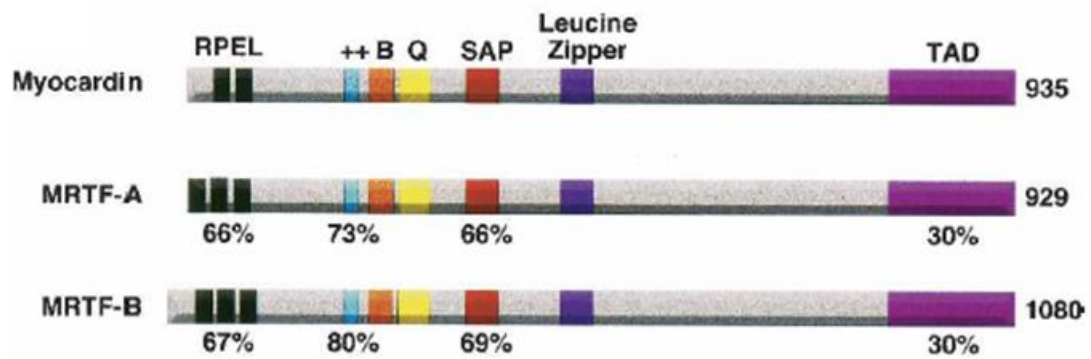


**Figure 11- Schematic representation of the structural domains of MRTF family members, whose function is referred in the main text**. From Pipes et al., 2006
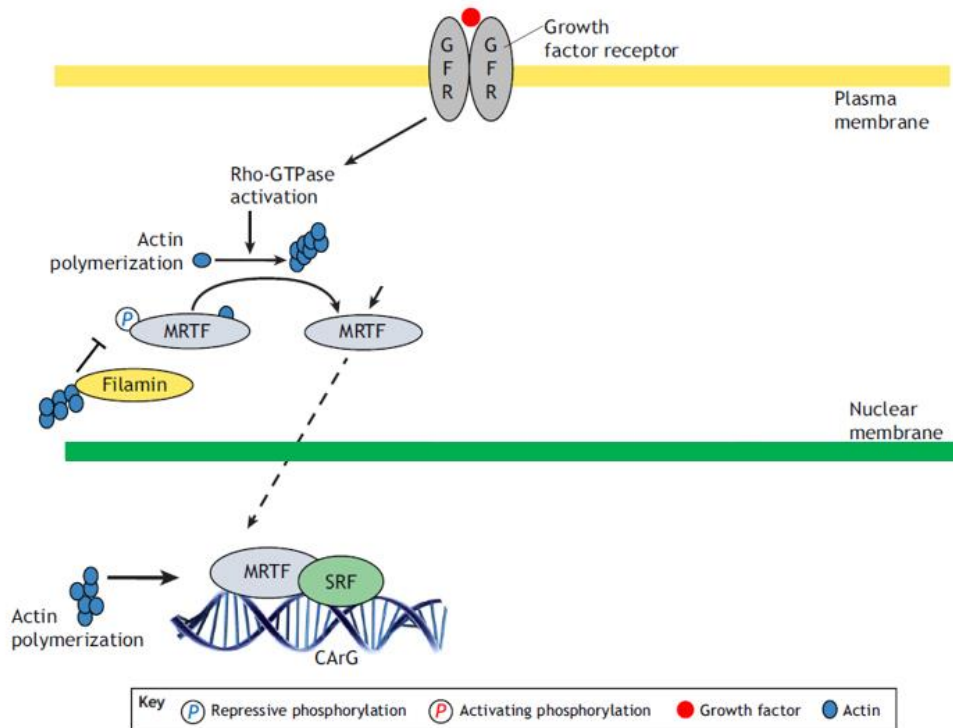
**Figure 12- Schematic representation of the MRTF/SRF signalling pathway**. MRTF activity is promoted by a decrease in the concentration of actin monomers in the cytoplasm which trap this co-transcription factor. Binding of growth factors to their corresponding receptors leads to Rho-GTPase activation and nuclear translocation of MRTF, which binds to SRF and induces the expression of SRF target genes. Conversely, an increase in the concentration of actin monomers traps MRTF in the cytoplasm blocking its activity. Adapted from Gau & Roy, 2018.

MRTF can also interact with YAP, a downstream effector of the Hippo pathway. This interaction allows MRTF to recruit the NcoA3 transcriptional activator to the YAP/TAZ-TEAD transcriptional complex and potentiate its transcriptional activity, promoting invasion and metastasis (Kim et al., 2017).

In addition, MRTF can act independent of SRF and bind directly to DNA. Asparuhova et al. were the first to describe that MRTF-A can act independent of SRF through its SAP domain, which binds to DNA and induce transcriptional activity independent of SRF (Asparuhova et al., 2011).

## 5.2. Role of MRTF-A in cancer

MRTF-A is a well described promotor of malignant progression as inducer of tumour cell invasion and metastization in many types of cancers, including breast cancer, where its overexpression is responsible for cell growth and ultimate patient poor survival (Medjkane et al., 2009; Seifert & Posern, 2017). Medjkane et al. have shown that MRTF-A depletion

reduces cell motility, indicating a key role of MRTF-A in promoting breast cancer cells invasion (Medjkane et al., 2009). The role of MRTF-A in cancer cell migration can be exerted through the SRF (Medjkane et al., 2009) or the YAP/TAZ-TEAD transcription factors (Kim et al., 2017). MRTF-A can also induce a stemness phenotype through interaction with SRF (Ikeda et al., 2018) or YAP/TAZ-TEAD (Plouffe et al., 2016; Shreberk-Shaked & Oren, 2019; Zheng & Pan, 2019). In addition to cell migration and stemness abilities, MRTF-A also promotes cell proliferation independently of its interaction with transcription factors through direct binding to DNA through its SAP domain (Gurbuz et al., 2014). Taken together, these observations demonstrate the importance of MRTF-A regulation by actin dynamics in the development of malignant phenotypes.

## 6. The MRTF/SRF could be a downstream P-cad effector in breast cancer cells

### 6.1. A humanized *Drosophila* model identified MRTF/SRF as a downstream P-cad effector

In order to investigate possible molecular pathways downstream of P-cad that could be responsible for the acquisition of tumourigenic phenotypes, the Janody's group, in collaboration with Eurico Morais de Sá's team, has generated a transgenic *Drosophila melanogaster* model carrying human P-cad inducible with the Gal4-UAS system that allows to temporal and spatial control P-cad expression during fly development.

When induced in GFP-expressing clones of cells from the follicle epithelium, human P-cad co-localizes with the fly E-cad (DE-cad) apically, concentrating specifically at the cellular membranes juxtaposed to other P-cad expressing cells (Figure 13 – upper panels). Cross section through the wing disc epithelium shows that P-cad also accumulated apically with DE-cad when expressed with the *nubbin*-Gal4 (*nub*-Gal4) driver (Figure 13 – bottom pannels). Thus, human P-cad is also able to establish *trans* junctional homophilic interactions in the fly epithelia.
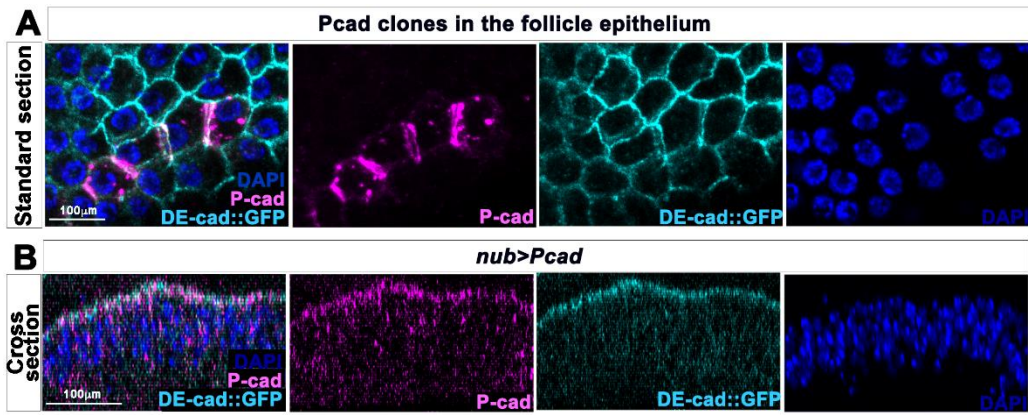
**Figure 13- Human P-cad co-localizes with *Drosophila* (D) E-cad in *Drosophila* epithelia.** (A) Standard confocal sections (top panels) or (B) cross sections (bottom panels) of third instar wing imaginal discs carrying a GFP knock in into the DE-cad locus (cyan) and expressing P-cad under *nub*-Gal4 control and stained with P-cad (magenta) and DAPI (blue). Scale bars = 100μm.

Moreover, P-cad shows similar genetic interactions with DE-cad in the wing disc primordium as those reported with human E-cad in cancer cells. In human and wing disc cells, P-cad can compensate for the loss of E-cad or DE-cad, respectively (Bazellières et al., 2015; Ribeiro et al., 2013 and data not shown). Conversely, E-cad or DE-cad are required for P-cad-induced tumour growth (Ribeiro et al., 2013) or wing differentiation defects (Figure 14.A), respectively.

Also, the Paredes' lab has demonstrated that P-cad requires α6β4-integrin and the Src oncogene to maintain a CSC phenotype (Ribeiro et al., 2018; Vieira et al., 2014). Similarly, our group has shown that knocking-down *Drosophila* Src or the integrin αPS2 supresses the P-cad wing phenotype (Figure 14.B).
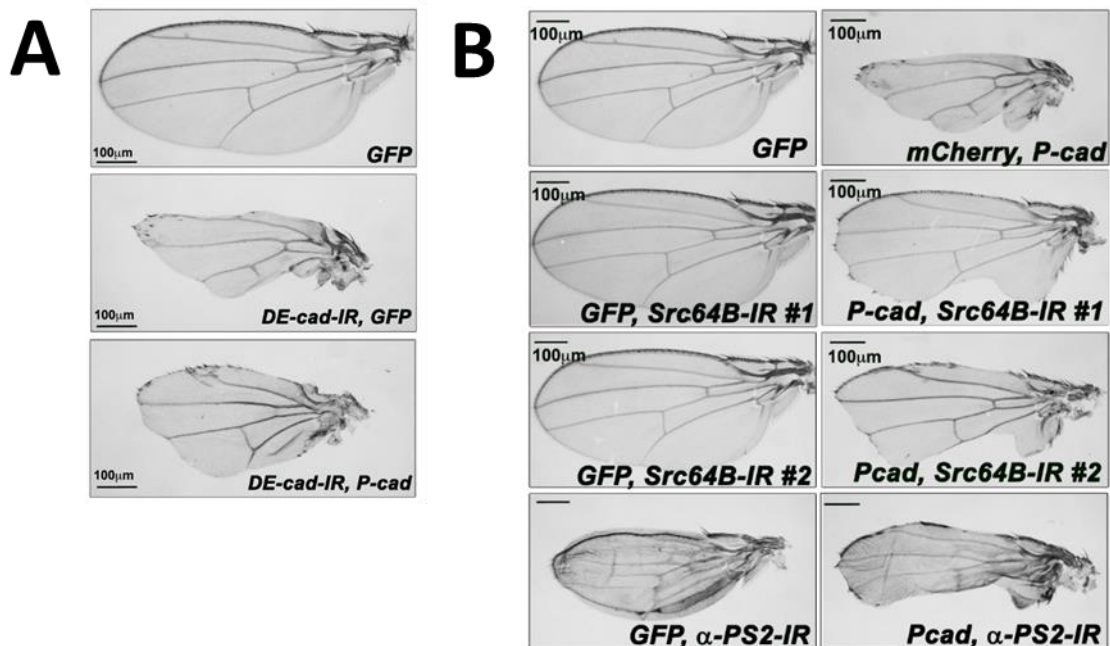


**Figure 14- Human P-cad requires DE-cad, Src and αPS2 to affect wing development.** (A) Adult wings in which *nub*-Gal4 drives UAS-*mCD8-GFP* (top panel) or UAS-*P-cad* and UAS-*mCherry*

(middle panel) or UAS-*DE-cad-IR* and UAS-*P-cad* (bottom panel). (B) Adult wings in which nub-Gal4 drives UAS-*mCD8-GFP* (top left panel) or UAS-*P-cad* and UAS-*mCherry* (top right panel) or UAS-*Src64B-IRJF03234* and UAS-*mCD8-GFP* (left second panel) or UAS-*Src64B-IRJF03234* and UAS-*P-cad* (right second panel) or UAS-*Src64B-IRHMC03327* and UAS-*mCD8-GFP* (left third panel) or UAS-*Src64B-IRHMC03327* and UAS-*P-cad* (right third panel) or UAS-*αPS2-IRJF02695* and UAS-*mCD8-GFP* (left bottom panel) or UAS-*αPS2-IRJF02695* and UAS-*P-cad* (right bottom panel). Scale bars = 100μm.

With these findings, our group has shown that human P-cad is functional in the *Drosophila* epithelia and that the consequences of overexpressing P-cad in the fly wing are reminiscent to the ones of overexpressing P-cad in breast cancer cells. So, it constitutes a good model to identify P-cad effectors that are relevant for the acquisition of a tumourigenic phenotype.

In a screen for suppressors of the P-cad wing phenotype, our group was able to identify components of the *Drosophila* MRTF/SRF signalling pathway. Knocking-down DMRTF or DSRF using RNA interference (IR), suppresses the P-cad-dependent wing phenotype (Figure 15.A), without affecting P-cad protein levels (Figure 15.B). Altogether, these results suggest that the MRTF-SRF pathway is a downstream effector of P-cad in the *Drosophila* model. However, a link between P-cad and the MRTF/SRF signalling pathway in breast carcinogenesis remains to be established.
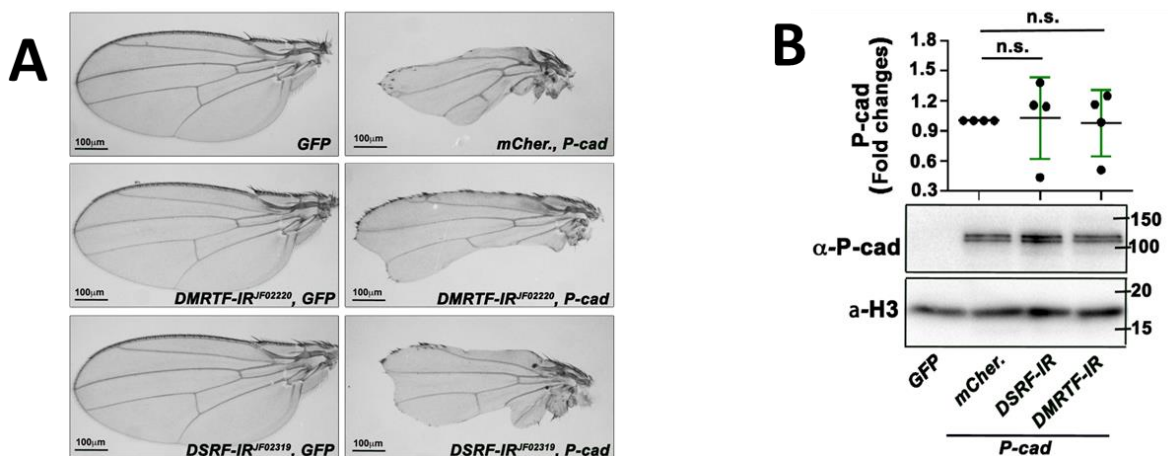


**Figure 15- P-cad expression of the fly wing epithelia promotes DMRTF and DSRF activity**. (A) adult wings in which *nub*-Gal4 drives UAS-*mCD8-GFP* (left top panel) or UAS-*P-cad* and UAS-*mCherry* (right top panel) or UAS-*DMRTF-IRJF02220* and UAS-*mCD8-GFP* (left second panel) or UAS-*DMRTF-IRJF02220* and UAS-*P-cad* (right second panel) or UAS-*DSRF-IRJF02319* and UAS-*mCD8-GFP* (left bottom panel) or UAS-*SRF-IRJF02319* and UAS-*P-cad* (right bottom panel). Scale bars = 100μm. (B) Western blots on protein extracts from wing imaginal discs expressing UAS-*mCD8-GFP* (lane 1) or UAS-*P-cad* and UAS-*mCherry* (lane 2) or UAS-*DMRTF-IRJF02220* and UAS-*P-cad* (lane 3) or UAS-*SRF-IRJF02319* and UAS-*P-cad* (lane 4) under *nub*-Gal4 control, blotted with

anti-P-cad and anti-Histone H3. Error bars indicate SD. n.s. indicates non-significant. Statistical significance was calculated using one-way ANOVA test.

## 6.2. P-cad expression and MRTF/SRF activity correlates in MCF10A-ER-Src cells

To validate the role of the MRTF/SRF activity downstream of P-cad, the Janody's group used a derivative of the MCF10A cell line established in 1990 by Soule et al. The MCF10A cell line is a spontaneously immortalized mammary epithelial cell line developed from culture of human fibrocystic mammary tissue in low calcium concentrations. These normal diploid cells lack tumourigenicity and anchorage-independent growth but depend on hormones and growth factors to maintain characteristics of a normal breast epithelium (Soule et al., 1990). This cell line can be cultured in monolayer, as well as three-dimensionally in matrigel (Debnath et al., 2003), which constitutes a great advantage to study tumour development. From this cell line, the laboratory of K. Struhl established the MCF10A-ER-Src cell line, which contains a fusion between the viral c-Src kinase orthologue and the ligand-binding domain of the ER, inducible with 4-OH-tamoxifen (TAM) treatment (Iliopoulos et al., 2009).

As represented in Figure 16, treatment of these cells with TAM leads to TAM association to the ER-binding domain, inducing Src activation. This results in a full morphological transformation within 36 hours, unlike MCF10A-ER-Src cells treated with the vehicle Ethanol (EtOH). Tavares et al. has shown that during the first 12 hours of TAM treatment, low levels of Src activity induces the transient assembly of actin stress fibres and the upregulation of the ABP Ena/VASP-like (EVL), which polarizes the actin stress fibres, leading to cell stiffening. In turn, cell stiffening triggers activation of Extracellular-signal Regulated Kinase (ERK), which upregulates Cyclin D1 to sustain cell proliferation. In addition, stress fibre-mediated cell stiffening potentiates Src activity and is absolutely required to induce malignant transformation (Tavares et al., 2017). Following this pre-malignant step, 24 hours after TAM treatment, MCF10A-ER-Src cells have disassembled their excessive stress fibres, become softer and have undergone EMT (Selvaggio et al., 2020; Tavares et al., 2017). Simultaneously, a sub-population of TAM-treated MCF10A-ER-Src cells have acquired CSCs characteristics, as defined by expression of the CD44 and CD24 markers, mammospheres formation and the ability to cause tumours in nude mice (Hirsch et al., 2009; Iliopoulos et al., 2009). Later on, 36 to 45 hours after TAM treatment, MCF10A-ER-Src cells acquire migrating and invading abilities (Tavares et al., 2017).
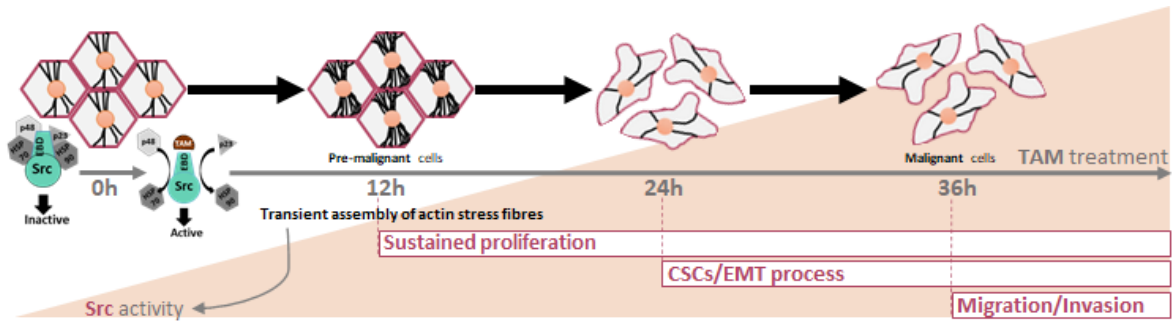
**Figure 16- Model by which MCF10A-ER-Src cells are transformed under TAM treatment within 36 hours.**

Using the MCF10A-ER-Src cell line, the Janody's group gathered preliminary data indicating that P-cad transiently accumulates in TAM-treated cells and that this transient effect is associated with the accumulation of F-actin stress fibres and an increase in MRTF/SRF signalling activity. Data from Figure 17.A show that TAM treatment leads to an increase of P-cad mRNA expression starting 2 hours after TAM treatment. P-cad expression is maintained significantly higher up to 12 hours after TAM treatment, before progressively decreasing 24 and 36 hours after TAM treatment. In addition, Fluorescent Activating Cell Sorting (FACS) of P-cad-positive cells indicates that a sub-population of cells is enriched in membrane-associated P-cad 6 hours after TAM treatment, when compared to EtOH-treated cells (Figure 17.B).
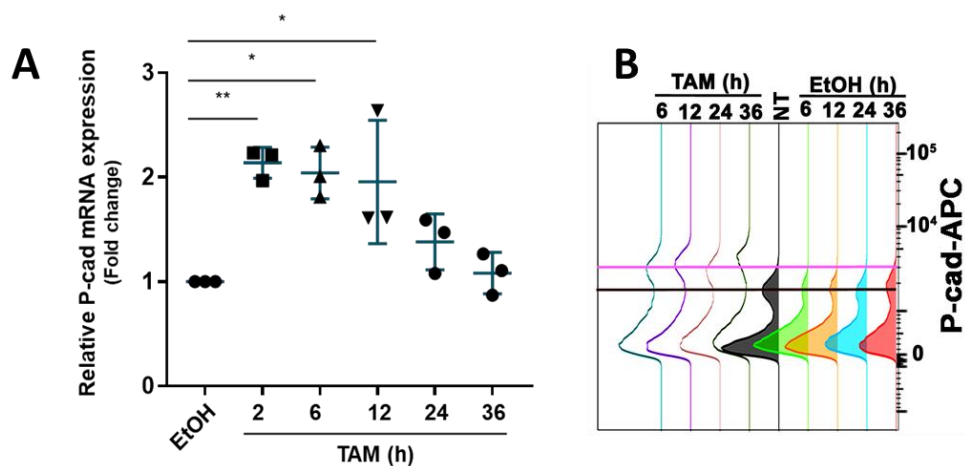


**Figure 17- TAM-treated MCF10A-ER-Src transiently up-regulate P-cad and accumulates P-cad at the cell membrane in a sub-population**. (A) Fold change quantification of P-cad mRNA levels between MCF10A-ER-Src cells treated with EtOH or TAM for 2, 6, 12, 24 and 36 hours. Error bars indicate standard deviation (SD). * indicates p-value<0.01. ** indicates p-value<0.001. Statistical significance was calculated using one-way ANOVA test. (B) Histogram of membrane-associated P-cad in MCF10A-ER-Src cells treated with EtOH or TAM for the same time points.

The transient accumulation of P-cad in TAM-treated MCF10A-ER-Src cells is associated with a transient increase in SRF transcriptional activity, as MCF10A-ER-Src cells transfected with an SRF luciferase reporter show a significant increase in luciferase activity

6 hours after TAM treatment, when compared to the ones treated with the vehicle EtOH (Figure 18.A). This increase in luciferase activity correlates with the significant accumulation of MRTF-A in the nucleus of MCF10A-ER-Src cells treated with TAM for 6 hours (Figure 18.B and C). Taken all together, these observations suggest that the transient accumulation of P-cad in TAM-treated MCF10A-ER-Src cells activates the actin/MRTF-A/SRF signalling pathway.
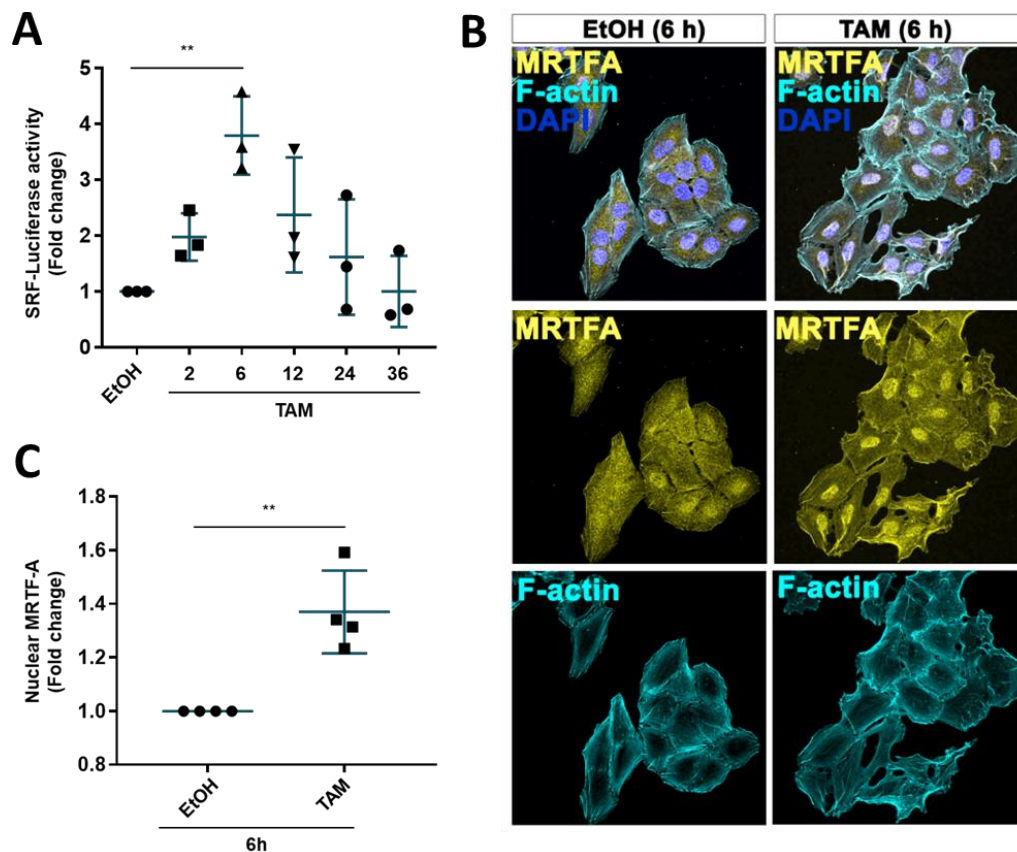


**Figure 18- MCF10A-ER-Src cells show a transient increase in SRF-Luciferase activity and accumulate MRTF-A in the nucleus 6 hours after TAM treatment**. (A) Fold change quantification of SRF-Luciferase activity in MCF10A-ER-Src cells transfected with a SRF Luciferase reporter treated with EtOH or TAM for 2, 6, 12, 24 and 36 hours. (B) Standard confocal sections of MCF10A-ER-Src cells treated with EtOH or TAM for 6 hours, stained with Phalloidin (cyan) to stain F-actin, anti-MRTF-A (magenta) and DAPI (blue). (C) Fold change quantification of nuclear MRTF-A in MCF10A-ER-Src cells treated with EtOH or TAM for 6 hours. Error bars indicate SD. ** indicates p-value<0.001. Statistical significance was calculated using unpaired t-test when comparing 2 conditions or one-way ANOVA test in case of multiple comparisons.

# CHAPTER II
# AIMS OF STUDY

This Master project was developed in the Cytoskeletal Regulation & Cancer group at i3S-Instituto de Investigação e Inovação em Saúde.

The work previously developed by Dr. Florence Janody's group using the *Drosophila* and the human MCF10A-ER-Src model led us to hypothesis that P-cad induces tumourigenicity through activation of the actin/MRTF-A/SRF signalling pathway in basal-like breast cancer cells.

In support of our hypothesis, Ribeiro et al. have shown that P-cad overexpression induces F-actin accumulation (Ribeiro et al., 2016). Moreover, alike P-cad, activation of the MRTF-A/SRF signalling pathway promotes breast cancer cell migration and invasion and the reacquisition of pluripotent phenotypes (Ikeda et al., 2018; Medjkane et al., 2009).

Therefore, the main aim of this project is to explore if P-cad induces tumourigenicity in basal-like breast cancer cells through activation of the actin/MRTF-A/SRF signalling pathway (Figure 19).

To achieve this goal, we asked two main questions:

1. <u>Does F-actin accumulation in TAM-treated MCF10A-ER-Src cells induces SRF transcriptional activity and cellular transformation?</u>

We analysed the effect of Latrunculin A (LatA) treatment, which binds G-actin, blocking their incorporation in filaments (Coué et al., 1987; Martin & Leder, 2001) on the ability of TAM-treated MCF10A-ER-Src cells to transiently activate the MRTF-A/SRF signalling pathway and to display features of cellular transformation. We also tested the possibility that, in turn, F-actin accumulation affect P-cad levels or localization.

2. <u>Does the transient activation of the MRTF-A/SRF signalling pathway in pre-malignant MCF10A-ER-Src cells promote cellular transformation?</u>

To address the role of the MRTF-A signalling pathway downstream of P-cad, we analysed the effect of blocking MRTF-A activity using the CCG-203971 inhibitor (Haak et al., 2017) on the ability of TAM-treated MCF10A-ER-Src cells to sustain proliferation in the absence of Epidermal Growth Factor (EGF), to grow mammospheres and to invade in collagen matrix.
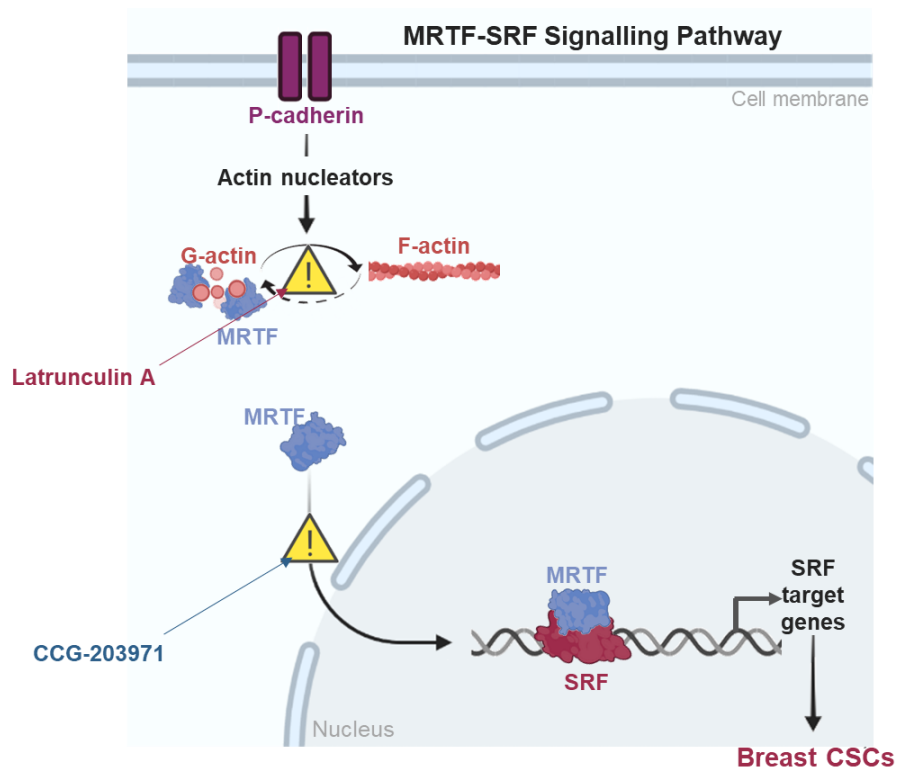
**Figure 19- Schematic of our hypothesis by which P-cad induces tumourigenicity through activation of the actin/MRTF-A/SRF signalling pathway in basal-like breast cancer cells**. To provide evidences sustaining this hypothesis, LatA was used to inhibit F-actin polymerization and CCG-203971 to inhibit the MRTF-A activity.

# CHAPTER III
# MATHERIALS AND METHODS

# 1. MCF10A-ER-Src cell line culture conditions

The MCF10A-ER-Src cell line was kindly provided by Kevin Struhl (Hirsch et al., 2009). Cells were cultured on standard tissue culture plastics in a 5% $CO_2$ humidified incubator at 37ºC in Complete Growth Media (CGM), composed of DMEM/F12 growth media (Alfagene, LTI11039-047), supplemented with 5% of Charcoal Stripped Horse Serum (CSHS), 20ng/mL human EGF (Peprotech, AF-100-15), 0.5µg/mL Hydrocortisone (Sigma, H0888), 100ng/mL Cholera toxin from Vibrio cholerae (Sigma, C8052), 10µg/mL Insulin (Sigma, I9278) and 0.5µg/mL Puromycin (Merck, 540411).

## 1.1. Horse Serum Charcoal Stripping

To decrease the level of estrogen and remove lipophilic materials as hormones and several growth factors that may impact on experiment's results, Horse Serum (Thermo Scientific, 16050-122) was inactivated for 30 min in a water bath at 56ºC with agitation, every 10 min and stripped twice with dextran-coated charcoal (Sigma, C6241-20G). After centrifugation at 200g and removal of all charcoal completely, CSHS was filtered using 0.2µm PES Filter system (VWR, 514-0332) and stored at -20ºC.

## 1.2. Cell subculture

When reaching 70% confluency, cell medium was removed from the flask and cells were washed with sterile Dulbecco's Phosphate Buffered Saline (PBS1X) (Biowest, L0615). Cells were then incubated with TrypLE™ Express (Alfagene, 12604-021) for 15 min in a 5% $CO_2$ humidified incubator at 37ºC to detach cells and washed with DMEM/F12 to stop the reaction. After centrifugation at 200g for 5 min, cells were resuspended in CGM and counted using 10µL of cell suspension in a Neubauer chamber. After determining cell density, cells were diluted in CGM to reduce confluency and the indicated number of cells per experiment was plated and left to adhere for 12 to 24 hours.

### 1.2.1. Cell Cryopreservation and defrosting

To establish stocks of cells maintained at -80ºC for later use, cell suspensions were centrifuged at 200g for 5 min and resuspended in freezing medium composed of 70% CGM, 20% CSHS and 10% Dimethyl sulfoxide (DMSO) (Sigma, D2650), at a final concentration of 750 000 cells per mL in Cryo-tubes (Starstedt, 72.379).

To culture cryopreserved cells, cryo-tubes were first quickly thawed in a 37ºC water bath and then resuspended in CGM. Cell suspensions were centrifuged at 200g for 5 min, supernatants were discarded, and cell pellets resuspended in CGM were plated in a plastic flask.

### 1.2.2. Drug treatments

To activate Src and induce transformation of the MCF10A-ER-Src cell line, cells were treated with 1µM 4-OH-TAM (Merck, H7904) for the indicated time. As a control, MCF10A-Er-Src cells were treated with the same volume of the vehicle EtOH for the same time.

To study the effects of inhibiting actin polymerization, MCF10A-ER-Src cells were treated with a final concentration of 0.5µM of Lat A (Labclinics, 10010630) for the indicated time.

To inhibit the MRTF-SRF signalling pathway, MCF10A-ER-Src cells were treated with a final concentration of 40µM of CCG-203971 (Merck, SML1422) for the indicated time.

### 2. Trypan-blue cell viability assay

To address the viability of MCF10A-ER-Src cells under treatment with LatA, 20 000 cells in 200µL of CGM were plated per well in a 96-well plate (Starstedt, 83.3924). 12 to 24 hours later, medium was removed, cells were washed with DMEM/F12 and incubated for 12, 24 or 36 hours with 0.5µM LatA or 1µM TAM+0.5µM LatA in cell culture medium restricted in supplements (DMEM/F12 growth medium supplemented with 0.5% CSHS, 0.5µg/mL hydrocortisone, 100ng/mL cholera toxin and 10µg/mL insulin). After treatment, medium was removed, cells were washed with PBS1X and detached from the plate using TrypLE$^{TM}$ Express for 15 min in a 5% $CO_2$ humidified incubator at 37ºC. After centrifugation at 200g for 5 min, cell pellets were resuspended in 20µL of cell culture medium restricted in supplements. For each condition, 5µL of cell suspension in the same volume of Trypan-Blue (Lonza, LONZ17-942E) were counted in a Neubauer chamber.

### 3. Immunofluorescence analysis

150 000 cells in 2mL of CGM were plated per well in a 6-well plate (Starstedt, 83.3920) containing 13mm coverslips of 1,5 thickness (VWR, 631-0150) previously coated with Poly-L-Lysine (Sigma, P78920) to facilitate cell adhesion.

After treatment, cells were washed with PBS$^{+/+}$ pH 7.2 (0.18% $CaCl_2$ and 0.05% $MgCl_2$ in PBS1X) and fixed with 25% Formaldehyde 16% Methanol-free (Sigma, 28908), 30% Piperazine-N,N'-bis(2-ethanesulfonic acid) (PIPES) 0.2M pH 6.8 (Sigma, P6757), 15% 4-(2-hydroxyethyl)-1-piperazineethanesulfonic acid) (HEPES) 0.2M pH 7 (Promega, H5302), 2% Ethylene glycol-bis(2-aminoethylether)-N,N,N',N' (EGTA) 0.5M pH 6,8 (Sigma, E3889), 0.4% $MgSO_4$ 1M and MiliQ water for 10 min at room-temperature (RT) followed by a wash with PBS1X.

Cells were then permeabilized with PBS-T (PBS1X supplemented with 0.1% Triton-X-100 (Sigma, T8787) for 2 min (note that, for P-cad staining, this step was not performed since P-cad is a protein localized at the membrane), followed by two washes with PBS1X. Cells were blocked for 1h at RT using a blocking buffer at pH 6.1, composed of 10mM MES pH 6.1 (Sigma, M8250), 150mM NaCl (Sigma, 31434), 5mM EGTA, pH 6.8, 5mM MgCl$_2$, 5mM Glucose (Alfagene, LTI41965-039), 2% Fetal Bovine Serum Premium heat-inactivated (Biowest, S008Y30304) and 1% Bovine Serum Albumin (BSA) (Sigma, A3294) in MiliQ water.

Primary antibody rabbit anti-Pcad (1:50 Cell signalling, 2130S) was incubated overnight at 4°C in blocking buffer. Coverslips were then washed twice with PBS1X and incubated with the secondary antibody Cy5-conjugated Donkey anti-rabbit (1:200 Jackson ImmunoResearch, 711-175-152) to detect P-cad together with Rhodamine-conjugated Phalloidin (Sigma, P1951) to detect F-actin in blocking buffer for 1 hour at RT. After two washes with PBS1X, cells were stained with DAPI (Sigma, D1377) for 10 min at RT, washed again with PBS1X and mounted in Vectashield (Baptista Marques, H-1000). Fluorescence images were acquired using a Leica SP5 confocal microscope using the 63X objective with immersion oil. Confocal microscope images were analysed using Fiji/Image J.

## 4. Western-blot

To obtain protein extracts for immunoblotting analysis, 150 000 cells in 2mL of CGM were plated per well in a 6-well plate. After treatment, cell pellets were resuspended in Lysis Buffer SDS-Free (50mM Tris(hydroxymethyl)aminomethane (Tris) pH 7.5 (VWR, 33621.260), 150mM NaCl, 1mM Ethylenediaminetetraacetic acid (EDTA) pH 8 (Sigma, E5134), 1mM EDTA pH 7 and 1% Triton (Sigma, T8787) in MiliQ water) containing 1% protease (Roche, 04693159001) and 1% phosphatase (Roche, 04906837001) inhibitors and incubated on ice for 30 min. Lysis products were centrifuged at 4°C for 30 min at 14 000 rpm and protein was quantified using the Bradford method. Laemmli Buffer 5X (2.88M Sodium Dodecil Sulfate (SDS) (L3771), 30mM Bromophenol blue (Sigma, 114405), 40mM Glycerol (Sigma, G5516), Tris pH 6.8 50mM and 1.2M Dithiothreitol (DTT) (NZYTech, MB03101) was added to a final concentration of 1X. Protein extracts were boiled for 5 min at 95°C and centrifuged for 10 min at 8 000 rpm. 30µg of protein were loaded in addition to the Precision Plus Kaleidoscope Standard molecular marker (Bio-rad, 1610395). Proteins were first stacked in a 5% SDS-PAGE gel (16.5% Acrylamide bis solution 30% (Bio-rad, #1610156), Tris pH 6.8 125mM, 0.1% SDS, 0.1% Amonium Persulphate (APS) (Sigma, A3678) and 0.1% N,N,N',N'-Tetramethyl-ethylenediamine (TEMED) (Sigma, T9281) for 15 min at 60V and then resolved in a 7% SDS-PAGE (23.9% Acrylamide 30%, Tris pH 8.8

375mM, 0.1% SDS, 0.1% APS and 0.1% TEMED) gel electrophoresis at 90V. Gels were then transferred on ice for 150 min using a constant amperage of 300mA to a 0.45μM PVDF blotting membrane (Amersham, 10600023), previously activated for 5 min in methanol. Membranes were then blocked with 5% milk in TBS-T (TBS with 0.1% Tween 20 (Sigma, P1379) and incubated overnight at 4ºC with the primary antibodies in 5% milk in TBS-T. On the next day, membranes were washed for 7 min four times with TBS-T and incubated 1 hour at RT with the secondary antibodies in 5% milk in TBS-T, followed by four washes of 7 min with TBS-T. Primary antibodies used were: mouse anti-P-cad (1:2500 BD, 610228), rabbit anti-p-Src (1:1000 Invitrogen, 44-6609), mouse anti-MRTF-A (1:1000 Santa Cruz, SC-390324) and mouse anti-HSC70 (1:8000 Santa Cruz, SC-7298), used as loading control. Secondary antibodies used were: HRP AP Donkey anti-mouse IgG (1:5000 Jackson Immunoresearch, 715-035-150) and HRP-conjugated AffiniPure Donkey anti-rabbit igG (1:5000 Jackson Immunoresearch, 711-035-152). Membranes were then exposed with 1:1 Immobilon Western Chemiluminescent HRP substrate (Milipore, P90719) and visualized at the ChemiDoc. Western-blot quantification was performed using Image Lab software.

## 4.1. Bradford protein quantification

Proteins were quantified using the Bradford method in a 96-well plate in duplicates with 1μL of sample added to 199μL of 1:5 Protein Dye Reagent Concentrate (Bradford reagent) (Bio-rad, #500-0006). To establish the calibration curve, BSA standards were analysed in duplicates. The plate was then incubated for 30 min at RT in the dark and the absorbances at 595nm wavelength were measured using Synergy Mx. BSA standards' absorbance was used to define a calibration curve and protein concentration was calculated.

## 5. Real-time PCR

## 5.1. RNA Extraction

To obtain samples for RNA extraction, 150 000 cells in 2mL of CGM were plated per well in a 6-well plate. After treatment, cell pellets were incubated with 40 mM Dithiothreitol (DTT) (NZYTech, MB03101) and RNAs were extracted using the NZY Total RNA Isolation Kit (NZYTech, MB013402) according to the manufacturer's instructions. mRNA concentrations were measured using Nanodrop. For cDNAs synthesis, 50ng/μL of Random Hexamers (NZYTech, MB12091) and 0.5mM of DNTP's mix (NZYTech, MB08701) were added to 0.5μg RNA samples and incubated at 65ºC for 5 min followed by 1 min chill on ice. To the RNA mix, 1X reaction buffer (NZYTech, 18091), 4U Ribonuclease Inhibitor (NZYTech, 17061) and 200U Reverse Transcriptase (NZYTech, MB083) were added.

Samples were placed in a thermocycler and cDNA was synthesized through the following cycle: starting with 10 min at 25ºC, followed by 50 min at 37ºC and 10 min at 70ºC.

## 5.2. PCR reaction

cDNA's were diluted in RNAse/DNAse-free water (Sigma, W4502) to a final concentration of 50ng/µL and for each reaction 1µL of cDNA was added to 9µL of master mix (1X GoTaq Buffer (NZYTech, NM101), 2.5mM $MgCl_2$, 200mM dNTP's, 0.3mM Forward Primer, 0.3mM Reverse Primer and 1.25U GoTaq Enzyme (NZYTech, MB35401). Samples were placed in a thermocycler and the following program was applied: 1 cycle at 95ºC for 2 min, 30 cycles extension at 95ºC for 1 min, 60ºC for 1 min and 72ºC for 1 min and finally 1 cycle at 72ºC for 5 min. 5µL of PCR products mix to 1µL of Gel-red (Biotium, 41003-T) Loading dye 3 colors and loaded onto a 2% agarose gel in TAE 1X (0.0489mM Tris Base (VWR, 33621.260), 0.0037mM EDTA and 1.14% Acetic Acid (VWR, 20108.292) Sequence of GAPDH primers used is showed in Table 2.

## 5.3. Real-time quantitative PCR (qRT-PCR)

Samples preparation for real-time quantitative analysis was performed on ice using iTaq Universal SYBR Green Supermix (Bio-rad, 64361172) according to the manufacturer's instructions. Briefly, a mastermix with 56% iTaq Universal SyBr Green Supermix (Bio-rad, 64361172) and 3.3% of each primer in MiliQ water was previously prepared for each sample and each reaction was analysed in triplicates with 9µL of mastermix and 1µL of cDNA 50ng/µL or DNAse/RNAse-free water for the blank. The reactions were performed using the following conditions: 1 cycle at 95ºC for 3 min, followed by 35 cycles of 20 seconds at 95ºC, 1 min at 60ºC, 15 seconds at 95ºC, 1 min at 60ºC and finally 15 seconds at 95ºC. qRT-PCR was performed in triplicates in CFX Touch Real Time detector system and relative fold change was calculated using ddCT method. Sequence of the primers used is showed in Table 2.

|  | Primer Sequence (5' – 3') |
| --- | --- |
| P-cad Forward | AGTGGAGGACCCCATGAACA |
| P-cad Reverse | TTGGGCTTGTGGTCATTCTG |
| GAPDH Forward | CTCTGCTCCTCCTGTTCGAC |
| GAPDH Reverse | ACCAAATCCGTTGACTCCGAC |

**Table 2- Sequence of primers used for qRT-PCR reaction.**

## 6. Dual Luciferase Renilla reporter assay

150 000 cells in 2mL of CGM were plated per well in a 6-well plate. After 12-24 hours, cells were transfected with 0.720µg of p3D.A-Luc and 1.44µg of pRL-TK plasmids in a cationic lipid transfection using Lipofectamine 2000 (Alfagene, 11668-019) according to the

manufacturer's instructions. After 12 hours, transfection medium was replaced by cell culture medium restricted in supplements for another 12 hours. Cells were then treated for 6 hours with EtOH or TAM in the presence or absence of LatA or CCG-203971 in cell culture medium restricted in supplements. After trypsinization, cell pellet was resuspended in 250µL of passive lysis buffer (PLB) 1X and thawed overnight at -20ºC.

Dual luciferase renilla reporter assay was performed using the Dual-Luciferase Reporter Assay system (Promega, PROME19600010) according to the manufacturer's instructions. Briefly, 80µL of sample were added in triplicates in a 96-well plate followed by 100µL of luciferase assay reagent II (LARII) and luminescence was detected using synergy Mx. Then, 100µL of 1X Stop and Glo solution were added, and luminescence was detected. Relative luciferase activity was quantified by normalizing Firefly Luciferase activity to their respective Renilla Luciferase activity. Plasmids were kindly provided by Guido Posern (University Halle-Wittenberg, Germany).

## 6.1.  Plasmid's expansion – Midi Prep

For bacterial transformation, 50ng of p3D.A-Luc and pRL-TK plasmids were incubated with Luria Broth Miller (LB) (GRISP, GCM04.0500) for 30 min and then heated up to 42ºC for 90 seconds, followed by a 2 min incubation on ice. 600µL of LB were added and a centrifugation was performed at 220rpm for 1 hour at 37ºC followed by a 2 min centrifugation at 6000 rpm at RT. In aseptic conditions, bacteria were seeded on LB, Agarose (Lonza (50004) plates supplemented with 100µg/mL Ampicilin (NZYTech, MB02102). Plates were incubated overnight at 37ºC with 200g agitation. After 12 hours, a well looked and isolated colony was selected and grown for 24 hours in LB with 100µg/mL Ampicilin at 37ºC with a 200g agitation.

A final volume of 100mL of overnight bacterial culture was harvested by centrifugation at 6000g for 15 min at 4ºC and the p3.D.A-Luc and pRL-TK plasmids were isolated using the QIAGEN Plasmid Midi Kit (Izasa, 50912143) according to the manufacturer's instructions. Briefly, pellets were resuspended in 4mL of Buffer P1. Identical volumes of Buffer P2 were then added. Samples were mixed by vigorous inversion and incubated at RT for 5 min until the solution turned blue. 4mL of Buffer P3 were added, mixed by vigorous inversion, and incubated for 15 min until the solution turned colorless. After a 10 min centrifugation at 14 000g at 4ºC, supernatants were loaded to a previously equilibrated QIAGEN-tip with 4mL of Buffer QBT and allowed to enter the resin by gravity flow. The QIAGEN-tip was then washed twice with 10mL of Buffer QC and DNA was eluted with 5mL of Buffer QF and precipitated with 3.5mL of isopropanol (PanReac AppliChem, 131070.1611). After a 45 min centrifugation at 14 000g at 4ºC, DNA pellets were washed

with 2mL of 70% EtOH at RT, air dried and resuspended in 50μL of MiliQ water and plasmids' DNA concentrations were measured using Nanodrop.

## 7. Collagen matrix invasion assay

20 000 cells in 200μL of CGM were plated per well in a 96-well plate previously coated with 30μL of 0.7% agarose (Lonza, 50004) in a laminar air flow cabinet. Cells were allowed to form spheroids within 24 hours. On the next day medium was removed and 60μL of 5mg/mL Collagen Type I (VWR, 734-1085) in 1M NaOH and 1X DMEM/F12 was added per well and cells were incubated in a 5% $CO_2$ humidified incubator at 37ºC for 1 hour. Spheroids were then treated with 4μM TAM or the same volume of EtOH in the presence or absence of 160μM CCG-203971. Plates were incubated at 37ºC with 5% $CO_2$ humidification for 36 hours and pictures were taken using 5x objective microscope in brightfield.

## 8. Mammospheres forming ability assay

150 000 cells in 2mL of CGM were plated per well in a 6-well plate in cell culture medium restricted in supplements. After treatment, cell pellets were collected using Versene (Alfagene, LTI15040-033) and resuspended in 1mL of PBS1X, passed three times through a 25 gauge needle using a syringe to obtain a single cell suspension and cell density was determined using a Neubauer chamber. According to cell count, 10 000 cells were plated per well in a 6-well plate previously coated with Poly(2-hydrocyethyl methacrylate) (PolyHEMA) in 2mL of mammosphere medium (1:1 DMEM/F12, 20ng/mL human EGF, 40μg/mL Insulin, 500ng/mL Hydrocortisone, 1% Penincilin/Streptomycin (Merck, 15070-063) and 1:1 Suplement B-27 Minus Vitamine A (Alfagene, LTI12587-010)) filtered with a 0.45μm filter (VWR, 514-4127). Cells were carefully incubated in a 5% $CO_2$ humidified incubator at 37ºC for 6 days and then pictures were acquired using the 5x objective in a brightfield microscope.

### 8.1. Poly-HEMA coating

6-well plates used for mammospheres forming ability assay were previously coated with a hydrophobic surface to provide non-adherent conditions. In a laminar air flow cabinet, 2mL of 1.2% PolyHEMA in 95% EtOH were added to each well and plates were then incubated at 54ºC in a non-$CO_2$ incubator for several days.

# CHAPTER IV
# RESULTS

To evaluate our hypothesis and explore the role of the actin/MRTF-A/SRF signalling pathway downstream of P-cad in basal-like breast cancer cells, we asked two main questions that are translated in the two aims of this project already described in chapter II.

## 1. Actin polymerization triggers MRTF/SRF signalling activity

Regarding our first aim, we tested if the transient accumulation of F-actin in pre-malignant TAM-treated MCF10A-ER-Src cells (Tavares et al., 2017), triggers MRTF-A/SRF signalling activity. To evaluate this end, we analysed the consequences of applying to pre-malignant TAM-treated MCF10A-ER-Src cells and control EtOH-treated cells, LatA, which binds G-actin, blocking their incorporation into filaments (Martin & Leder, 2001).

### 1.1. LatA treatment inhibits F-actin assembly but does not compromise cell viability

As LatA treatment is expected to reduce the pool of actin filaments (Coué et al., 1987; Martin & Leder, 2001), we first evaluated if a concentration of 0.5µM of LatA was effective in reducing F-actin levels by immunofluorescence analysis.

Confocal sections on immunofluorescence analysis of MCF10A-ER-Src cells treated with EtOH or TAM in the presence or absence of LatA for 12, 24 and 36 hours and stain with Phalloidin, which binds F-actin, showed a striking reduction in actin filament levels in LatA-treated MCF10A-ER-Src cells, compared to those that were not treated with LatA (Figure 20.A).

To discard the possibility that the consequences of LatA treatment resulted from apoptosis, MCF10A-ER-Src cells' viability was assessed using Trypan-blue after treatment with EtOH or TAM in the presence of 0.5µM LatA for 12, 24 and 36 hours. We found that cells showed over 80% viability rate in all experimental conditions (Figure 20.B), indicating that LatA has no major effect on cell survival during the 36 hours of treatment.

Together, these data showed that LatA treatment inhibits F-actin accumulation in MCF10A-ER-Src cells without compromising their viability.
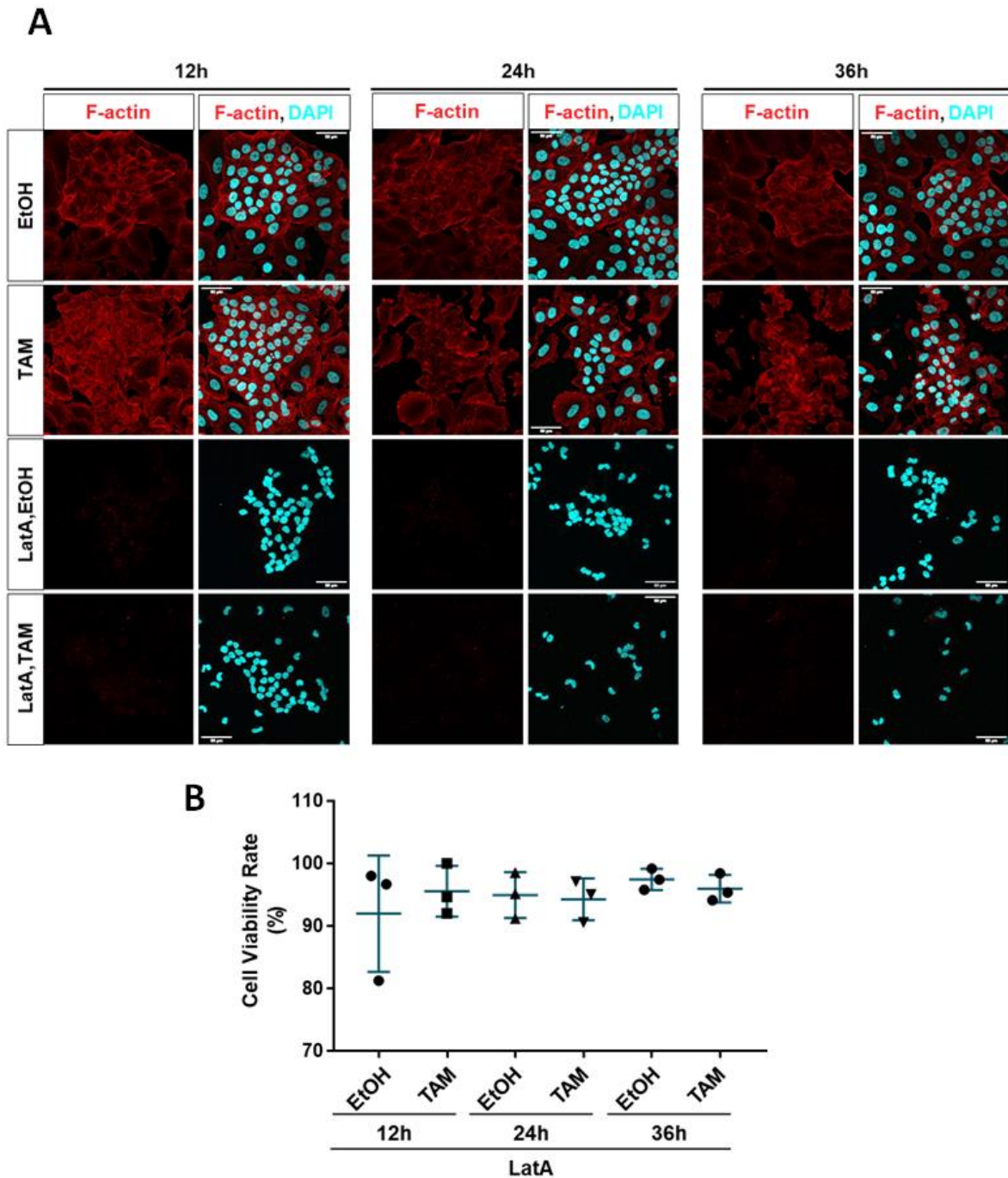
**Figure 20- MCF10A-ER-Src cells co-treated with LatA and EtOH or TAM for 12, 24 and 36 hours are viable and fail to assemble actin filaments**. (A) Standard confocal sections of MCF10A-ER-Src cells treated with EtOH or TAM in the presence or absence of 0.5μM LatA for 12, 24 and 36h, stained with Phalloidin (red) to stain F-actin and DAPI (blue) to stain the nuclei. Scale bar = 50μm. (B) Viability rate (%) of MCF10A-ER-Src cells treated with 0.5μM of LatA and EtOH or TAM for 12, 24 and 36 hours. Error bars indicate SD. Statistical significance was calculated using one-way ANOVA test.

## 1.2. LatA treatment prevents SRF transcriptional activity in TAM-treated MCF10A-ER-Src cells

Then, we investigated if the transient F-actin accumulation taking place in pre-malignant TAM-treated MCF10A-ER-Src cells was required to an increased MRTF-A/SRF signalling activity. To this end, we evaluated the consequence of inhibiting F-actin accumulation using LatA on SRF transcriptional activity.

MCF10A-ER-Src cells were transfected with a SRF minimal Luciferase reporter and treated with EtOH or TAM in the presence or absence of LatA for 6 hours. As expected, quantification of SRF-Luciferase activity showed an average 3-fold increase in SRF-Luciferase activity in MCF10A-ER-Src cells treated with TAM when compared to EtOH treated ones. On the other hand, LatA significantly abrogated the increase in SRF-Luciferase activity in EtOH-treated MCF10A-ER-Src cells (Figure 21).

Thus, LatA treatment prevents SRF transcriptional activity in TAM-treated MCF10A-ER-Src cells. These observations are consistent with a model by which the transient accumulation of F-actin in pre-malignant TAM-treated MCF10A-ER-Src cells reduces the pool of G-actin, triggering the dissociation of the G-actin:MRTF-A complex and consequently an increase in SRF transcriptional activity through the association between SRF and MRTF-A.
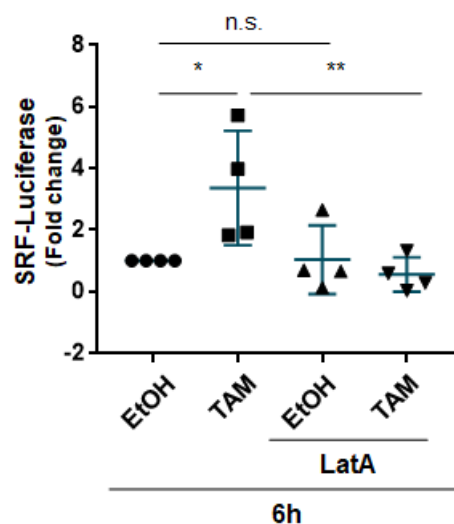


**Figure 21- LatA prevents the upregulation of the SRF-Luciferase reporter in TAM-treated MCF10A-ER-Src cells**. Fold change quantification of SRF-Luciferase activity in MCF10A-ER-Src cells transfected with the SRF-responsive-Luciferase reporter gene and treated for 6 hours with EtOH or TAM in the presence or absence of 0.5µM LatA. Error bars indicate SD. * indicates p-value<0.01. ** indicates p-value<0.001. Statistical significance was calculated using one-way ANOVA test, which compares the means of the four independent groups between each other's.

### 1.3. LatA treatment could prevent cellular transformation

Then, we evaluated the role of F-actin polymerization on the ability of TAM-induced MCF10A-ER-Src to undergo cellular transformation. To achieve this goal, we first evaluated if preventing F-actin accumulation using LatA hampers pre-malignant MCF10A-ER-Src cells to acquire morphological transformed features over time.

Brightfield imaging of MCF10A-ER-Src cells treated with EtOH or TAM for 12, 24 and 36 hours in the absence of LatA showed that, TAM-treated MCF10A-ER-Src cells maintained an epithelial-like phenotype up to 12 hours after treatment, to then acquire a mesenchymal phenotype starting 24 hours after treatment (Figure 22.A). This was in contrast to EtOH-treated cells, which maintained an epithelial-like morphology during the 36 hours of treatment. However, in the presence of LatA, EtOH- and TAM-treated MCF10A-ER-Src cells lose their epithelial morphology and undergo a morphological rounding as soon as 12 hours after treatment. This round phenotype was maintained 24 and 36 hours after EtOH or TAM treatment (Figure 22.A), precluding us to conclude on the morphological transformed states of these cells.

As a stepwise increase in the activity of ER-Src and of endogenous pSrc during the 36 hours of TAM treatment is associated with the sequential acquisition of pre-malignant and malignant phenotypes (Tavares et al., 2017), we then tested the effect of LatA on the phosphorylation levels of ER-Src (ER-pSrc). Western-blot analysis on protein extracts from MCF10A-ER-Src cells treated with EtOH or TAM in the absence of LatA for 12, 24 and 36 hours, blotted with anti-pSrc showed an increase in ER-pSrc levels in cells treated with TAM, which was only significantly different 36 hours after treatment, when compared with cells treated with EtOH (Figure 22.B and C). LatA could abrogate ER-Src activity, as ER-pSrc levels were significantly reduced in cells co-treated with TAM and LatA for 36 hours, compared with those treated with TAM only (Figure 22.B and C). These observations suggest that LatA treatment prevents TAM-induced cellular transformation.

A

| | 0h | 12h | 24h | 36h |
|---|---|---|---|---|
| EtOH | | | | |
| TAM | | | | |
| LatA, EtOH | | | | |
| LatA, TAM | | | | |

B

α-ER-pSrc
α-HSC70

α-ER-pSrc
α-HSC70

C
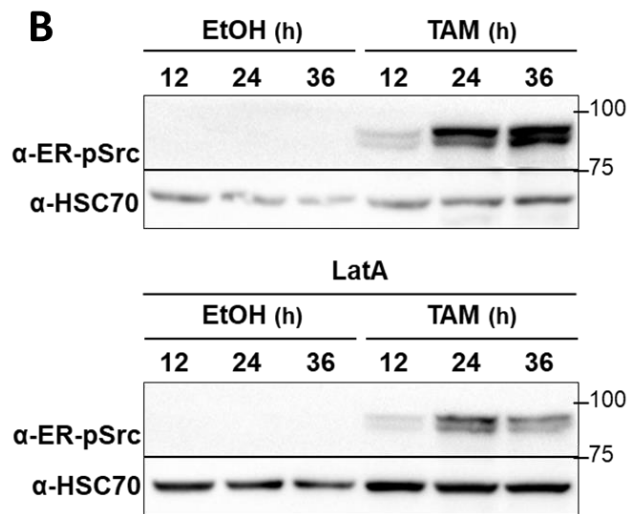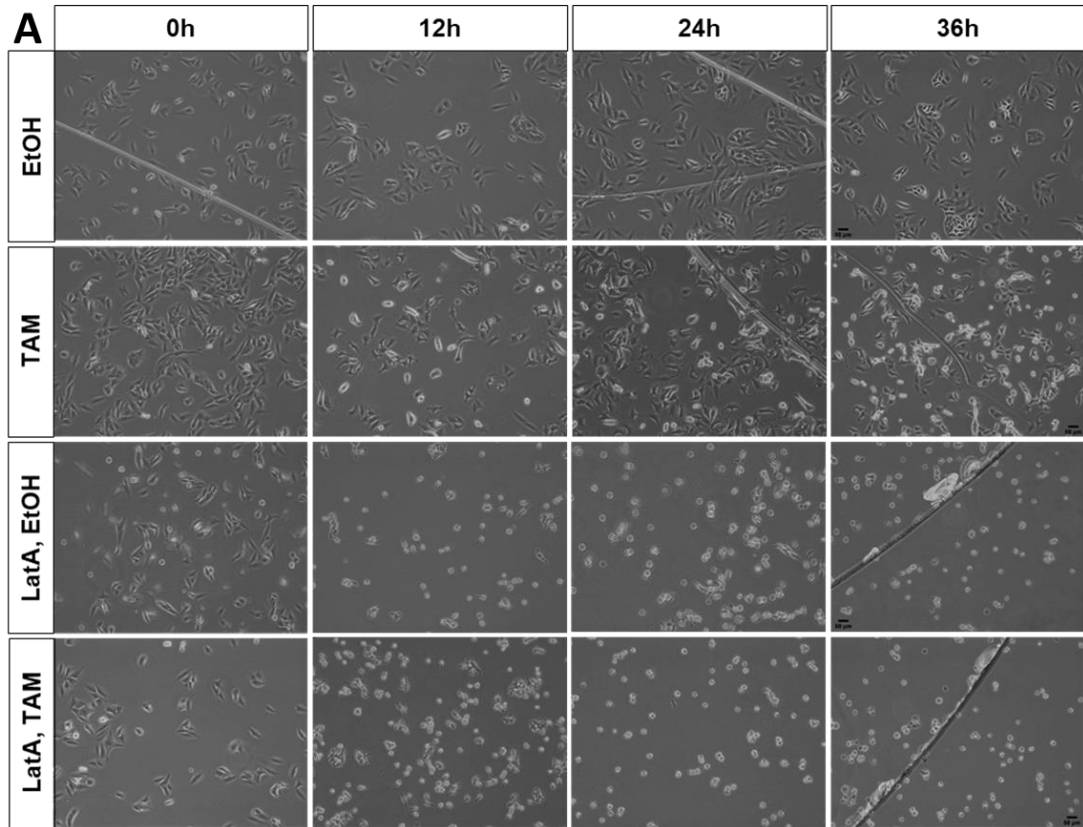
**Figure 22- LatA treatment induces morphological rounding of MCF10A-ER-Src cells treated with EtOH or TAM and reduces the phosphorylation levels of ER-Src**. (A) Images acquired with 5X objective on brightfield microscope of MCF10A-ER-Src cells treated with EtOH or TAM in the presence or absence of 0.5µM LatA for 12, 24 and 36 hours. Scale b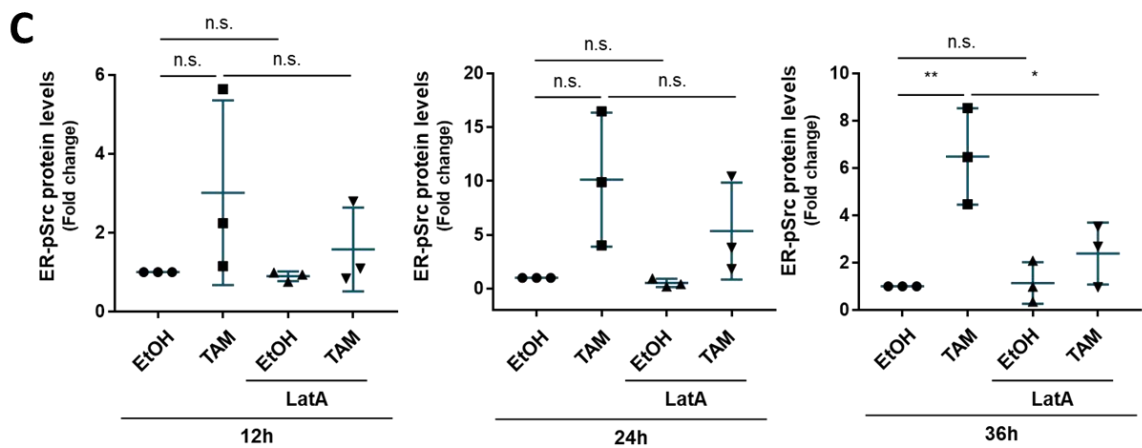ars = 50µm. (B) Western-blots on protein extracts from MCF10A-ER-Src cells treated for 12, 24 and 36 hours with EtOH or TAM (upper panels) or with 0.5µM LatA and EtOH or TAM (bottom panels), blotted with anti-pSrc or anti-HSC70. (C) Fold change quantification or ER-pSrc levels in MCF10A-ER-Src cells treated with EtOH or TAM in the presence or absence of 0.5µM LatA for 12, 24 and 36 hours, normalized to HSC70. Error bars indicate SD. n.s. indicates non-significant. Statistical significance was calculated using non-parametric t-test.

## 1.4. LatA treatment affects P-cad localization and could stabilize P-cad in pre-malignant cells without affecting P-cad expression

We hypothesize that P-cad promotes the activation of the actin/MRTF-A/SRF signalling pathway through F-actin. As the actin cytoskeleton also controls cadherin organization at AJs (Indra et al., 2018), we tested the possibility that the transient increase in F-actin in pre-malignant TAM-treated MCF10A-ER-Src induces activation of the MRTF-A/SRF signalling pathway by enhancing P-cad activity. To this end, we analysed P-cad expression and localization in EtOH- and TAM-treated MCF10A-ER-Src cells when actin polymerization was inhibited with LatA treatment.

We first tested if LatA affect P-cad expression in EtOH- and TAM-treated MCF10A-ER-Src cells by quantitative RT-PCR. As expected, quantification of P-cad mRNA expression levels indicated that P-cad was significantly upregulated in cells treated with TAM for 24 or 36 hours, compared to those treated with EtOH for the same time. In the presence of LatA P-cad mRNA levels were not significantly affected in MCF10A-ER-Src cells treated with TAM at all timepoints analysed. Surprisingly, in cells treated with EtOH for 12, 24 or 36 hours, LatA significantly induced P-cad expression (Figure 23.A). These observations suggest that in un-transformed MCF10A-ER-Src cells, the actin cytoskeleton prevents P-cad expression. In contrast, in cells undergoing transformation, P-cad expression is independent of the actin cytoskeleton.

To confirm that the transient accumulation of F-actin in pre-malignant TAM-treated MCF10A-ER-Src cells does not affect P-cad protein stability, we then tested the effect of LatA on P-cad protein levels by Western-Blot. We first confirmed that P-cad accumulates during transformation in TAM-treated MCF10A-ER-Src cells by western-blot. Quantification of P-cad protein levels between cells treated with EtOH or TAM for 2, 6, 12, 24 and 36 hours showed that TAM treatment induces a transient increase in P-cad protein levels, that was significantly higher 12 hours after treatment, compared to P-cad protein levels in cells

treated with EtOH for the same time (Figure 23. B and C, in collaboration with Patrícia Guerreiro).

Then, we evaluated if LatA treatment affects P-cad levels. Quantifications indicated that P-cad levels were not significantly different between MCF10A-ER-Src cells treated with TAM or EtOH in the presence or absence of LatA at all time points analysed. Yet, as previously observed (Figure 23.B and C), P-cad levels were in average increased 2 folds in cells treated with TAM for 12 hours, while this increase was only 1.46 folds in the presence of LatA (Figure 23.D), suggesting that F-actin accumulation could stabilize P-cad. Additional replicates would be required to confirm this hypothesis.

Finally, we analysed LatA effect on P-cad localization using immunofluorescence analysis. Standard confocal sections (Figure 23.F) and cross sections (Figure 23.G) showed that, in the absence of LatA, MCF10A-ER-Src cells treated with EtOH or TAM for 12 hours localized P-cad at the membrane, only in cells that form cell-cell contacts. However, in the presence of LatA, P-cad lost its membrane-associated localization and accumulated in the cytoplasm in both EtOH and TAM-treated cells.

Together, these data show that the actin cytoskeleton affects P-cad localization. In addition, they suggest that the transient accumulation of F-actin in pre-malignant MCF10A-ER-Src cells could stabilize P-cad but does not affect its expression.
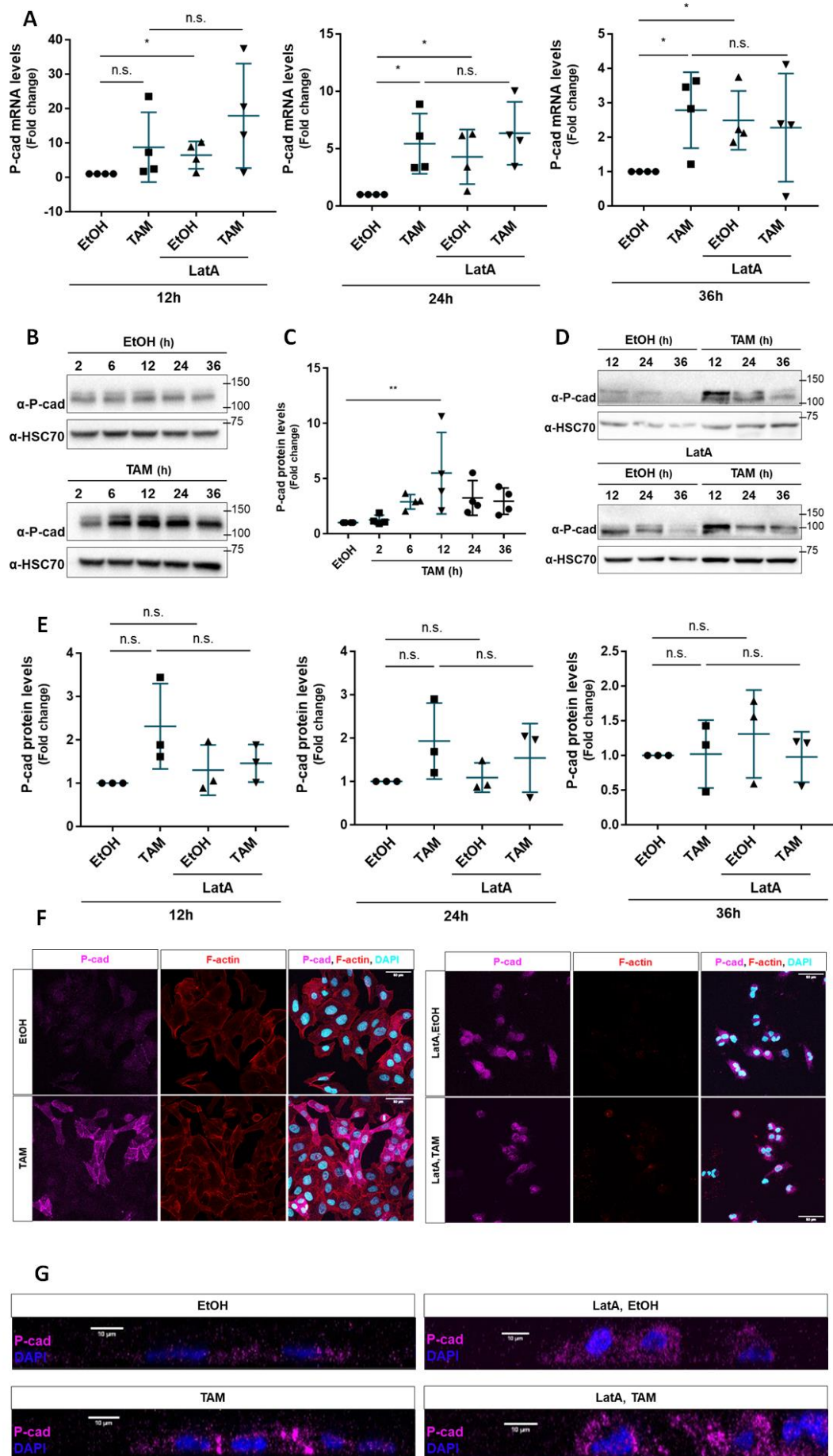
**Figure 23- LatA treatment does not affect P-cad mRNA or protein expression levels of MCF10A-ER-Src cells treated with EtOH or TAM in the presence or absence of 0.5μM LatA for 12, 24 and 36 hours but prevents P-cad to localize at the cell membrane of MCF10A-ER-Src cells treated with EtOH or TAM in the presence or absence of 0.5μM LatA for 12 hours**. (A) Fold change P-cad mRNA levels in extracts from MCF10A-ER-Src cells treated with EtOH or TAM in the presence or absence of 0.5μM LatA for 12, 24 and 36 hours. Error bars indicate SD. * indicates p-value<0.01 and n.s. indicates non-significant. Statistical significance was calculated using one-way ANOVA test, which compares the means of four independent groups between each other's. (B) Western-blots on protein extracts from MCF10A-ER-Src cells treated for 2, 6, 12, 24 and 36 hours with EtOH (upper panels) or TAM (bottom panels), blotted with anti-Pcad or anti-HSC70. (C) Fold change quantification of P-cad levels between MCF10A-ER-Src cells treated with EtOH and those treated with TAM for the same time points, normalized to HSC70. Error bars indicate SD. ** indicates p-value<0.001. Statistical significance was calculated using one-way ANOVA test. (D) Western-blots on protein extracts from MCF10A-ER-Src cells treated for 12, 24 and 36 hours with EtOH or TAM (upper panels) or 0.5μM LatA and EtOH or TAM (bottom panels), blotted with anti-P-cad or anti-HSC70. (E) Fold change quantification of P-cad levels between MCF10A-ER-Src cells treated with EtOH or TAM in the presence or absence of 0.5μM LatA for 12, 24 and 36 hours, normalized to HSC70. Error bars indicate SD. n.s. indicates non-significant. Statistical significance was calculated using one-way ANOVA test. (F) Standard confocal sections of MCF10A-ER-Src cells treated with EtOH or TAM in the presence or absence of 0.5μM LatA for 12 hours, stained with anti-Pcad (purple), Phalloidin (red) to stain F-actin and DAPI (blue) to stain the nuclei. Scale bars = 50μm. (G) Cross sections of MCF10A-ER-Src cells treated with EtOH or TAM in the presence or absence of 0.5μM LatA for 12 hours, stained with anti-Pcad (purple) and DAPI (blue) to stain the nuclei. Scale bars = 10μm.

## 2. MRTF-A activity is required in pre-malignant MCF10A-ER-Src cells to promote cellular transformation

The second aim of this project was to determine the role of the transient increase in MRTF-A/SRF signalling activity in pre-malignant TAM-treated MCF10A-ER-Src cells.

### 2.1. TAM treatment correlates with the transient accumulation of MRTF-A

Prior to analyse the consequences of inhibiting MRTF-A/SRF signalling activity, we evaluated if MRTF-A protein levels were altered during cellular transformation (in collaboration with Sara Canato).

Western-blot on protein extracts from MCF10A-ER-Src cells treated with EtOH or TAM showed that MRTF-A levels were transiently accumulated in cells treated with TAM for 6, 12 and 24 hours when compared with those treated with EtOH (Figure 24.A and B). These observations indicate that the transient increase in SRF transcriptional activity (Figure 18.A

and 21) is associated with a transient accumulation of MRTF-A in pre-malignant cells that amass actin filaments.
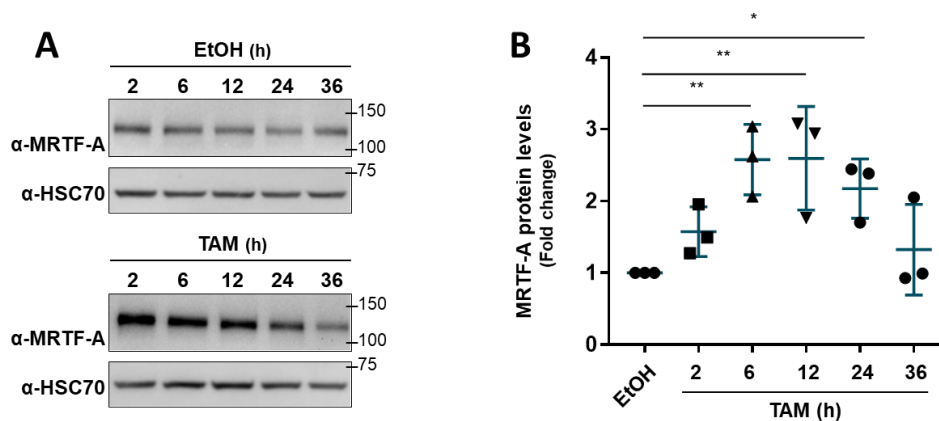


**Figure 24- MRTF-A transiently accumulates in MCF10A-ER-Src cells 6, 12 and 24 hours after TAM treatment**. (A) Western-blots on protein extracts from MCF10A-ER-Src cells treated for 2, 6, 12, 24 and 36 hours with EtOH (upper panels) or TAM (bottom panels), blotted with anti-MRTF-A or anti-HSC70. (B) Fold change quantification of MRTF-A levels between MCF10A-ER-Src cells treated with EtOH or TAM for the same time points, normalized to HSC70. Error bars indicate SD. * indicates p-value<0.01. ** indicates p-value<0.001. Statistical significance was calculated using one-way ANOVA test, which compares the mean of each independent group with the mean of the control group.

## 2.2. CCG-203971 treatment abrogates SRF transcriptional activity in TAM-treated MCF10A-ER-Src cells

To decipher the role of the transient increase in MRTF-A/SRF signalling activity in pre-malignant TAM-treated MCF10A-ER-Src cells, we took advantage of the small molecule inhibitor CCG-203971, which blocks the nuclear localization and activity of MRTF-A (Haak et al., 2017). We first confirmed that treating cells with 40µM of CCG-203971 could abrogate the transient increase in SRF transcriptional activity in TAM-treated MCf10A-ER-Src cells using the minimal SRF-Luciferase reporter as read-out.

As expected, we observed a significant increase of SRF-Luciferase activity in MCF10A-ER-Src cells treated with TAM when compared with cells treated with EtOH for the same time (Figure 25), which is in concordance with our previous results (Figure 18.A and 21). SRF-dependent Luciferase activity was not significantly different in MCF10A-ER-Src cells treated with EtOH for 6 hours. In contrast, CCG-203971 significantly abolished SRF-Luciferase activity in cells treated with TAM for 6 hours. These observations confirmed that the transient increase in SRF transcriptional activity in pre-malignant MCF10A-ER-Src cells is dependent on MRTF-A activity and validate the use of CCG-203971 to analyse the consequences of inhibiting MRTF-A activity on the acquisition of transformed features.
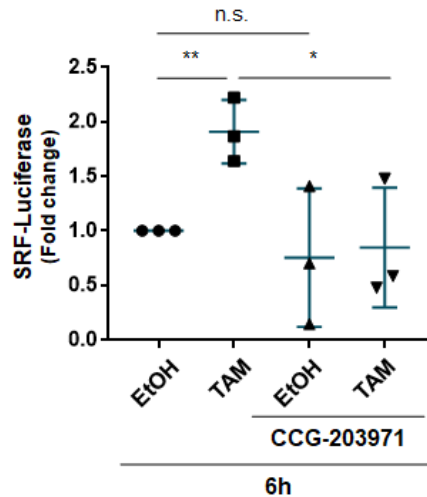
**Figure 25- CCG-203971 prevents the upregulation of the SRF-Luciferase reporter in TAM-treated MCF10A-ER-Src cells**. Fold change quantification of Luciferase activity in MCF10A-ER-Src cells transfected with the SRF-responsive-Luciferase reporter gene and treated with EtOH or TAM in the presence or absence of 40µM CCG-203971 for 6 hours. Error bars indicate SD. * indicates p-value<0.01. ** indicates p-value<0.001. n.s. indicates non-significant. Statistical significance was calculated using one-way ANOVA test, which compares the means of the four independent groups between each other's.

## 2.3. CCG-203971 treatment could prevent TAM-treated MCF10A-ER-Src cells to acquire morphological transformed features

To analyse the consequences of inhibiting MRTF-A/SRF signalling activity in pre-malignant MCF10A-ER-Src cells on the acquisition of transformed features, we first analysed if in the presence of CCG-203971, TAM-treated MCF10A-ER-Src cells fail to acquire morphological transformed features using brightfield microscope. As previously reported (Tavares et al., 2017), while MCF10A-ER-Src cells treated with EtOH for 2, 6, 12, 24 or 36 hours maintained an epithelial-like morphology, those that were treated with TAM acquired morphological transformation features 36 hours after TAM treatment associated with cell detachment (Figure 26). After 24 and 36 hours, CCG-203971 treatment affected the morphology of EtOH and TAM-treated cells, which started to lose their epithelial-like morphology. However, although pictures were taken under low cells confluency, upon CCG-203971 treatment, EtOH and TAM-treated cells do not show much differences in morphology but the presence of CCG-203971 in TAM-treated cells appeared to reduce the number of cells detaching from their substratum.

These observations suggest that inhibiting MRTF-A activity in pre-malignant TAM-treated MCF10A-ER-Src cells could prevent the acquisition of transformed features. Additional studies would be required to confirm this hypothesis.
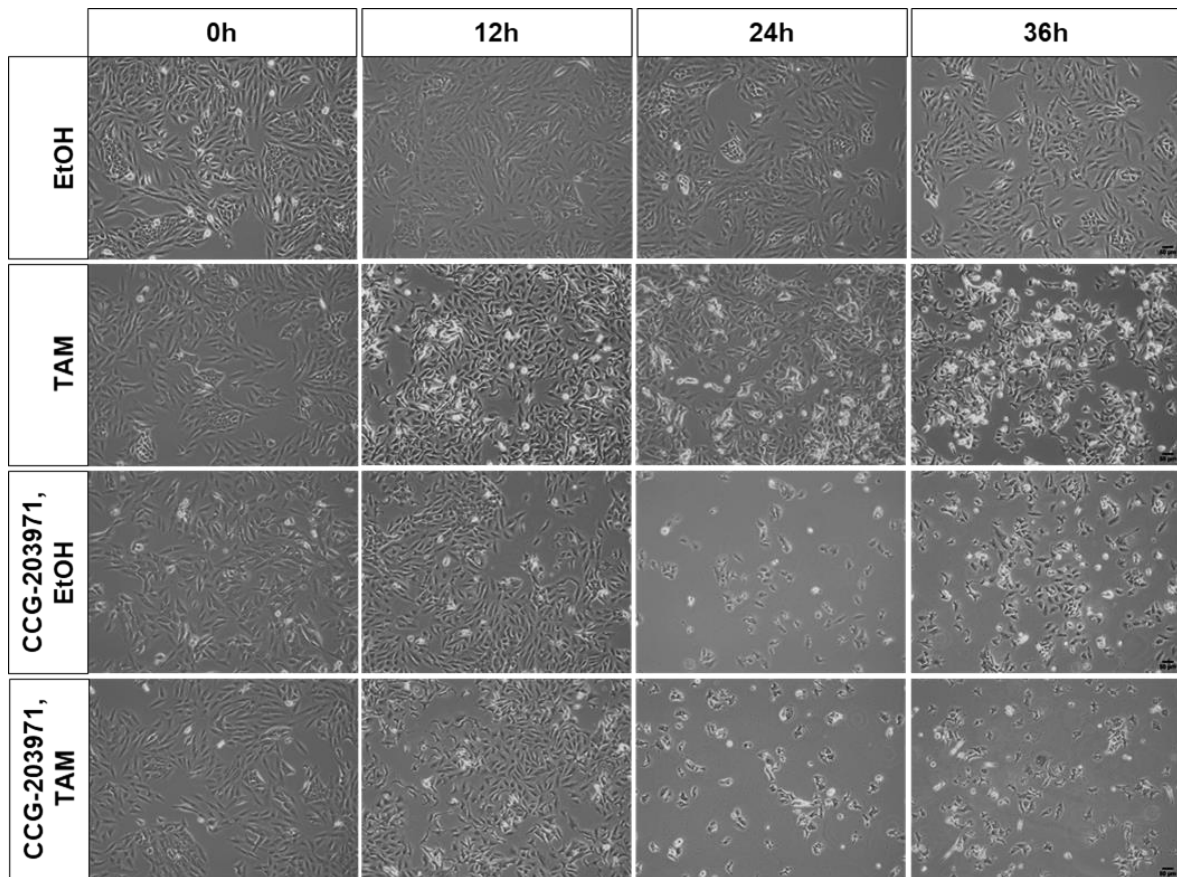
**Figure 26- Treatment with 40µM CCG-203971 could prevent cellular transformation of MCF10A-ER-Src cells**. Images acquired with 10X objective on brightfield microscope of MCF10A-ER-Src cells treated with EtOH or TAM in the presence or absence of 40µM CCG-203971 for 12, 24 and 36 hours. Scale bars = 50µm.

## 2.4. CCG-203971 treatment prevents TAM-treated MCF10A-ER-Src cells to acquire invading abilities

To validate the role of the transient increase in MRTF-A activity in pre-malignant TAM-treated MCF10A-ER-Src cells in promoting malignant transformation, we accessed if the presence of CCG-203971 affect the ability of TAM-treated MCF10A-ER-Src cells to invade using invasion assay in collagen matrix.

Primary spheroids of MCF10A-ER-Src cells treated with EtOH for 36 hours, maintained a round shape with well-defined borders. In contrast, those that were treated with TAM for the same time displayed irregular borders with cells spreading into the collagen matrix (Figure 27.A), indicating that MRC10A-ER-Src cells treated with TAM for 36 hours have acquired invasive abilities. The presence of CCG-203971 had no major effect on EtOH-treated spheroids. However, it suppressed the ability of TAM-treated cells to invade, as these spheroids maintained a round shape. Quantification of the number of spheroids that displayed invasive fronts indicates that CCG-203971 reduced drastically the number of

invading TAM-treated spheroids (Figure 27.B). Consistent with this observation, while we observed a significant decrease of the circularity of MCF10A-ER-Src spheroids upon TAM treatment, this effect was abrogated in the presence of CCG-203971 (Figure 27.C). These observations suggest that the transient increase in MRTF-A activity in pre-malignant TAM-treated MCF10A-ER-Src cells is required for the acquisition of invading abilities.
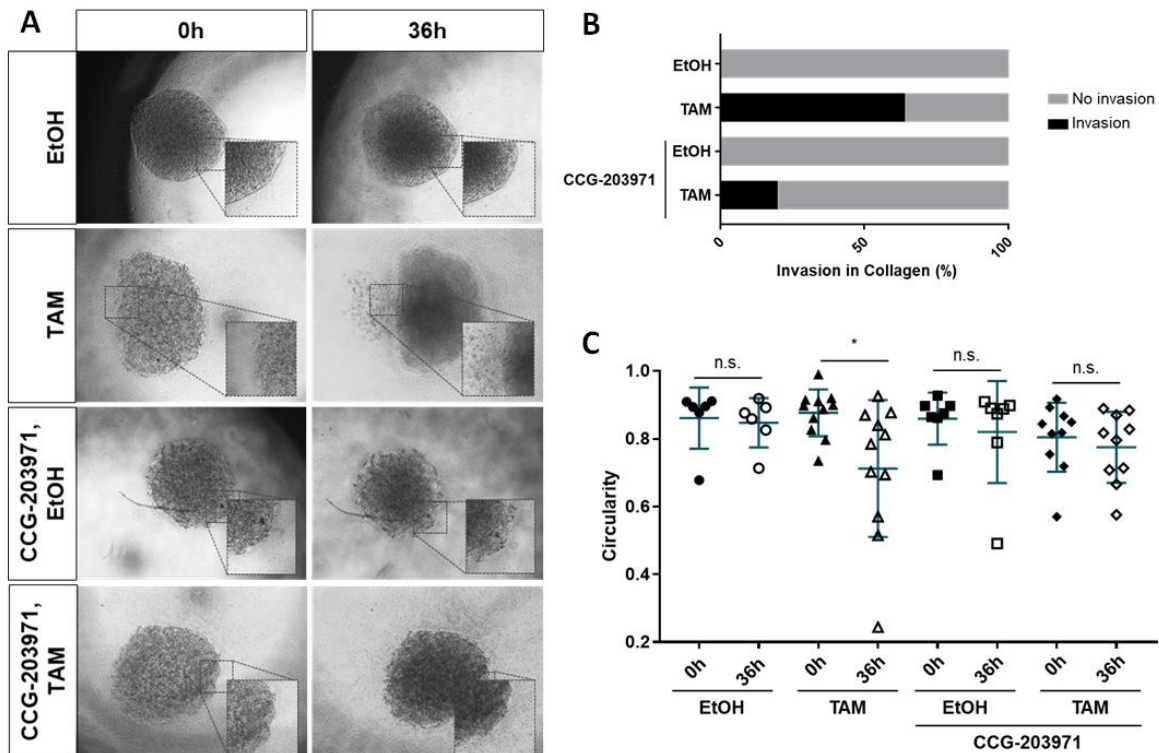


**Figure 27- Treatment with 40µM of CCG-203971 prevents TAM-treated MCF10A-ER-Src cells to invade in collagen**. (A) Images acquired with 5X objective on brightfield microscope of MCF10A-ER-Src cell spheroids embedded in 5mg/mL collagen and treated with EtOH or TAM for 36 hours in the presence or absence of CCG-203971. (B) Quantification of the number of MCF10A-ER-Src spheroids invading in collagen after treatment with EtOH or TAM for 36 hours in the presence or absence of CCG-203971. (C) Quantification of the circularity of MCF10A-ER-Src spheroids circularity treated with EtOH or TAM for 36 hours in the presence or absence of CCG-203971. Error bars indicate SD. * indicates p-value<0.01. Statistical significance was calculated using one-way ANOVA test, which compares the means of the four independent groups between each other's.

## 2.5. CCG-203971 treatment could prevent TAM-treated MCF10A-ER-Src cells to acquire stemness properties

As MCF10A-ER-Src cells treated with TAM for 36 hours acquire ability to grow mammospheres due to the emergence of cells with CSC properties (Hirsch et al., 2009), we analysed if MRTF-A/SRF signalling was required for this process. TAM-treated MCF10A-ER-Src cells were able to grow bigger mammospheres when compared with MCF10A-ER-Src cells treated with EtOH. In the presence of CCG-203971, EtOH-treated

MCF10A-ER-Src spheres were not significantly different compared to those grown in the absence of CCG-203971. However, CCG-203971 drastically reduced the size of TAM-treated MCF10A-ER-Src spheres (Figure 28). These observations suggest that inhibiting MRTF-A activity in pre-malignant TAM-treated MCF10A-ER-Src cells could prevent the acquisition of stemness properties. Additional replicates and quantification of mammospheres forming efficiency would be required to confirm these observations.
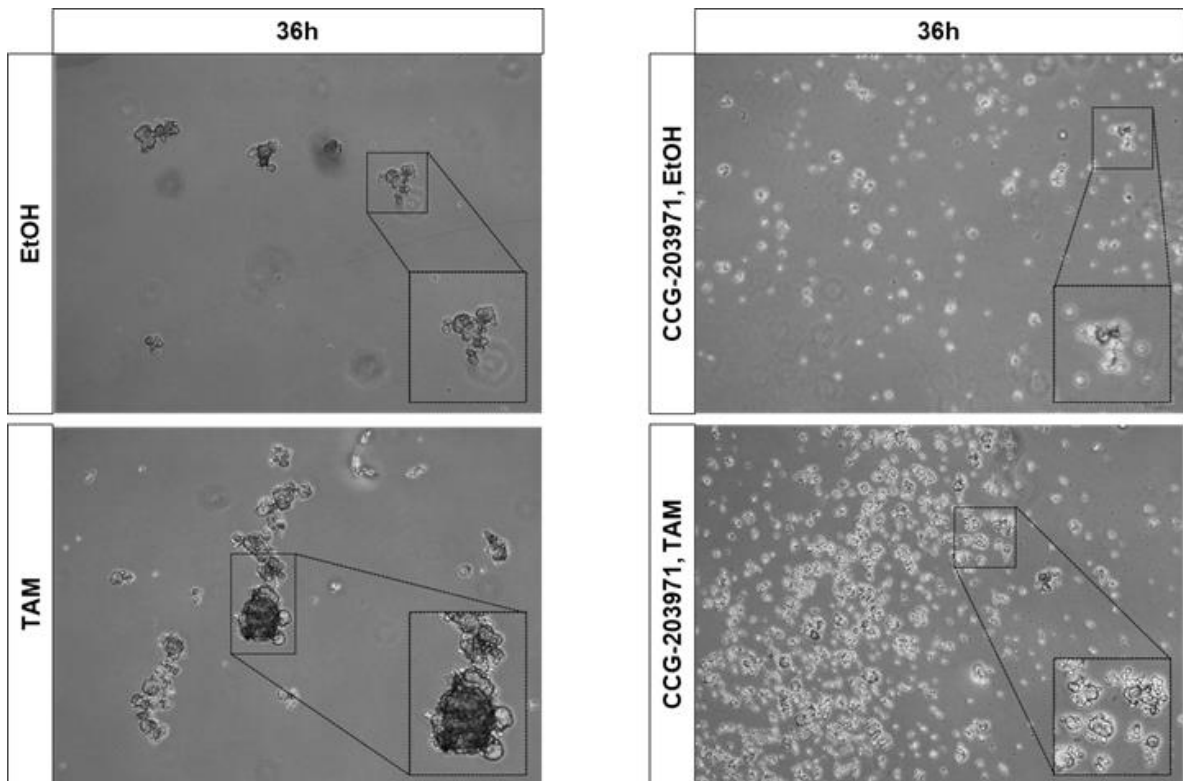


**Figure 28- Treatment with 40μM of CCG-203971 appears to prevent the growth of TAM-treated MCF10A-ER-Src mammospheres**. Images acquired with 5X objective on brightfield microscope of MCF10A-ER-Src mammospheres after treatment with EtOH or TAM for 36 hours in the presence or absence of CCG-203941.

# CHAPTER V

# DISCUSSION

## 1. P-cad could induce the activation of MRTF-A/SRF signalling through F-actin

Our work is consistent with a model by which the transient accumulation of F-actin in pre-malignant TAM-treated MCF10A-ER-Src cells by P-cad induces the activation of the MRTF-A/SRF signalling pathway (Figure 29). First, we found that the transient accumulation of F-actin in pre-malignant TAM-treated MCF10A-ER-Src cells (Tavares et al., 2017), is associated with a transient accumulation of P-cad (Figure 23.B and C) and of MRTF-A (Figure 24), as well as with the upregulation of a minimal SRF-dependent Luciferase reporter (Figure 18.A and 21). Second, we have shown that inhibiting F-actin accumulation in pre-malignant TAM-treated MCF10A-ER-Src cells (Figure 20.A), prevents the upregulation of a SRF-dependent minimal reporter (Figure 21). The effect of the F-actin inhibitor LatA on MRTF-A/SRF transcriptional activity is likely specific, as LatA-treated cells do not undergo apoptosis (Figure 20.B). Moreover, LatA has been shown to block the dissociation of the G-actin:MRTF-A complex and to induce MRTF-A translocation to the nucleus and MRTF-A/SRF transcriptional activity (Miralles et al., 2003; Sotiropoulos et al., 1999). Third, in the Drosophila wing, human P-cad genetically interacts with the fly MRTF and SRF (Figure 15) and promotes MRTF nuclear accumulation (C. Lopes, personal communication). Fourth, our preliminary data indicate that knocking down P-cad in TAM-treated MCF10A-ER-Src cells abrogates the upregulation of the SRF-dependent Luciferase reporter (T. Jesus, personal communication). Fifth, P-cad has been shown to promote F-actin stress fibre assembly and to affect acto-myosin-dependent cell stiffening (Ribeiro et al., 2016).

P-cad could promote F-actin assembly, leading to MRTF-A activation through several mechanisms. One mechanism can involve the activation of Rac1 due to the inhibition of E-cad function, as P-cad affects the ability of E-cad to interact with p120ctn at AJs (Ribeiro et al., 2013) and that the loss of E-cad-dependent AJs trigger the activation of the MRTF-A/SRF signalling pathway through Rac1 (Ribeiro et al., 2018). P-cad could also promote F-actin assembly through Integrin regulation. Consistent with this hypothesis, P-cad functional effects involved α6β4 integrins (Vieira et al., 2014). The intracellular domain of integrins connects to the actin cytoskeleton allowing adhesion to the ECM and controls Rho GTPases activity (Brakebusch et al., 2002; Defilippi et al., 1999). Furthermore, in breast cancer cells lines, integrins, such as αV- and β1 have been shown to activate MRTF-A/SRF (Hermann et al., 2016). In addition, in fibroblast cell lines, integrins trigger the nuclear translocation of MRTF-A through the LINC complex (linker of nucleoskeleton and cytoskeleton) or through formins (Plessner et al., 2015). P-cad could also induce F-actin polymerization through Src, as Src is a critical mediator of P-cad in breast cancer cells (Ribeiro et al., 2018) and is a

well-known regulator of the actin cytoskeleton (Ortiz et al., 2021). In turn, F-actin assembly could feedback on P-cad by promoting its stability since P-cad levels could be reduced upon LatA treatment in TAM-treated MCF10A-ER-Src cells (Figure 23.E). Consistent with this hypothesis, the actin cytoskeleton has been shown to stabilize cadherins (Budnar & Yap, 2013). We also observed that the actin cytoskeleton is required to localize P-cad at the cell membrane in EtOH and TAM-treated MCF10A-ER-Src cells (Figure 23.F and G). However, as the actin cytoskeleton is required to maintain AJs (Rimm et al., 1995), the cytoplasmatic accumulation of P-cad in LatA-treated cells can be an indirect consequence of AJ disassembly.

## 2. The transient activation of the P-cad/F-actin/MRTF-A/SRF signalling axis in pre-malignant cells is required for cellular transformation

Our observations suggest that activation of the MRTF-A/SRF signalling pathway in pre-malignant TAM-treated MCF10A-ER-Src cells is required for cellular transformation (Figure 29). First, we have shown that inhibition of MRTF-A/SRF signalling in pre-malignant TAM-treated MCF10A-ER-Src cells could prevent the acquisition of morphological transformed features (Figure 26). In addition, we provided evidences that MRTF-A activation appears to be required for the acquisition of invasive (Figure 27) and stemness properties (Figure 28). In breast cancer, MRTF-A has been described to promote malignant progression by inducing tumour cells invasion and metastization (Medjkane et al., 2009) through its interaction with SRF (Ikeda et al., 2018). Moreover, in normal pancreatic cells, overexpressing MRTF-A induces stem cells features and EMT (Song et al., 2016). However, the transient increase in MRTF-A/SRF signalling activity in pre-malignant TAM-treated MCF10A-ER-Src cells by P-cad is unlikely to directly promote CSC activity and invading ability, as at the time cells acquire CSC features, 24 hours after TAM treatment (Hirsch et al., 2009; Iliopoulos et al., 2009), or invading abilities, 36 hours of TAM treatment (Tavares et al., 2017), SRF transcriptional activity has lost its ability to trigger gene expression (Figure 25). Instead, the transient increase of MRTF-A/SRF transcriptional activity in pre-malignant TAM-treated MCF10A-ER-Src cells could be required to promote the gain of sustained proliferative abilities, as well as to induce the transition toward a fully transformed state. Consistent with this hypothesis, the ability of TAM-treated MCF10A-ER-Src cells to sustain proliferation in the absence of growth factors, is concomitant with the transient activation of MRTF-A (Tavares et al., 2017 and Figure 24). Moreover, overexpressing MRTF-A in untransformed MCF10A acini has been shown to promote proliferation and EMT (Seifert & Posern, 2017). Thus, while P-cad has only been implicated

in controlling malignant phenotypes in fully transformed cells (Ribeiro et al., 2010; Ribeiro et al., 2013; Vieira et al., 2014), our observations suggest a novel role of P-cad in pre-malignant cells. Consistent with our findings, P-cad upregulation in breast and colon cancer cells appears in the earlier stages of the malignant process in most cases (Hardy et al., 2002; Paredes et al., 2002).

Although we provide evidences that in pre-malignant TAM-treated MCF10A-ER-Src cells, MRTF-A acts through SRF, we cannot exclude the possibility that MRTF-A also promote cellular transformation independently of SRF or through additional transcription factors, as MRTF-A has been shown to control gene expression through YAP-TAZ/TEAD (Kim et al., 2017) or through direct binding to DNA (Gurbuz et al., 2014). Moreover, in breast cancer cells, MRTF-A has been proposed to trigger the expression of a specific set of pro-proliferative genes, independently of SRF (Gurbuz et al., 2014). We cannot either exclude the possibility that 24 and 36 hours after TAM treatment, a small sub-population of MCF10A-ER-Src cells maintain high MRTF-A/SRF activity, which promote stemness and invading abilities, as our data looking at SRF-Luciferase activity were performed on the whole cell population. Consistent with this possibility, P-cad remains enriched at the membrane in a sup-population of TAM-treated MCF10A-ER-Src cells 24 and 36 hours after TAM treatment (Figure 17).
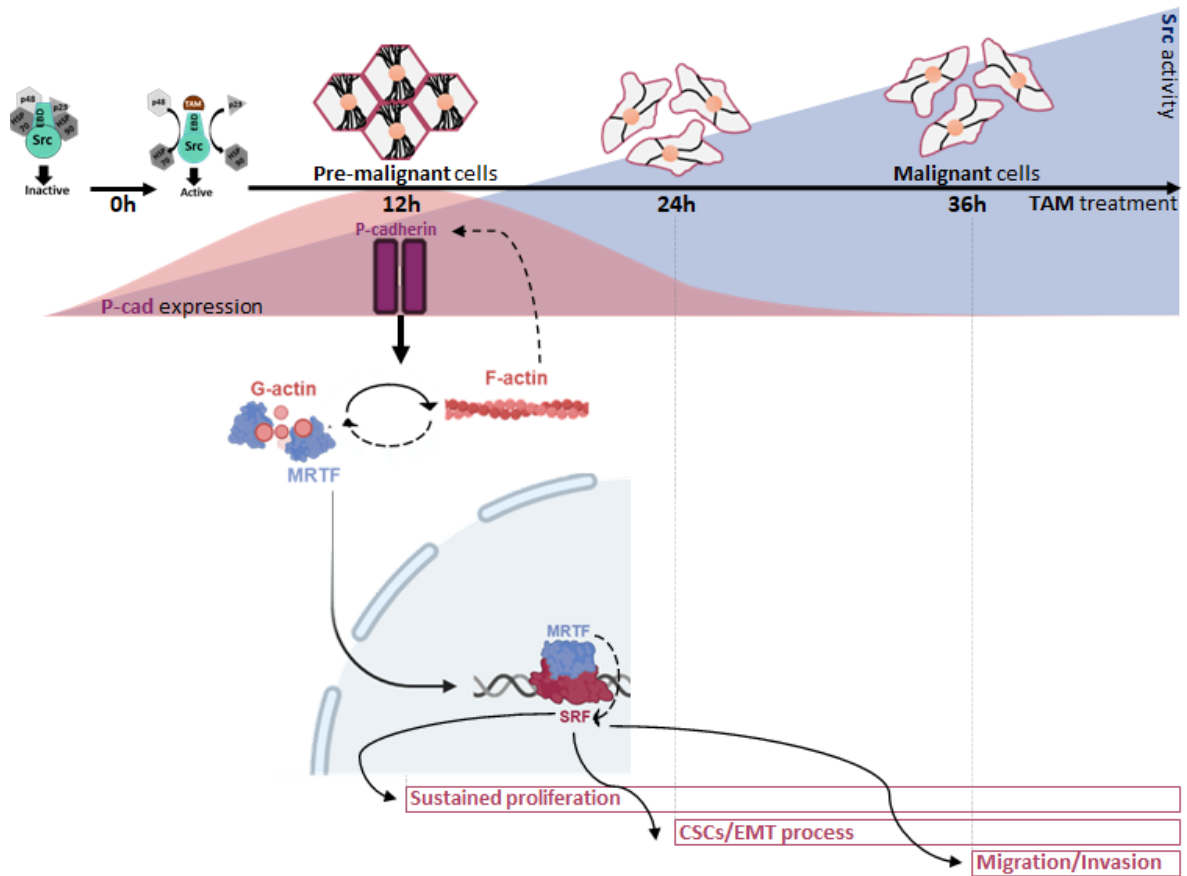
**Figure 29- Model of the role of the P-cad/F-actin/MRTF-A/SRF signalling axis in basal-like TNBC cells.**

# CHAPTER VI
# CONCLUSION AND FUTURE PERSPECTIVES

In summary, we have provided evidences that the MRTF-A/SRF signalling pathway is activated by P-cad, through regulation of actin polymerization in pre-malignant breast cancer cells, and that this transient mechanism is required for malignant progression (Figure 29). Our work suggests that the P-cad/F-actin/MRTF-A/SRF signalling axis could be used as a prognostic read out to predict pre-malignant basal-like TNBC that will evolve to aggressive cancer. Our work also opens the possibility that targeting this pathway could be used as a therapeutic strategy to prevent the progression of a subset of pre-malignant basal-like TNBCs.

# CHAPTER VII
# REFERENCES

Ades, F., Zardavas, D., Bozovic-Spasojevic, I., Pugliano, L., Fumagalli, D., de Azambuja, E., Viale, G., Sotiriou, C., & Piccart, M. (2014). Luminal B breast cancer: molecular characterization, clinical management, and future perspectives. *J Clin Oncol*, *32*(25), 2794-2803. https://doi.org/10.1200/jco.2013.54.1870

Albergaria, A., Ribeiro, A. S., Vieira, A. F., Sousa, B., Nobre, A. R., Seruca, R., Schmitt, F., & Paredes, J. (2011). P-cadherin role in normal breast development and cancer. *Int J Dev Biol*, *55*(7-9), 811-822. https://doi.org/10.1387/ijdb.113382aa

Alluri, P., & Newman, L. A. (2014). Basal-like and triple-negative breast cancers: searching for positives among many negatives. *Surgical oncology clinics of North America*, *23*(3), 567-577. https://doi.org/10.1016/j.soc.2014.03.003

Ambekar, R., Lau, T.-Y., Walsh, M., Bhargava, R., & Toussaint, K. C., Jr. (2012). Quantifying collagen structure in breast biopsies using second-harmonic generation imaging. *Biomedical optics express*, *3*(9), 2021-2035. https://doi.org/10.1364/BOE.3.002021

Asparuhova, M. B., Ferralli, J., Chiquet, M., & Chiquet-Ehrismann, R. (2011). The transcriptional regulator megakaryoblastic leukemia-1 mediates serum response factor-independent activation of tenascin-C transcription by mechanical stress. *Faseb j*, *25*(10), 3477-3488. https://doi.org/10.1096/fj.11-187310

Atashzar, M. R., Baharlou, R., Karami, J., Abdollahi, H., Rezaei, R., Pourramezan, F., & Zoljalali Moghaddam, S. H. (2020). Cancer stem cells: A review from origin to therapeutic implications. *J Cell Physiol*, *235*(2), 790-803. https://doi.org/10.1002/jcp.29044

Baranwal, S., & Alahari, S. K. (2009). Molecular mechanisms controlling E-cadherin expression in breast cancer. *Biochem Biophys Res Commun*, *384*(1), 6-11. https://doi.org/10.1016/j.bbrc.2009.04.051

Bazellières, E., Conte, V., Elosegui-Artola, A., Serra-Picamal, X., Bintanel-Morcillo, M., Roca-Cusachs, P., Muñoz, J. J., Sales-Pardo, M., Guimerà, R., & Trepat, X. (2015). Control of cell-cell forces and collective cell dynamics by the intercellular adhesome. *Nat Cell Biol*, *17*(4), 409-420. https://doi.org/10.1038/ncb3135

Blanchoin, L., Boujemaa-Paterski, R., Sykes, C., & Plastino, J. (2014). Actin dynamics, architecture, and mechanics in cell motility. *Physiol Rev*, *94*(1), 235-263. https://doi.org/10.1152/physrev.00018.2013

Brakebusch, C., Bouvard, D., Stanchi, F., Sakai, T., & Fässler, R. (2002). Integrins in invasive growth. *J Clin Invest*, *109*(8), 999-1006. https://doi.org/10.1172/jci15468

Bruner, H. C., & Derksen, P. W. B. (2018). Loss of E-Cadherin-Dependent Cell-Cell Adhesion and the Development and Progression of Cancer. Cold Spring Harb Perspect Biol, 10(3). https://doi.org/10.1101/cshperspect.a029330

Budnar, S., & Yap, A. S. (2013). A mechanobiological perspective on cadherins and the actin-myosin cytoskeleton. *F1000prime reports*, *5*, 35-35. https://doi.org/10.12703/P5-35

Chen, Y. H., Hancock, B. A., Solzak, J. P., Brinza, D., Scafe, C., Miller, K. D., & Radovich, M. (2017). Next-generation sequencing of circulating tumour DNA to predict recurrence in triple-negative breast cancer patients with residual disease after neoadjuvant chemotherapy. NPJ Breast Cancer, 3, 24. https://doi.org/10.1038/s41523-017-0028-4

Chesarone, M. A., & Goode, B. L. (2009). Actin nucleation and elongation factors: mechanisms and interplay. Curr Opin Cell Biol, 21(1), 28-37. https://doi.org/10.1016/j.ceb.2008.12.001

Cheung, L. W., Leung, P. C., & Wong, A. S. (2010). Cadherin switching and activation of p120 catenin signaling are mediators of gonadotropin-releasing hormone to promote tumour cell migration and invasion in ovarian cancer. Oncogene, 29(16), 2427-2440. https://doi.org/10.1038/onc.2009.523

Choo, J. R., & Nielsen, T. O. (2010). Biomarkers for Basal-like Breast Cancer. Cancers, 2(2), 1040-1065. https://doi.org/10.3390/cancers2021040

Coué, M., Brenner, S. L., Spector, I., & Korn, E. D. (1987). Inhibition of actin polymerization by latrunculin A. FEBS Letters, 213(2), 316-318. https://doi.org/https://doi.org/10.1016/0014-5793(87)81513-2

da Silva-Diz, V., Lorenzo-Sanz, L., Bernat-Peguera, A., Lopez-Cerda, M., & Muñoz, P. (2018). Cancer cell plasticity: Impact on tumour progression and therapy response. Semin Cancer Biol, 53, 48-58. https://doi.org/10.1016/j.semcancer.2018.08.009

David, J. M., & Rajasekaran, A. K. (2012). Dishonorable discharge: the oncogenic roles of cleaved E-cadherin fragments. Cancer research, 72(12), 2917-2923. https://doi.org/10.1158/0008-5472.CAN-11-3498

Debnath, J., Muthuswamy, S. K., & Brugge, J. S. (2003). Morphogenesis and oncogenesis of MCF-10A mammary epithelial acini grown in three-dimensional basement membrane cultures. Methods, 30(3), 256-268. https://doi.org/10.1016/s1046-2023(03)00032-x

Defilippi, P., Olivo, C., Venturino, M., Dolce, L., Silengo, L., & Tarone, G. (1999). Actin cytoskeleton organization in response to integrin-mediated adhesion. *Microsc Res Tech*, *47*(1), 67-78. https://doi.org/10.1002/(sici)1097-0029(19991001)47:1<67::Aid-jemt7>3.0.Co;2-p

Drăgănescu, M., & Carmocan, C. (2017). Hormone Therapy in Breast Cancer. Chirurgia (Bucur), 112(4), 413-417. https://doi.org/10.21614/chirurgia.112.4.413

Farahani, E., Patra, H. K., Jangamreddy, J. R., Rashedi, I., Kawalec, M., Rao Pariti, R. K., Batakis, P., & Wiechec, E. (2014). Cell adhesion molecules and their relation to (cancer) cell stemness. Carcinogenesis, 35(4), 747-759. https://doi.org/10.1093/carcin/bgu045

Feinberg, A. P., Ohlsson, R., & Henikoff, S. (2006). The epigenetic progenitor origin of human cancer. Nat Rev Genet, 7(1), 21-33. https://doi.org/10.1038/nrg1748

Fleming, T. P., Javed, Q., & Hay, M. (1992). Epithelial differentiation and intercellular junction formation in the mouse early embryo. Dev Suppl, 105-112.

Fougner, C., Bergholtz, H., Norum, J. H., & Sørlie, T. (2020). Re-definition of claudin-low as a breast cancer phenotype. Nat Commun, 11(1), 1787. https://doi.org/10.1038/s41467-020-15574-5

Francavilla, C., Maddaluno, L., & Cavallaro, U. (2009). The functional role of cell adhesion molecules in tumour angiogenesis. *Seminars in Cancer Biology*, *19*, 298-309. https://doi.org/10.1016/j.semcancer.2009.05.004

Fu, N. Y., Nolan, E., Lindeman, G. J., & Visvader, J. E. (2019). Stem Cells and the Differentiation Hierarchy in Mammary Gland Development. *Physiological Reviews*, *100*(2), 489-523. https://doi.org/10.1152/physrev.00040.2018

Garrido-Castro, A. C., Lin, N. U., & Polyak, K. (2019). Insights into Molecular Classifications of Triple-Negative Breast Cancer: Improving Patient Selection for Treatment. *Cancer discovery*, *9*(2), 176-198. https://doi.org/10.1158/2159-8290.CD-18-1177

Gasparics, Á., & Sebe, A. (2018). MRTFs- master regulators of EMT. *Dev Dyn, 247*(3), 396-404. https://doi.org/10.1002/dvdy.24544

Gau, D., & Roy, P. (2018). SRF'ing and SAP'ing - the role of MRTF proteins in cell migration. *J Cell Sci*, *131*(19). https://doi.org/10.1242/jcs.218222

Ghebeh, H., Al-Khaldi, S., Olabi, S., Al-Dhfyan, A., Al-Mohanna, F., Barnawi, R., Tulbah, A., Al-Tweigeri, T., Ajarim, D., & Al-Alwan, M. (2014). Fascin is involved in the chemotherapeutic resistance of breast cancer cells predominantly via the PI3K/Akt pathway. *Br J Cancer*, *111*(8), 1552-1561. https://doi.org/10.1038/bjc.2014.453

Gurbuz, I., Ferralli, J., Roloff, T., Chiquet-Ehrismann, R., & Asparuhova, M. B. (2014). SAP domain-dependent Mkl1 signaling stimulates proliferation and cell migration by induction of a distinct gene set indicative of poor prognosis in breast cancer patients. *Molecular Cancer*, *13*(1), 22. https://doi.org/10.1186/1476-4598-13-22

Haak, A. J., Appleton, K. M., Lisabeth, E. M., Misek, S. A., Ji, Y., Wade, S. M., Bell, J. L., Rockwell, C. E., Airik, M., Krook, M. A., Larsen, S. D., Verhaegen, M., Lawlor, E. R., & Neubig, R. R. (2017). Pharmacological Inhibition of Myocardin-related Transcription Factor Pathway Blocks Lung Metastases of RhoC-Overexpressing

Melanoma. *Mol Cancer Ther*, *16*(1), 193-204. https://doi.org/10.1158/1535-7163.Mct-16-0482

Hanahan, D., & Weinberg, R. A. (2011). Hallmarks of cancer: the next generation. *Cell*, *144*(5), 646-674. https://doi.org/10.1016/j.cell.2011.02.013

Hansen, R. K., & Bissell, M. J. (2000). Tissue architecture and breast cancer: the role of extracellular matrix and steroid hormones. *Endocrine-related cancer*, *7*(2), 95-113. https://doi.org/10.1677/erc.0.0070095

Hardy, R. G., Tselepis, C., Hoyland, J., Wallis, Y., Pretlow, T. P., Talbot, I., Sanders, D. S. A., Matthews, G., Morton, D., & Jankowski, J. A. Z. (2002). Aberrant P-cadherin expression is an early event in hyperplastic and dysplastic transformation in the colon. *Gut*, *50*(4), 513. https://doi.org/10.1136/gut.50.4.513

Harjunpää, H., Llort Asens, M., Guenther, C., & Fagerholm, S. C. (2019). Cell Adhesion Molecules and Their Roles and Regulation in the Immune and Tumour Microenvironment. *Front Immunol*, *10*, 1078. https://doi.org/10.3389/fimmu.2019.01078

Hermann, M. R., Jakobson, M., Colo, G. P., Rognoni, E., Jakobson, M., Kupatt, C., Posern, G., & Fässler, R. (2016). Integrins synergise to induce expression of the MRTF-A-SRF target gene ISG15 for promoting cancer cell invasion. *J Cell Sci*, *129*(7), 1391-1403. https://doi.org/10.1242/jcs.177592

Hirsch, H. A., Iliopoulos, D., Tsichlis, P. N., & Struhl, K. (2009). Metformin selectively targets cancer stem cells, and acts together with chemotherapy to block tumour growth and prolong remission. *Cancer Res*, *69*(19), 7507-7511. https://doi.org/10.1158/0008-5472.Can-09-2994

Horne, H. N., Oh, H., Sherman, M. E., Palakal, M., Hewitt, S. M., Schmidt, M. K., Milne, R. L., Hardisson, D., Benitez, J., Blomqvist, C., Bolla, M. K., Brenner, H., Chang-Claude, J., Cora, R., Couch, F. J., Cuk, K., Devilee, P., Easton, D. F., Eccles, D. M., Eilber, U., Hartikainen, J. M., Heikkilä, P., Holleczek, B., Hooning, M. J., Jones, M., Keeman, R., Mannermaa, A., Martens, J. W. M., Muranen, T. A., Nevanlinna, H., Olson, J. E., Orr, N., Perez, J. I. A., Pharoah, P. D. P., Ruddy, K. J., Saum, K. U., Schoemaker, M. J., Seynaeve, C., Sironen, R., Smit, V., Swerdlow, A. J., Tengström, M., Thomas, A. S., Timmermans, A. M., Tollenaar, R., Troester, M. A., van Asperen, C. J., van Deurzen, C. H. M., Van Leeuwen, F. F., Van't Veer, L. J., García-Closas, M., & Figueroa, J. D. (2018). E-cadherin breast tumour expression, risk factors and survival: Pooled analysis of 5,933 cases from 12 studies in the Breast Cancer Association Consortium. *Sci Rep*, *8*(1), 6574. https://doi.org/10.1038/s41598-018-23733-4

Ikeda, T., Hikichi, T., Miura, H., Shibata, H., Mitsunaga, K., Yamada, Y., Woltjen, K., Miyamoto, K., Hiratani, I., Yamada, Y., Hotta, A., Yamamoto, T., Okita, K., & Masui, S. (2018). Srf destabilizes cellular identity by suppressing cell-type-specific gene expression programs. *Nat Commun*, *9*(1), 1387. https://doi.org/10.1038/s41467-018-03748-1

Iliopoulos, D., Hirsch, H. A., & Struhl, K. (2009). An epigenetic switch involving NF-kappaB, Lin28, Let-7 MicroRNA, and IL6 links inflammation to cell transformation. *Cell*, *139*(4), 693-706. https://doi.org/10.1016/j.cell.2009.10.014

Indra, I., Choi, J., Chen, C. S., Troyanovsky, R. B., Shapiro, L., Honig, B., & Troyanovsky, S. M. (2018). Spatial and temporal organization of cadherin in punctate adherens junctions. *Proc Natl Acad Sci U S A*, *115*(19), E4406-e4415. https://doi.org/10.1073/pnas.1720826115

Jie, D., Zhongmin, Z., Guoqing, L., Sheng, L., Yi, Z., Jing, W., & Liang, Z. (2013). Positive expression of LSD1 and negative expression of E-cadherin correlate with metastasis and poor prognosis of colon cancer. *Dig Dis Sci*, *58*(6), 1581-1589. https://doi.org/10.1007/s10620-012-2552-2

Kaszak, I., Witkowska-Piłaszewicz, O., Niewiadomska, Z., Dworecka-Kaszak, B., Ngosa Toka, F., & Jurka, P. (2020). Role of Cadherins in Cancer-A Review. *Int J Mol Sci*, *21*(20). https://doi.org/10.3390/ijms21207624

Kim, T., Hwang, D., Lee, D., Kim, J. H., Kim, S. Y., & Lim, D. S. (2017). MRTF potentiates TEAD-YAP transcriptional activity causing metastasis. *Embo j, 36*(4), 520-535. https://doi.org/10.15252/embj.201695137

Knudsen, K. A., & Wheelock, M. J. (2005). Cadherins and the mammary gland [https://doi.org/10.1002/jcb.20419]. *Journal of Cellular Biochemistry, 95*(3), 488-496. https://doi.org/https://doi.org/10.1002/jcb.20419

Kustermans, G., Piette, J., & Legrand-Poels, S. (2008). Actin-targeting natural compounds as tools to study the role of actin cytoskeleton in signal transduction. *Biochem Pharmacol, 76*(11), 1310-1322. https://doi.org/10.1016/j.bcp.2008.05.028

Lee, E. Y., & Muller, W. J. (2010). Oncogenes and tumour suppressor genes. *Cold Spring Harb Perspect Biol, 2*(10), a003236. https://doi.org/10.1101/cshperspect.a003236

Lewczuk, Ł., Pryczynicz, A., & Guzińska-Ustymowicz, K. (2019). Cell adhesion molecules in endometrial cancer - A systematic review. *Adv Med Sci, 64*(2), 423-429. https://doi.org/10.1016/j.advms.2019.08.003

Liga-Portuguesa-Contra-o-Cancro. (2021). Accessed 09/01/2021 from https://www.ligacontracancro.pt/cancro-da-mama/

Liu, X., Ory, V., Chapman, S., Yuan, H., Albanese, C., Kallakury, B., Timofeeva, O. A., Nealon, C., Dakic, A., Simic, V., Haddad, B. R., Rhim, J. S., Dritschilo, A., Riegel, A., McBride, A., & Schlegel, R. (2012). ROCK inhibitor and feeder cells induce the conditional reprogramming of epithelial cells. Am J Pathol, 180(2), 599-607. https://doi.org/10.1016/j.ajpath.2011.10.036

López-Lázaro, M. (2018). The stem cell division theory of cancer. *Critical Reviews in Oncology/Hematology, 123*, 95-113. https://doi.org/https://doi.org/10.1016/j.critrevonc.2018.01.010

Malhotra, G. K., Zhao, X., Band, H., & Band, V. (2010). Histological, molecular and functional subtypes of breast cancers. Cancer Biol Ther, 10(10), 955-960. https://doi.org/10.4161/cbt.10.10.13879

Marra, A., Trapani, D., Viale, G., Criscitiello, C., & Curigliano, G. (2020). Practical classification of triple-negative breast cancer: intratumoural heterogeneity, mechanisms of drug resistance, and novel therapies. npj Breast Cancer, 6(1), 54. https://doi.org/10.1038/s41523-020-00197-2

Martin, S. S., & Leder, P. (2001). Human MCF10A mammary epithelial cells undergo apoptosis following actin depolymerization that is independent of attachment and rescued by Bcl-2. Mol Cell Biol, 21(19), 6529-6536. https://doi.org/10.1128/mcb.21.19.6529-6536.2001

Mbalaviele, G., Dunstan, C. R., Sasaki, A., Williams, P. J., Mundy, G. R., & Yoneda, T. (1996). E-cadherin expression in human breast cancer cells suppresses the development of osteolytic bone metastases in an experimental metastasis model. Cancer Res, 56(17), 4063-4070.

Medjkane, S., Perez-Sanchez, C., Gaggioli, C., Sahai, E., & Treisman, R. (2009). Myocardin-related transcription factors and SRF are required for cytoskeletal dynamics and experimental metastasis. Nat Cell Biol, 11(3), 257-268. https://doi.org/10.1038/ncb1833

Mendonsa, A. M., Na, T. Y., & Gumbiner, B. M. (2018). E-cadherin in contact inhibition and cancer. Oncogene, 37(35), 4769-4780. https://doi.org/10.1038/s41388-018-0304-2

Miralles, F., Posern, G., Zaromytidou, A. I., & Treisman, R. (2003). Actin dynamics control SRF activity by regulation of its coactivator MAL. *Cell, 113*(3), 329-342. https://doi.org/10.1016/s0092-8674(03)00278-2

Mithraprabhu, S., Khong, T., & Spencer, A. (2014). Overcoming inherent resistance to histone deacetylase inhibitors in multiple myeloma cells by targeting pathways integral to the actin cytoskeleton. *Cell Death Dis, 5*(3), e1134. https://doi.org/10.1038/cddis.2014.98

Montesano, R., & Hall, J. (2001). Environmental causes of human cancers. *European Journal of Cancer, 37*, 67-87. https://doi.org/10.1016/S0959-8049(01)00266-0

Nassar, D., & Blanpain, C. (2016). Cancer Stem Cells: Basic Concepts and Therapeutic Implications. *Annu Rev Pathol*, *11*, 47-76. https://doi.org/10.1146/annurev-pathol-012615-044438

Navarro, P., Gómez, M., Pizarro, A., Gamallo, C., Quintanilla, M., & Cano, A. (1991). A role for the E-cadherin cell-cell adhesion molecule during tumour progression of mouse epidermal carcinogenesis. *J Cell Biol*, *115*(2), 517-533. https://doi.org/10.1083/jcb.115.2.517

NCHS. (2021). *Centers for Disease Control and Prevention*. Retrieved 27-01-2021 from https://www.cdc.gov/nchs/fastats/leading-causes-of-death.htm

NIH. (2021). *National Cancer Institute*. Accessed 27-01-2021 from https://www.cancer.gov/about-cancer/understanding/what-is-cancer

Nose, A., & Takeichi, M. (1986). A novel cadherin cell adhesion molecule: its expression patterns associated with implantation and organogenesis of mouse embryos. *J Cell Biol*, *103*(6 Pt 2), 2649-2658. https://doi.org/10.1083/jcb.103.6.2649

Ohata, H., Ishiguro, T., Aihara, Y., Sato, A., Sakai, H., Sekine, S., Taniguchi, H., Akasu, T., Fujita, S., Nakagama, H., & Okamoto, K. (2012). Induction of the stem-like cell regulator CD44 by Rho kinase inhibition contributes to the maintenance of colon cancer-initiating cells. *Cancer Res*, *72*(19), 5101-5110. https://doi.org/10.1158/0008-5472.Can-11-3812

Ortiz, M. A., Mikhailova, T., Li, X., Porter, B. A., Bah, A., & Kotula, L. (2021). Src family kinases, adaptor proteins and the actin cytoskeleton in epithelial-to-mesenchymal transition. *Cell communication and signaling : CCS*, *19*(1), 67-67. https://doi.org/10.1186/s12964-021-00750-x

Pandit, P., Patil, R., Palwe, V., Gandhe, S., Patil, R., & Nagarkar, R. (2020). Prevalence of Molecular Subtypes of Breast Cancer: A Single Institutional Experience of 2062 Patients. *Eur J Breast Health*, *16*(1), 39-43. https://doi.org/10.5152/ejbh.2019.4997

Paredes, J., Albergaria, A., Oliveira, J. T., Jerónimo, C., Milanezi, F., & Schmitt, F. C. (2005). P-cadherin overexpression is an indicator of clinical outcome in invasive breast carcinomas and is associated with CDH3 promoter hypomethylation. *Clin Cancer Res*, *11*(16), 5869-5877. https://doi.org/10.1158/1078-0432.Ccr-05-0059

Paredes, J., Correia, A. L., Ribeiro, A. S., Albergaria, A., Milanezi, F., & Schmitt, F. C. (2007). P-cadherin expression in breast cancer: a review. *Breast Cancer Res*, *9*(5), 214. https://doi.org/10.1186/bcr1774

Paredes, J., Figueiredo, J., Albergaria, A., Oliveira, P., Carvalho, J., Ribeiro, A. S., Caldeira, J., Costa, Â. M., Simões-Correia, J., Oliveira, M. J., Pinheiro, H., Pinho, S. S., Mateus, R., Reis, C. A., Leite, M., Fernandes, M. S., Schmitt, F., Carneiro, F., Figueiredo, C., Oliveira, C., & Seruca, R. (2012). Epithelial E- and P-cadherins: Role and clinical significance in cancer. *Biochimica et Biophysica Acta (BBA) - Reviews on Cancer*, *1826*(2), 297-311. https://doi.org/https://doi.org/10.1016/j.bbcan.2012.05.002

Paredes, J., Milanezi, F., Viegas, L., Amendoeira, I., & Schmitt, F. (2002). P-cadherin expression is associated with high-grade ductal carcinoma in situ of the breast. *Virchows Arch*, *440*(1), 16-21. https://doi.org/10.1007/s004280100487

Paredes, J., Stove, C., Stove, V., Milanezi, F., Van Marck, V., Derycke, L., Mareel, M., Bracke, M., & Schmitt, F. (2004). P-cadherin is up-regulated by the antiestrogen ICI 182,780 and promotes invasion of human breast cancer cells. *Cancer Res*, *64*(22), 8309-8317. https://doi.org/10.1158/0008-5472.Can-04-0795

Parsa, N. (2012). Environmental factors inducing human cancers. *Iranian journal of public health*, 41(11), 1-9. https://pubmed.ncbi.nlm.nih.gov/23304670

Pattabiraman, D. R., & Weinberg, R. A. (2014). Tackling the cancer stem cells - what challenges do they pose? Nat Rev Drug Discov, 13(7), 497-512. https://doi.org/10.1038/nrd4253

Pawłowski, R., Rajakylä, E. K., Vartiainen, M. K., & Treisman, R. (2010). An actin-regulated importin α/β-dependent extended bipartite NLS directs nuclear import of MRTF-A. *Embo j, 29*(20), 3448-3458. https://doi.org/10.1038/emboj.2010.216

Peralta Soler, A., Knudsen, K. A., Salazar, H., Han, A. C., & Keshgegian, A. A. (1999). P-cadherin expression in breast carcinoma indicates poor survival. *Cancer*, *86*(7), 1263-1272. https://doi.org/10.1002/(sici)1097-0142(19991001)86:7<1263::aid-cncr23>3.3.co;2-u

Pipes, G. C., Creemers, E. E., & Olson, E. N. (2006). The myocardin family of transcriptional coactivators: versatile regulators of cell growth, migration, and myogenesis. *Genes Dev*, *20*(12), 1545-1556. https://doi.org/10.1101/gad.1428006

Plessner, M., Melak, M., Chinchilla, P., Baarlink, C., & Grosse, R. (2015). Nuclear F-actin formation and reorganization upon cell spreading. *J Biol Chem*, *290*(18), 11209-11216. https://doi.org/10.1074/jbc.M114.627166

Plouffe, S. W., Meng, Z., Lin, K. C., Lin, B., Hong, A. W., Chun, J. V., & Guan, K.-L. (2016). Characterization of Hippo Pathway Components by Gene Inactivation. *Molecular cell*, *64*(5), 993-1008. https://doi.org/10.1016/j.molcel.2016.10.034

Posern, G., & Treisman, R. (2006). Actin' together: serum response factor, its cofactors and the link to signal transduction. *Trends Cell Biol*, *16*(11), 588-596. https://doi.org/10.1016/j.tcb.2006.09.008

Prat, A., Parker, J. S., Karginova, O., Fan, C., Livasy, C., Herschkowitz, J. I., He, X., & Perou, C. M. (2010). Phenotypic and molecular characterization of the claudin-low intrinsic subtype of breast cancer. *Breast Cancer Res*, *12*(5), R68. https://doi.org/10.1186/bcr2635

Rakha, E. A., Reis-Filho, J. S., Baehner, F., Dabbs, D. J., Decker, T., Eusebi, V., Fox, S. B., Ichihara, S., Jacquemier, J., Lakhani, S. R., Palacios, J., Richardson, A. L., Schnitt, S. J., Schmitt, F. C., Tan, P. H., Tse, G. M., Badve, S., & Ellis, I. O. (2010). Breast cancer prognostic classification in the molecular era: the role of histological grade. *Breast Cancer Res*, *12*(4), 207. https://doi.org/10.1186/bcr2607

Ribeiro, A. S., Albergaria, A., Sousa, B., Correia, A. L., Bracke, M., Seruca, R., Schmitt, F. C., & Paredes, J. (2010). Extracellular cleavage and shedding of P-cadherin: a mechanism underlying the invasive behaviour of breast cancer cells. *Oncogene*, *29*(3), 392-402. https://doi.org/10.1038/onc.2009.338

Ribeiro, A. S., Carvalho, F. A., Figueiredo, J., Carvalho, R., Mestre, T., Monteiro, J., Guedes, A. F., Fonseca, M., Sanches, J., Seruca, R., Santos, N. C., & Paredes, J. (2016). Atomic force microscopy and graph analysis to study the P-cadherin/SFK mechanotransduction signalling in breast cancer cells. *Nanoscale*, *8*(46), 19390-19401. https://doi.org/10.1039/c6nr04465d

Ribeiro, A. S., Nobre, A. R., Mendes, N., Almeida, J., Vieira, A. F., Sousa, B., Carvalho, F. A., Monteiro, J., Polónia, A., Fonseca, M., Sanches, J. M., Santos, N. C., Seruca, R., & Paredes, J. (2018). SRC inhibition prevents P-cadherin mediated signaling and function in basal-like breast cancer cells. *Cell Commun Signal*, *16*(1), 75. https://doi.org/10.1186/s12964-018-0286-2

Ribeiro, B. S., Laura Carreto, Nuno Mendes, Ana Rita Nobre, Sara Ricardo, André, Albergaria, J. F. C.-T., Rene Gerhard, Ola Söderberg, Raquel Seruca, Manuel A Santos, Fernando, & Paredes, S. a. J. (2013). 'P-cadherin functional role is dependent on E-cadherin cellular context: a proof of concept using the breast cancer model'. *J Pathol*, *239*(1), 122. https://doi.org/10.1002/path.4722

Rimm, D. L., Koslov, E. R., Kebriaei, P., Cianci, C. D., & Morrow, J. S. (1995). Alpha 1(E)-catenin is an actin-binding and -bundling protein mediating the attachment of F-actin to the membrane adhesion complex. *Proc Natl Acad Sci U S A*, *92*(19), 8813-8817. https://doi.org/10.1073/pnas.92.19.8813

Rodriguez, F. J., Lewis-Tuffin, L. J., & Anastasiadis, P. Z. (2012). E-cadherin's dark side: possible role in tumour progression. *Biochim Biophys Acta*, *1826*(1), 23-31. https://doi.org/10.1016/j.bbcan.2012.03.002

Rossi, F., Noren, H., Jove, R., Beljanski, V., & Grinnemo, K.-H. (2020). Differences and similarities between cancer and somatic stem cells: therapeutic implications. *Stem Cell Research & Therapy*, *11*(1), 489. https://doi.org/10.1186/s13287-020-02018-6

Saito, M., Tucker, D. K., Kohlhorst, D., Niessen, C. M., & Kowalczyk, A. P. (2012). Classical and desmosomal cadherins at a glance. *J Cell Sci*, *125*(Pt 11), 2547-2552. https://doi.org/10.1242/jcs.066654

Samanta, D., & Almo, S. C. (2015). Nectin family of cell-adhesion molecules: structural and molecular aspects of function and specificity. *Cell Mol Life Sci*, *72*(4), 645-658. https://doi.org/10.1007/s00018-014-1763-4

Saria, M. G. (2018). Overview of Cancer. In *Your Guide to Cancer Prevention* (pp. 1-6). https://www.ons.org/books/your-guide-cancer-prevention

Sarrió, D., Palacios, J., Hergueta-Redondo, M., Gómez-López, G., Cano, A., & Moreno-Bueno, G. (2009). Functional characterization of E- and P-cadherin in invasive breast cancer cells. *BMC Cancer*, *9*, 74. https://doi.org/10.1186/1471-2407-9-74

Schettini, F., Pascual, T., Conte, B., Chic, N., Brasó-Maristany, F., Galván, P., Martínez, O., Adamo, B., Vidal, M., Muñoz, M., Fernández-Martinez, A., Rognoni, C., Griguolo, G., Guarneri, V., Conte, P. F., Locci, M., Brase, J. C., Gonzalez-Farre, B., Villagrasa, P., De Placido, S., Schiff, R., Veeraraghavan, J., Rimawi, M. F., Osborne, C. K., Pernas, S., Perou, C. M., Carey, L. A., & Prat, A. (2020). HER2-enriched subtype and pathological complete response in HER2-positive breast cancer: A systematic review and meta-analysis. *Cancer Treat Rev*, *84*, 101965. https://doi.org/10.1016/j.ctrv.2020.101965

Schmitt, F., Ricardo, S., Vieira, A. F., Dionísio, M. R., & Paredes, J. (2012). Cancer stem cell markers in breast neoplasias: their relevance and distribution in distinct molecular subtypes. *Virchows Arch*, *460*(6), 545-553. https://doi.org/10.1007/s00428-012-1237-8

Seifert, A., & Posern, G. (2017). Tightly controlled MRTF-A activity regulates epithelial differentiation during formation of mammary acini. *Breast Cancer Research*, *19*(1), 68. https://doi.org/10.1186/s13058-017-0860-3

Selvaggio, G., Canato, S., Pawar, A., Monteiro, P. T., Guerreiro, P. S., Brás, M. M., Janody, F., & Chaouiya, C. (2020). Hybrid Epithelial-Mesenchymal Phenotypes Are Controlled by Microenvironmental Factors. *Cancer Res*, *80*(11), 2407-2420. https://doi.org/10.1158/0008-5472.Can-19-3147

Seo, J., & Kim, J. (2018). Regulation of Hippo signaling by actin remodeling. *BMB reports*, *51*(3), 151-156. https://doi.org/10.5483/bmbrep.2018.51.3.012

Shreberk-Shaked, M., & Oren, M. (2019). New insights into YAP/TAZ nucleo-cytoplasmic shuttling: new cancer therapeutic opportunities? *Mol Oncol, 13*(6), 1335-1341. https://doi.org/10.1002/1878-0261.12498

Sidorenko, E., & Vartiainen, M. K. (2019). Nucleoskeletal regulation of transcription: Actin on MRTF. *Exp Biol Med (Maywood)*, *244*(15), 1372-1381. https://doi.org/10.1177/1535370219854669

Sisson, T. H., Ajayi, I. O., Subbotina, N., Dodi, A. E., Rodansky, E. S., Chibucos, L. N., Kim, K. K., Keshamouni, V. G., White, E. S., Zhou, Y., Higgins, P. D. R., Larsen, S. D., Neubig, R. R., & Horowitz, J. C. (2015). Inhibition of Myocardin-Related Transcription Factor/Serum Response Factor Signaling Decreases Lung Fibrosis and Promotes Mesenchymal Cell Apoptosis. *The American Journal of Pathology*, *185*(4), 969-986. https://doi.org/https://doi.org/10.1016/j.ajpath.2014.12.005

Song, Z., Liu, Z., Sun, J., Sun, F. L., Li, C. Z., Sun, J. Z., & Xu, L. Y. (2016). The MRTF-A/B function as oncogenes in pancreatic cancer. *Oncol Rep*, *35*(1), 127-138. https://doi.org/10.3892/or.2015.4329

Sotiropoulos, A., Gineitis, D., Copeland, J., & Treisman, R. (1999). Signal-Regulated Activation of Serum Response Factor Is Mediated by Changes in Actin Dynamics. *Cell*, *98*(2), 159-169. https://doi.org/https://doi.org/10.1016/S0092-8674(00)81011-9

Soule, H. D., Maloney, T. M., Wolman, S. R., Peterson, W. D., Jr., Brenz, R., McGrath, C. M., Russo, J., Pauley, R. J., Jones, R. F., & Brooks, S. C. (1990). Isolation and characterization of a spontaneously immortalized human breast epithelial cell line, MCF-10. *Cancer Res*, *50*(18), 6075-6086.

Sun, Y. S., Zhao, Z., Yang, Z. N., Xu, F., Lu, H. J., Zhu, Z. Y., Shi, W., Jiang, J., Yao, P. P., & Zhu, H. P. (2017). Risk Factors and Preventions of Breast Cancer. *Int J Biol Sci*, *13*(11), 1387-1397. https://doi.org/10.7150/ijbs.21635

Sung, H., Ferlay, J., Siegel, R. L., Laversanne, M., Soerjomataram, I., Jemal, A., & Bray, F. (2021). Global Cancer Statistics 2020: GLOBOCAN Estimates of Incidence and Mortality Worldwide for 36 Cancers in 185 Countries. *CA Cancer J Clin*, *71*(3), 209-249. https://doi.org/10.3322/caac.21660

Takada, Y., Ye, X., & Simon, S. (2007). The integrins. *Genome biology*, *8*(5), 215-215. https://doi.org/10.1186/gb-2007-8-5-215

Takeichi, M. (1977). Functional correlation between cell adhesive properties and some cell surface proteins. *J Cell Biol*, *75*(2 Pt 1), 464-474. https://doi.org/10.1083/jcb.75.2.464

Taniuchi, K., Nakagawa, H., Hosokawa, M., Nakamura, T., Eguchi, H., Ohigashi, H., Ishikawa, O., Katagiri, T., & Nakamura, Y. (2005). Overexpressed P-cadherin/CDH3 promotes motility of pancreatic cancer cells by interacting with p120ctn and activating rho-family GTPases. *Cancer Res*, *65*(8), 3092-3099. https://doi.org/10.1158/0008.5472.Can-04-3646

Tavares, S., Vieira, A. F., Taubenberger, A. V., Araújo, M., Martins, N. P., Brás-Pereira, C., Polónia, A., Herbig, M., Barreto, C., Otto, O., Cardoso, J., Pereira-Leal, J. B., Guck, J., Paredes, J., & Janody, F. (2017). Actin stress fiber organization promotes cell stiffening and proliferation of pre-invasive breast cancer cells. *Nat Commun*, *8*, 15237. https://doi.org/10.1038/ncomms15237

Toft, D. J., & Cryns, V. L. (2011). Minireview: Basal-like breast cancer: from molecular profiles to targeted therapies. *Mol Endocrinol*, *25*(2), 199-211. https://doi.org/10.1210/me.2010-0164

Toh, T. B., Lim, J. J., & Chow, E. K. (2017). Epigenetics in cancer stem cells. *Mol Cancer*, *16*(1), 29. https://doi.org/10.1186/s12943-017-0596-9

Toledo-Guzmán, M. E., Bigoni-Ordóñez, G. D., Ibáñez Hernández, M., & Ortiz-Sánchez, E. (2018). Cancer stem cell impact on clinical oncology. *World journal of stem cells*, *10*(12), 183-195. https://doi.org/10.4252/wjsc.v10.i12.183

Turashvili, G., & Brogi, E. (2017). Tumour Heterogeneity in Breast Cancer. *Front Med (Lausanne)*, *4*, 227. https://doi.org/10.3389/fmed.2017.00227

van Roy, F., & Berx, G. (2008). The cell-cell adhesion molecule E-cadherin. *Cell Mol Life Sci*, *65*(23), 3756-3788. https://doi.org/10.1007/s00018-008-8281-1

Vartiainen, M. K., Guettler, S., Larijani, B., & Treisman, R. (2007). Nuclear actin regulates dynamic subcellular localization and activity of the SRF cofactor MAL. *Science*, *316*(5832), 1749-1752. https://doi.org/10.1126/science.1141084

Vernieri, C., Milano, M., Brambilla, M., Mennitto, A., Maggi, C., Cona, M. S., Prisciandaro, M., Fabbroni, C., Celio, L., Mariani, G., Bianchi, G. V., Capri, G., & de Braud, F. (2019). Resistance mechanisms to anti-HER2 therapies in HER2-positive breast cancer: Current knowledge, new research directions and therapeutic perspectives. *Crit Rev Oncol Hematol*, *139*, 53-66. https://doi.org/10.1016/j.critrevonc.2019.05.001

Vieira, A. F., & Paredes, J. (2015). P-cadherin and the journey to cancer metastasis. *Mol Cancer*, *14*, 178. https://doi.org/10.1186/s12943-015-0448-4

Vieira, A. F., Ribeiro, A. S., Dionísio, M. R., Sousa, B., Nobre, A. R., Albergaria, A., Santiago-Gómez, A., Mendes, N., Gerhard, R., Schmitt, F., Clarke, R. B., & Paredes, J. (2014). P-cadherin signals through the laminin receptor α6β4 integrin to induce stem cell and invasive properties in basal-like breast cancer cells. *Oncotarget*, *5*(3), 679-692. https://doi.org/10.18632/oncotarget.1459

Vieira, A. F., Ricardo, S., Ablett, M. P., Dionísio, M. R., Mendes, N., Albergaria, A., Farnie, G., Gerhard, R., Cameselle-Teijeiro, J. F., Seruca, R., Schmitt, F., Clarke, R. B., & Paredes, J. (2012). P-cadherin is coexpressed with CD44 and CD49f and mediates stem cell properties in basal-like breast cancer. *Stem Cells*, *30*(5), 854-864. https://doi.org/10.1002/stem.1075

Visvader, J. E., & Lindeman, G. J. (2012). Cancer Stem Cells: Current Status and Evolving Complexities. *Cell Stem Cell*, *10*(6), 717-728. https://doi.org/https://doi.org/10.1016/j.stem.2012.05.007

Wang, D., Chang, P. S., Wang, Z., Sutherland, L., Richardson, J. A., Small, E., Krieg, P. A., & Olson, E. N. (2001). Activation of cardiac gene expression by myocardin, a transcriptional cofactor for serum response factor. *Cell*, *105*(7), 851-862. https://doi.org/10.1016/s0092-8674(01)00404-4

Watanabe, K., Ueno, M., Kamiya, D., Nishiyama, A., Matsumura, M., Wataya, T., Takahashi, J. B., Nishikawa, S., Nishikawa, S., Muguruma, K., & Sasai, Y. (2007). A ROCK inhibitor permits survival of dissociated human embryonic stem cells. *Nat Biotechnol*, *25*(6), 681-686. https://doi.org/10.1038/nbt1310

Weigelt, B., Geyer, F. C., & Reis-Filho, J. S. (2010). Histological types of breast cancer: how special are they? *Mol Oncol*, *4*(3), 192-208. https://doi.org/10.1016/j.molonc.2010.04.004

WHO. (2021). *International Agency for Cancer Research (IARC) - Cancer Today*. Accessed 27-01-2021 from https://gco.iarc.fr/today/online-analysis-table?v=2020&mode=cancer&mode_population=continents&population=900&populations=900&key=asr&sex=0&cancer=39&type=1&statistic=5&prevalence=0&population_group=0&ages_group%5B%5D=0&ages_group%5B%5D=17&group_cancer=1&i

Witsch, E., Sela, M., & Yarden, Y. (2010). Roles for growth factors in cancer progression. *Physiology (Bethesda)*, *25*(2), 85-101. https://doi.org/10.1152/physiol.00045.2009

Wong, S. H. M., Fang, C. M., Chuah, L. H., Leong, C. O., & Ngai, S. C. (2018). E-cadherin: Its dysregulation in carcinogenesis and clinical implications. *Crit Rev Oncol Hematol*, *121*, 11-22. https://doi.org/10.1016/j.critrevonc.2017.11.010

Xing, X., Tang, Y. B., Yuan, G., Wang, Y., Wang, J., Yang, Y., & Chen, M. (2013). The prognostic value of E-cadherin in gastric cancer: a meta-analysis. *Int J Cancer*, *132*(11), 2589-2596. https://doi.org/10.1002/ijc.27947

Xuan Zhang, Z. P., Chunxia Ji, Xiaoyan Zhang, Jianqing Xu and Jin Wang. (2017). Novel Insights into the Role of the Cytoskeleton in Cancer. In J. C. Jimenez-Lopez (Ed.), *Cytoskeleton - Structure, Dynamics, Function and Disease*. https://doi.org/10.5772/66860

Yadav, B. S., Chanana, P., & Jhamb, S. (2015). Biomarkers in triple negative breast cancer: A review. *World journal of clinical oncology*, *6*(6), 252-263. https://doi.org/10.5306/wjco.v6.i6.252

Yamaguchi, H., & Condeelis, J. (2007). Regulation of the actin cytoskeleton in cancer cell migration and invasion. *Biochimica et Biophysica Acta (BBA) - Molecular Cell Research*, *1773*(5), 642-652. https://doi.org/https://doi.org/10.1016/j.bbamcr.2006.07.001

Yin, L., Liu, T., Li, C., Yan, G., Li, C., Zhang, J., & Wang, L. (2020). The MRTF-A/miR-155/SOX1 pathway mediates gastric cancer migration and invasion. *Cancer Cell Int*, *20*, 303. https://doi.org/10.1186/s12935-020-01395-5

Yip, C. H., Smith, R. A., Anderson, B. O., Miller, A. B., Thomas, D. B., Ang, E. S., Caffarella, R. S., Corbex, M., Kreps, G. L., & McTiernan, A. (2008). Guideline implementation for breast healthcare in low- and middle-income countries: early detection resource allocation. *Cancer*, *113*(8 Suppl), 2244-2256. https://doi.org/10.1002/cncr.23842

Zheng, Y., & Pan, D. (2019). The Hippo Signaling Pathway in Development and Disease. *Developmental cell*, *50*(3), 264-282. https://doi.org/10.1016/j.devcel.2019.06.003